

1 Mass Spectrometry and Fourier Transform Infrared Spectroscopy for
2
3 Analysis of Biological Materials
4
5

6 By
7
8

9 Timothy J. Anderson
10
11
12
13

14 A dissertation submitted to the graduate faculty
15
16 In partial fulfillment of the requirements for the degree of
17
18 DOCTOR OF PHILOSOPHY
19
20
21
22

23 Major: Analytical Chemistry
24
25
26 Program of Study Committee:
27
28 R. Sam Houk, Major Professor
29 Young-Jin Lee
30 Emily Smith
31 Joseph Burnett
32 Jesudoss Kingston
33
34
35
36
37
38
39

40 Iowa State University
41
42 Ames, Iowa
43
44

45
46 Copyright © Timothy James Anderson, 2014. All rights reserved.

TABLE OF CONTENTS		
47	LIST OF FIGURES	vi
48	LIST OF TABLES	vii
50	CHAPTER 1. GENERAL INTRODUCTION	1
51	Mass Spectrometry	1
52	Modern Mass Spectrometers and Detectors	2
53	Quadrupole Mass Spectrometer	3
54	Time-of-Flight Mass Spectrometer	4
55	Fourier Transform Ion Cyclotron Resonance and Orbitrap Mass	
56	Spectrometers	5
57	Detectors	7
58	Separation Techniques Coupled to Mass Spectrometry	8
59	Gas Chromatography	9
60	Liquid Chromatography	9
61	Ion Mobility Spectrometry	11
62	Ionization Techniques	12
63	Electron Ionization	13
64	Electrospray Ionization	13
65	Laser Desorption/Ionization	14
66	Mass Spectrometry for Proteomics	16
67	Mass Spectrometry for Metabolomics	18
68	Fourier Transform Infrared Spectroscopy	19
69	Fourier Transform Infrared-Photoacoustic Spectroscopy	21
70	FTIR-PAS Utilized for Biological Materials	22

93	Dissertation Overview	23
94		
95	References	24
96		
97	CHAPTER 2. HIGH RESOLUTION TIME-OF-FLIGHT MASS SPECTROMETRY	
98	FINGERPRINTING OF METABOLITES FROM CECUM AND DISTAL COLON	
99	CONTENTS OF RATS FED RESISTANT STARCH	37
100		
101	Abstract	38
102		
103	Keywords	38
104		
105	Introduction	39
106		
107	Materials and Methods	42
108		
109	Animal Study	42
110		
111	Starch Diet Materials	43
112		
113	Preparation of OS-HA7 Starch Diet	43
114		
115	Preparation of StA-HA7 Starch Diet	43
116		
117	Rat Cecal Samples	44
118		
119	Rat Distal Colon Samples	44
120		
121	Metabolite Extraction for Cecal and Distal Colon Samples	45
122		
123	Mass Spectrometry	46
124		
125	Statistical Analysis	47
126		
127	Results and Discussion	48
128		
129	Mass Spectrometry	48
130		
131	Statistical Analysis of Cecal Contents	51
132		
133	Statistical Analysis of Distal Colon Contents	52
134		
135	Biomarkers from Resistant Starch Diets	54
136		
137	Conclusions	56
138		

139	Acknowledgement	57
140		
141	References	58
142		
143	CHAPTER 3. COMPREHENSIVE IDENTIFICATION OF ALPHA-ZEIN PROTEINS BY	
144	HIGH-PERFORMANCE LIQUID CHROMATOGRAPHY ACCURATE MASS TIME-OF-	
145	FLIGHT MASS SPECTROMETRY	72
146		
147	Abstract	73
148		
149	Keywords	73
150		
151	Introduction	74
152		
153	Materials and Methods	76
154		
155	Alpha-Zein Protein Extraction	76
156		
157	HPLC-TOF MS	77
158		
159	Results and Discussion	78
160		
161	Previous MS Studies of Zein Proteins	78
162		
163	Measured Mass Spectra and M_r Values	79
164		
165	Comparison of Observed Alpha-Zein Proteins with Database Entries	80
166		
167	Alpha-Zein Proteins without Database Entries	83
168		
169	Comparison of Proteins from CGM and DDGS	85
170		
171	Acknowledgements	86
172		
173	References	87
174		
175	CHAPTER 4. ANALYSIS OF RESISTANT STARCHES IN RAT CECAL CONTENTS	
176	USING FOURIER TRANSFORM INFRARED PHOTOACOUSTIC SPECTROSCOPY	96
177		
178	Abstract	97
179		
180	Keywords	97
181		
182	Introduction	98
183		
184	Materials and Methods	101

185	Rat Animal Study	101
186		
187	Starch Diets Fed to Rats	102
188		
189	Rat Cecal Samples	102
190		
191	Enzymatic Assay for Starch Content	103
192		
193	FTIR-PAS	103
194		
195	PLS and PCA	103
196		
197	Results and Discussion	105
198		
199	Enzymatic Assay for Starch Content	105
200		
201	FTIR-PAS	106
202		
203	Abbreviations	107
204		
205	Funding Sources	108
206		
207	Conflict of Interest	108
208		
209	Acknowledgment	108
210		
211	References	109
212		
213	CHAPTER 5. GENERAL CONCLUSIONS	116
214		
215	ACKNOWLEDGEMENTS	119
216		
217		
218		
219		
220		
221		
222		
223		
224		
225		
226		
227		
228		
229		
230		

231	LIST OF FIGURES	
232		
233	Figure 1-1. Diagram of quadrupole rod system	30
234		
235	Figure 1-2. Diagram of time-of-flight reflectron	31
236		
237	Figure 1-3. Diagram of FT-ICR cell	32
238		
239	Figure 1-4. Diagram of Orbitrap detector	33
240		
241	Figure 1-5. Picture of travelling wave ion mobility device	34
242		
243	Figure 1-6. Diagram of travelling wave separation over time	35
244		
245	Figure 1-7. Picture and schematic of FTIR-PAS apparatus	36
246		
247	Figure 2-1. Flow diagram of study and treatment schedule for treatments	65
248		
249	Figure 2-2. Mass spectra of cecal content samples from diets	66
250		
251	Figure 2-3. Mass spectra of distal colon content samples from diets	67
252		
253	Figure 2-4. Selected mass spectra of cecal and distal colon samples from diets	68
254		
255	Figure 2-5. PLS-DA of cecal verification-set diet treatments	69
256		
257	Figure 2-6. PLS-DA of cecal and distal-colon verification-set antibiotic treatment	70
258		
259	Figure 2-7. PLS-DA of distal-colon-content verification-set diet treatments	71
260		
261	Figure 3-1. α -Zein protein bands from CGM and DDGS using SDS-PAGE	94
262		
263	Figure 3-2. Mass spectrum of a mixture of zein proteins	95
264		
265	Figure 4-1. FTIR PAS spectra collected from rat cecal contents	113
266		
267	Figure 4-2. PLS plot of enzymatic starch assay vs predicted values by FTIR-PAS	114
268		
269	Figure 4-3. PCA plot of principal components according to resistant starch diets	115
270		
271		
272		
273		
274		
275		
276		

277	LIST OF TABLES	
278		
279	Table 2-1. Metabolite peaks found in rat cecal and distal colon samples	62
280		
281	Table 2-2. Cecal biomarkers with contribution to class matched to KEGG database	63
282		
283	Table 2-3. Distal Biomarkers with contribution to class matched to KEGG database	64
284		
285	Table 3-1. α -Zein Proteins observed with mass spectrometry using protein database	90
286		
287	Table 3-2. Comparison of α -zein proteins to database proteins previously identified	91
288		
289	Table 3-3. Comparison of α -zein proteins to non-database proteins previously identified	92
290		
291	Table 3-4. α -Zein proteins not previously reported and with no database Entries	93
292		
293	Table 4-1. Enzymatic assay analysis of <i>in vivo</i> starch in cecal contents by rat	112
294		
295		

296
297
298
299
300
301

CHAPTER 1

GENERAL INTRODUCTION

302 Mass Spectrometry

303 Chemistry at its most basic foundation is the study of elements and compounds.
304 Analytical chemistry strives to produce and utilize instruments or tools that assist scientists in
305 qualitatively and quantitatively understanding matter. Few analytical tools have had as large an
306 impact on chemistry as the mass spectrometer (MS). A MS analyzes materials based on their
307 mass-to-charge ratio (m/z). As long as an element or a material has a positive or negative charge
308 in gas phase, the MS has the potential to observe it.

309 The foundation of mass spectrometry began in the mid-19th century, first with the
310 observation of canal rays by Goldstein in 1886 (1). Canal rays are beams of positive ions
311 produced from gas discharge tubes. It was shown by Wien in 1898 that the trajectory of canal
312 rays could be altered using electric and magnetic fields (1). This observation proved that canal
313 rays were charged particles. In that same year Thomson was able to deduce the mass-to-charge
314 ratio of the electron (1). In 1905 Thompson began to study canal rays by following Wien's
315 experiments. The instrument Thomson developed used magnetic and electric fields to deflect
316 gas ions from their original path. Improvements to the instrumentation allowed him to observe
317 deflection parabolas of various ions from hydrogen, oxygen, chlorine, and phosgene. He
318 replaced the photographic plate with a metal plate that had a slit, and then he placed a second
319 plate attached to an electroscope to determine ion abundance vs mass (2).

320 In 1913 Thomson analyzed neon and observed parabolas at m/z 20 and 22. The m/z 22
321 isotope parabola in the spectrum of neon disproved the proposed view that all elements consisted

322 of atoms with a single mass number. Thomson's assistant, Aston, continued detailed studies of
323 isotopes. In 1919 Aston built a new mass spectrograph which could collimate the parabolas into
324 discrete lines, and had a resolution of 130. The instrument first used an electric field between
325 parallel plates to separate the ions, second an electromagnet with a gap between the poles
326 focused the ions to a spectrographic photoplate. The new instrument had the capability to not
327 only accurately separate isotopes of neon, it could record the isotope abundances. By 1924,
328 through the use of the mass spectrograph, fifty three of the known eighty elements had been
329 measured for mass and abundance (1, 2). Based on the pivotal work of these early pioneers, MS
330 has become critical for analytical chemistry and the broader scientific community from World
331 War II into present times. A comprehensive history of critical MS discoveries can be found
332 elsewhere (2).

333

334 *Modern Mass Spectrometers and Detectors*

335 In the past twenty years the use of MS for biological materials has matured. A variety of
336 commercial instruments have emerged to meet these needs. MS instruments produced today can
337 have high resolution, high mass ranges, rapid scan rates, and are relatively user friendly.
338 However, modern instruments still produce results similar to Thomson's first mass spectrometer.
339 MS instruments still measure intensity and m/z of the ionized elements or chemical compounds
340 of interest. The following descriptions are brief functional overviews of the most common
341 modern MS instruments used for biological analysis.

342

343

344

345 Quadrupole Mass Spectrometer

346 In the early 1950's a German physicist named Paul developed the quadrupole mass
347 analyzer (3-5). Figure 1-1 shows that the quadrupole mass selectors consist of four hyperbolic or
348 cylindrical metal rods equivalently spaced from each other (6). The rods positioned directly
349 opposite each other carry the same positive or negative voltage Φ_0 . The adjacent rods share the
350 same magnitude of applied voltage; however they carry the inverse charge, considering there is
351 no bias voltage. The constant voltage Φ_0 on the quadrupole rod is the summation of a direct
352 current (DC) voltage U and radio frequency (RF) voltage V with a driving frequency ω , as
353 shown below:

354

355 $\Phi_0 = U + V \cos \omega t$. (7)

356

357 The applied voltages on the rods produce a field that deflects the ions as they pass between the
358 rods. The field that is produced from a respective applied voltage to the rods permits stable
359 oscillations of only a narrow range of m/z ions. All other ions that traverse the quadrupole field
360 oscillate with increasingly unstable amplitudes until they hit the rods (7). The quadrupole can
361 thus be used for MS to select masses and measure their intensity with the appropriate detector.

362 A popular version of the quadrupole mass spectrometer is the triple quadrupole mass
363 spectrometer used for tandem mass spectrometry (8). The first quadrupole in the instrument is
364 generally a mass selector for a m/z species of interest. The selected ions pass into a second
365 multipole with only a RF voltage that is set to excite the ions for fragmentation (9). A buffer gas
366 of either N_2 , He, or Ar is introduced into the second quadrupole. The transfer of kinetic energy

367 from collisions with the buffer gas causes ion fragmentation. After fragmentation, the ions are
368 transferred to a third quadrupole that measures the ion fragments of the parent ion.

369

370 Time-of-Flight Mass Spectrometer

371 Time-of-flight (TOF) MS was first proposed in 1946 by William Stephens (10). By 1948
372 a functional TOF instrument called the Velocitron was built by Cameron and Eggers (11). TOF
373 instruments function as indicated by their name; they measure the flight time of a packet of ions
374 from the injection source to the detector. An extraction pulse accelerates ions, then a m/z
375 dependent separation occurs as they then traverse a field free zone to reach the detector (12).
376 Due to the function of the TOF instrument, it has many proposed benefits, such as microsecond
377 scan times for entire spectra, nearly unlimited mass range, and high resolution (12). The TOF
378 instrument can achieve fast scan times because it can measure the entire m/z range in a single
379 scan; however, there is a limit to the scan speed of the instruments. To prohibit spectral overlap
380 with the previous scan, the instrument cannot begin the next scan pulse until the slowest ion from
381 the previous scan has reached the detector (13). The high mass range for TOF is achieved by
382 altering the extraction pulse and other various instrument parameters to allow massive ions to be
383 separated. Ions as large as intact virus capsids have been measured using TOF MS (14).

384 TOF instruments began as low resolution instruments. It was common for basic linear
385 TOF instruments to have a resolution of approximately 100 (15). Effective flight length, the
386 thickness of the injected ion packet, and the extraction pulse shape are factors that affect TOF
387 instrument resolution. The relation of effective flight length (L_{eff}) and thickness of ion packet
388 (Δz) to TOF resolution (R_{FWHM}) is shown below (13):

389

390 $R_{FWHM} \approx L_{eff} / 2\Delta z$.

391

392 To improve TOF resolution, innovations to instrumentation have been developed to increase L_{eff}
393 and decrease Δz (12, 15). To improve resolution of TOF instrumentation, the reflectron was
394 devised to compensate for kinetic energy spread. Figure 1-2 details a reflectron instrument,
395 which allows the bending and altering of the ion path so as to make as efficient use of the
396 chamber space as possible and optimize L_{eff} . For early instruments Δz was a major hindrance
397 because it was extremely difficult to focus all of the ions on the same “starting line”. Orthogonal
398 time of flight helped alleviate this issue by using lenses and slits to produce a narrow axial ion
399 packet prior to the entrance of the TOF. The ions are injected by an ion modulator which
400 orthogonally accelerates the ions (16). Most modern TOF instruments combine orthogonal ion
401 injection and reflectron configurations to maximize the L_{eff} and Δz relationship to produce TOF
402 resolutions greater than 10,000 (13).

403

Fourier Transform Ion Cyclotron Resonance and Orbitrap Mass Spectrometers

404 The highest resolution MS are Fourier transform ion cyclotron resonance (FT-ICR)
405 instruments reaching resolutions of 1,000,000 or greater (17). The instrument was invented in
406 1974 by Marshall and Comisarow (18). FT-ICR MS functions as a trapping and analyzing
407 device for ions in three-dimensional space, as shown in Figure 1-3. Ions are injected into a cell
408 with a strong magnetic field applied in the same direction as injected ions. The magnetic field
409 exerts a rotational force on the ions perpendicular to the magnetic field. As the ion packet is
410 injected into the cell, the fore and aft plates are charged to trap the ions in the cell (19).

412 Many aspects of FT-ICR MS make it a powerful technique for biological analysis. The
413 ultra-high resolution is obtained because the ions trapped within the ICR cell move extremely
414 fast and they have small orbital radii, also, the ion cyclotron frequencies are almost completely
415 independent of the spread of velocity in the axial direction. An ion can oscillate between the
416 detector plates ~500,000 times per second (19). Such a large number of data points in such a
417 short time can produce incredible signal-to-noise ratios. The FT-ICR instrument is also a
418 popular choice for tandem mass spectrometry. The excitation plates can increase the kinetic
419 energy of ions at selected m/z values for CID and subsequent MSⁿ experiments can be carried
420 out (19).

421 The Orbitrap instrument is the newest high resolution MS. The first practical orbital
422 trapping instrument, used purely for ion trapping was first devised by Kingdon in 1923 (20).
423 Later, in 1981 Knight produced a modified trap device that improved upon the instrument
424 proposed by Kindgon (21). It wasn't until 2000 that Makarov demonstrated with an early orbital
425 trapping instrument that the orbitrap could be used as a MS (22). Figure 1-4 shows that the
426 Orbitrap consists of a Saturn shaped central electrode that is slim at both ends, but converges into
427 a slightly larger diameter at its center. The central electrode is surrounded by two symmetrical
428 electrodes (22-24). Ions enter the Orbitrap off axis from the center rod's equatorial position and
429 are allowed to settle into ring-like orbits around the rod. The rings oscillate back and forth over
430 the electrode at a frequency dependent upon their m/z. The current image of the charged rings is
431 recorded by the split outer electrodes and converted into signal amplitude vs time. The spectrum
432 is converted via Fourier transform into intensity vs frequency, and then the plot is inverted into
433 intensity vs m/z (22-24).

434

435 Detectors

436 One of the most important, but least appreciated components of a MS is the detector. The
437 electron multiplier (EM) is the most widely used detector for biological TOF and quadrupole MS
438 instruments. A conventional EM detector for many scanning quadrupole instruments is
439 comprised of a dynode that is positioned to collect the ions of interest from the MS. The EM is
440 built with many dynodes, each subsequent dynode has a lower voltage until terminating with an
441 anode (25). The ions that hit the dynode release secondary electrons from the initial collision
442 producing a cascade of electrons. The cascade then reaches the detector anode which converts
443 the electron current into signal to be analyzed. EM detectors are useful for biological
444 instruments because scanning across a spectrum may provide few ions for detection. The EM
445 amplifies the signal and allows low ion counts to be recorded. A negative aspect of EM
446 detectors is the ability for loss of signal linearity when the detector is saturated with too many
447 ions and the secondary electron cascade overwhelms the anode (25).

448 For TOF instruments a different EM detector called the microchannel plate (MCP) is a
449 popular choice. The MCP is a thin disk that consists of numerous parallel semiconducting
450 channels that traverse the plate. As an ion hits the entrance of the cavity, secondary electrons are
451 released and start a cascade down the detector (25, 26). It also has provides an extremely fast
452 response time. However, there are many downsides to MCP detectors. If an ion hits a cavity, it
453 drains the electron density of adjacent cells for several microseconds (26). If another ion hits at
454 the same point within that period it is not counted, and causes decreased detection linearity.
455 Lastly, MCP plates are relatively fragile and must be handled carefully and maintained in low
456 pressure conditions.

457 Cryogenic detectors are another detector variant useful for biological TOF MS
458 instruments. The cryogenic detector measures the thermal energy produced by ions impinging
459 upon a superconducting film (26). They have been used successfully in TOF devices to measure
460 extremely large molecules greater than a MDa (27). Cryogenic detectors also have the capability
461 of discerning the charge of large molecular species (25, 26). The cryogenic detector has a major
462 downside; the detector must be maintained at very low temperature (~2 K). Despite the
463 difficulties with combining an MS instrument to a cryogenic detector, a commercial matrix
464 assisted laser desorption ionization (MALDI) TOF instrument called the “macromizer” has been
465 produced (25).

466 MS instruments that utilize image-current detectors have begun to be used heavily for
467 biological MS. As described above, the image-current devices detect ion frequencies between
468 two electrodes as they oscillate in an ion trap. The major benefits to image-current devices are
469 due to their ruggedness, high resolution, and non-destructive ion analysis. The downsides are
470 that FT-ICR instruments must be cryogenically cooled and have space charge constraints. The
471 major downsides to Orbitrap instrument are a) space charge concerns, and b) acquisition times
472 can be greater than a second to obtain high accuracy and resolution.

473

474 *Separation Techniques Coupled to Mass Spectrometry*

475 From the 1920’s until the 1950’s mass spectrometry was pivotal for many important
476 breakthroughs to better understanding elemental ions and simple molecular ions. It wasn’t until
477 1955, at the Dow Chemical Company, that MS got a new wind when gas chromatography (GC)
478 device and MS were coupled together (28). The pairing of these two devices showed that by
479 applying a separation prior to analysis that compound identities and quantitative measurements

480 could be made. Since then a multitude of separation techniques have been coupled to MS. The
481 following are brief discussions of the major separation techniques paired with MS for biological
482 analysis.

483

484 Gas Chromatography

485 The GC excels at separating a wide variety of volatile compounds (29). Samples are
486 primarily dissolved and prepared in volatile solvents. The solvent is then injected by syringe into
487 a heated port that vaporizes the solvent along with the dissolved analytes. The sample then flows
488 through an oven-heated fused silica capillary tube that is commonly coated or filled with a
489 stationary phase (30). The stationary phase is a material that has the potential to interact with the
490 various analytes based on its unique side-group specificity (30). If an analyte interacts with the
491 stationary phase it is apt to flow more slowly than other analytes, thus allowing a separation to
492 occur. As the analytes leave the column they are directed to the MS. If the separation has been
493 performed adequately, the individual compounds can be identified in order of retention without
494 overlap using electron impact ionization (EI) described below.

495

496 Liquid Chromatography

497 For separating compounds which are high molecular weight, non-volatile, or unstable at
498 high temperatures, liquid chromatography (LC) is a favorable technique (31). Sample
499 preparation is generally simple. A sample can either be prepared by extraction from a biological
500 material, or by dissolving desired compounds into the appropriate solvent. The sample “plug” is
501 then injected into the LC solvent flow that runs through the system. The solvent flow is set to a
502 certain pressure, temperature, and solvent gradient prior to reaching the column (31). With basic

503 reverse-phase LC setups, the column is generally packed with porous silica particles that are
504 typically 2 to 50 μm and bonded with C₁₈ stationary phase. The sample analytes interact with the
505 stationary phase and the polar compounds pass through the column more quickly than the non-
506 polar compounds which interact strongly with the stationary phase (31). Commonly, a solvent
507 gradient that gradually increases the concentration of less-polar solvent is utilized. As the LC
508 solvent becomes more concentrated with a less-polar solvent, the interaction of the analyte with
509 the mobile phase increases, while the interaction of the analyte with the stationary phase is
510 lessened. This allows for faster run times and better resolution of eluent peaks (31). After
511 separation, the analytes must be converted to the gas phase for MS detection. Electrospray
512 ionization (ESI) is a common method of interfacing LC and MS and is discussed below.

513 LC excels in the breadth of the analytes it can separate. It can separate the smallest of
514 dissolved chemical species to extremely high molecular weight proteins. To improve and speed
515 up the separation of analytes there are mainly three improvements applied to LC. The first is to
516 alter the stationary phase bead. By decreasing the size of the bead the surface area is increased
517 to allow analyte interaction (31). However, the beads are also porous and dwell time is an issue.
518 The interaction can be improved by using a solid core and porous coating to decrease the dwell
519 time (32). The second is to utilize high pressure instrumentation that reduces dead volume and
520 allows the sample to move quickly through a column and decrease longitudinal band broadening
521 (31). Also, high pressure instrumentation is important with smaller stationary phase beads, as
522 new volume flow constraints are produced. The third is the use of specialized stationary phases
523 for enhanced separation for specific analytes. In the case of chiral separation, a special chiral
524 stationary phase must be used to provide an interaction that separates the nearly identical
525 analytes (33).

526 For basic protein analysis by gel filtration/size exclusion chromatography, a porous gel
527 stationary phase is utilized to separate the proteins based on shape and size (34). Larger proteins
528 elute first, while smaller proteins dwell in the pores and thus elute more slowly. Along with the
529 pore-size, varying types of stationary phase can be entrapped within the gel to interact with the
530 protein functional groups to further enhance the separation.

531

532 **Ion Mobility Spectrometry**

533 For complex biological mixtures, ion mobility spectrometry (IMS) has the capability to
534 separate a variety of compounds, for example, isomeric reverse peptides, proteins by charge
535 state, and large protein complexes (35-37). IMS in conjunction with MS can provide important
536 structural information about gas-phase biomolecular ions (38, 39). A variety of many
537 conformation-based biomolecular studies have utilized IMS MS to probe protein folding,
538 oligosaccharide characterization, and even determine whether proteins retain solution phase
539 characteristics in the gas phase (36, 40-47).

540 Commonly, IMS utilizes a drift tube. The drift tube is filled with a buffer gas, typically
541 He, and has a uniform electric field applied axially down the drift tube. As an ion moves through
542 the drift tube its drift time through the IMS device is related to the number of collisions with
543 buffer gas, the electric field applied, its initial velocity, and the length of the drift tube (48). This
544 relation allows ions to be separated based upon their charge state and size. Ions which are highly
545 charged traverse the drift tube faster than low charge state ions. Ions which are compact have
546 fewer collisions with the buffer gas and traverse the drift tube more quickly than those with
547 elongated conformations.

548 Recently, another form of IMS, called traveling wave IMS has been utilized. A
549 photograph of a traveling wave device is shown in Figure 1-5. Figure 1-6 shows a diagram of
550 travelling wave IMS separation. Traveling wave IMS follows the same principles of basic IMS
551 by separating by charge and size, however it utilizes time varying AC symmetrical potential
552 waves for separation (49). The wave speed and wave amplitude can both be modulated to
553 produce a desired separation of ions. The separation can be visualized by thinking of ions as
554 buoys on the ocean. A small buoy will not have the ability to crest a wave that washes over it
555 and will be taken along with the wave. Larger buoys will crest the wave and propagate more
556 slowly. Based upon this separation method smaller, and highly charged ions are carried further
557 per wave event than larger less charged ions and thus produce a sizable separation after many
558 wave events.

559

560 *Ionization Techniques*

561 The field of mass spectrometry relies heavily on the production of ions. Because of the
562 various properties inherent to each analyte compound, the production of ions can be one of the
563 most difficult and frustrating aspects of mass spectrometry. Compounds which do not have such
564 satisfactory side-groups have to be ionized using various high energy ionization techniques, such
565 as, electron ionization (EI), which is discussed further below. A great number of ionization
566 techniques exist for mass spectrometry, some extremely specialized for the production of a
567 specific ion species.

568

569

570

571 Electron Ionization

572 The ionization method EI was the first major biological ionization method, and is still
573 one of the most popular (50). It was first used by Dempster (51) and was further developed by
574 Nier (52). Currently, EI is the most commonly used ion source utilized with GC-MS
575 instruments. GC excels at volatilizing complex solvent mixtures prior to the column for
576 selective separation, and then injection to the EI source for ionization (53). The EI source
577 requires that an analyte vapor is passed through a reduced pressured chamber that crosses an
578 electron beam produced by a tungsten or rhenium filament (50). The electron beam is most
579 commonly tuned to approximately 70 eV for optimal analyte ionization (54). The ionization
580 process causes the neutral analyte molecule to lose an electron through a molecule/electron
581 collision interaction (50). The ionization process is very energetic and it is common that the ion
582 produced is unstable and fragments into smaller ionized species. Due to the large number of
583 highly energetic ions produced from an analyte, fragmentation is extensive and a nearly complete
584 distribution of the analyte's unique structural characteristics can be elucidated from the mass
585 spectrum (50). The mechanism of analyte ionization by EI is deceptively complex and has been
586 thoroughly described elsewhere (55).

587

588 Electrospray Ionization

589 Electrospray ionization (ESI), unlike EI, is a “soft” ionization technique which rarely
590 causes large scale fragmentation of analyte molecules. ESI is also a much more selective
591 ionization method than EI. ESI negative and positive ion production is most commonly centered
592 around the abstraction or addition of protons to the analyte, respectively. Because of this
593 reliance on protons for ionization, ESI is typically useful for protein and peptide analytes due to

594 the abundance of acidic and basic side groups. Regular ESI consists of a solvent system that
595 includes the analyte of interest. The solvent is pumped through a capillary at flow rates of 1 to
596 100 μ L/min, along with an applied voltage to the solution of approximately 2 to 5 kV. As the
597 solution is electrically charged, a gradient is produced within the capillary and a Taylor cone is
598 produced as the solution is expelled (56). The excess charge in the solution migrates to the
599 exterior of the solvent. As the charge builds upon the surface of the solvent, droplets are
600 expelled from the Taylor cone in a stream. The rate of the droplet formation increases until the
601 Rayleigh limit, where the positive and negative charge hit equilibrium in conjunction with the
602 surface tension of the solution. The highly charged droplets burst repeatedly as the repulsive
603 charge splits the droplets apart until only gas phase ions of the analyte remain. Due to the excess
604 charge placed within each droplet, it is common for peptides or protein analyte ions of multiple
605 charge states to be produced.

606 In many situations only very small samples of protein or peptides are available for
607 analysis. A popular form of ESI that accommodates this scenario is nano-ESI. The flow rates
608 utilized for nano-ESI are substantially lower, approximately 10 to 40 nL/min. The inner
609 diameter of the capillary used for nano-ESI is also significantly decreased to 200 nm, in
610 comparison to 1 to 2 μ m for ESI (57). The combination of the low flow rate and the decreased
611 capillary size typically allows nano-ESI to produce finer droplets than ESI, which accounts for
612 the generally more stable spray observed with nano-ESI.

613

614 Laser Desorption/Ionization

615 MALDI is a popular technique to ionize biological analytes. Typically proteins or
616 peptides are ionized using MALDI, but many other biological compounds can also be ionized.

617 The matrix is the key player in the ionization of the analyte. MALDI matrices are usually
618 organic acids, such as 2,5-dihydroxybenzoic acid (DHB) or α -cyano-4-hydroxycinnamic acid
619 (CHCA) that absorb the wavelength of light emitted by a UV laser (58, 59). The sample
620 preparation entails co-crystallization of the analyte with the matrix at a ratio that can be as high
621 as 1000:1 matrix to analyte. During analysis, the laser irradiates the sample, the matrix absorbs
622 the light and causes a small desorption event that releases matrix and analyte. The energetically
623 excited matrix donates or abstracts a proton from the analyte causing it to become ionized. The
624 analyte is usually singly charged, but in some instances, MALDI ions are doubly charged (60).
625 The basic understanding of the matrix and analyte ionization is relatively well understood;
626 however, the exact mechanism of the charge transfer from the matrix to analyte is still uncertain
627 (61-63).

628 MALDI is a powerful ionization technique for biological sample analysis; but, it has a
629 few major disadvantages. Some of the most glaring issues lie with the matrix. The matrix, as
630 described previously, must be used in amounts that are much higher than the analyte. Since the
631 matrix is ionized along with the analyte, it is common for large background signals from matrix
632 and its fragment ions to drown out low molecular weight (M_r) analytes. Careless MALDI
633 sample preparation commonly produces homogenous crystals that are not co-crystallized with
634 the analyte, thus producing poor analyte ionization, reproducibility, and signal stability. Some
635 analyte compounds, such as small nonpolar lipids, will not co-crystallize at all with traditional
636 MALDI matrix and produce poor signal quality. Last, MALDI most often performs best at
637 modest vacuum pressures (~ 1 torr). At these pressures it is common to lose many volatile
638 analytes of interest prior to sample analysis.

639 Because of complications with MALDI discerning volatile analytes, atmospheric pressure
640 laser desorption (AP LDI) has gained popularity (64, 65). Imaging of biological tissues has been
641 popular for MALDI, but a great deal of focus has been placed on AP LDI because of the
642 potential to observe both volatile and nonvolatile analytes (66-70). However, AP LDI has a
643 variety of negative aspects. Because AP LDI is performed at atmospheric conditions, ionization
644 and sensitivity are significantly reduced in comparison to MALDI. At atmospheric pressure, an
645 ion encounters countless collisions with the gases in the atmosphere. Many of these atmospheric
646 components will buffer the ions from reaching the MS source, or scavenge the charge from the
647 ion itself. It is a highly unlikely event that ions from AP LDI will reach the MS. To remedy
648 these issues, a variety of post ionization techniques have been developed. Laser ablation
649 electrospray ionization (LAESI), ablates large portions of sample, then utilizes ESI to ionize
650 neutral analyte from the ablation plume (71, 72). Electrospray assisted desorption/ionization
651 (ELDI) uses low laser power to desorb analyte from a sample and then uses ESI to post ionize,
652 similarly to LAESI (73). Laser ablation atmospheric pressure photoionization (LA APPI) ablates
653 the sample, and as it is liberated a vacuum UV lamp is used to assist in ionizing UV absorbing
654 analyte molecules (74). APPI post ionization can be utilized as a secondary ionization method
655 when a UV absorbing dopant, such as toluene is used. This dopant can absorb the UV light,
656 ionize, and then collide and transfer charge to the analyte before it enters the MS.

657

658 *Mass Spectrometry for Proteomics*

659 MS is a powerful tool that has been used to assist in the identification of proteins. The
660 first step to comprehensively identify a protein is to use the M_r . High resolution MS
661 instrumentation and the use of deconvolution can assist in the determination of a protein M_r ;

662 however, due to the complexity of proteins, it is not possible to accurately identify the protein's
663 primary sequence. A common and more involved method of using MS to identify the primary
664 sequence of a protein is bottom-up proteomics. Generally, a purified unknown protein is
665 subjected to a proteolytic digestion that lyses the protein into peptide fragments. The digest is
666 then analyzed using LC-MS, or LC-MS/MS for a more complete view of the protein sequence
667 (75). The LC separation allows for separation of isobaric peptides prior to MS/MS analysis.
668 MS/MS is performed using collision-induced dissociation (CID). CID is performed in a
669 multipole and contains a collision gas of N₂ or Ar. The peptide ions are accelerated within the
670 multipole and will fragment as they strike the collision gas, resulting in b- and y-ion fragments
671 (76). Through the use of various software and databases, the fragment ion information can be
672 used with M_r to determine the de novo sequence of the protein (77-79).

673 A more recent method is top-down proteomics developed by McLafferty et al. (80) The
674 whole protein is introduced into the instrument and each of the charge states is isolated and
675 dissociated. The accurate mass of the parent protein and the fragments are then scrutinized and
676 the protein is identified. The main benefit to top-down proteomics is that there is little sample
677 preparation; however, a specialized high-resolution instrument that can isolate and dissociate
678 proteins is necessary. Top-down proteomic techniques have shifted, and the most common are
679 electron transfer dissociation (ETD) (81) and electron capture dissociation (ECD) (82-84). In
680 ETD an ion/ion reaction occurs as the protein is trapped in the instrument with a radical anion,
681 such as azobenzene ($[(C_6H_5)_2N_2]^{-\bullet}$). The radical anion trapped with the protein donates the spare
682 electron to the protein cation, which destabilizes the protein backbone and causes it to fragment.
683 ECD accomplishes the same fragmentation mechanism as ETD, yet uses free electrons captured

684 and trapped with the proteins. Since ETD and ECD fragment through a different mechanism
685 than CID, the fragments produced are c- and y-ions (64).

686

687 *Mass Spectrometry for Metabolomics*

688 Metabolomics is currently considered the final major “omics”. Metabolomics does not
689 neatly fit within the same categorical structure as the other “omics”, such as genomics,
690 transcriptomics, and proteomics which study DNA, all forms of RNA, and proteins, respectively.
691 The first three “omics” encompass only characterizing the nucleic acids and the combination of
692 the 22 amino acids. However, metabolomics encompasses all compounds which are produced
693 by living cells. Because of this broad classification, and the wide variety of compounds that can
694 be observed as metabolites, metabolomics is a still growing and very complex field of biology.

695 There are two forms of metabolomics that are generally utilized. The first is targeted
696 analysis, where the identification and quantification of metabolites have been pre-selected prior
697 to the analysis (85). Targeted analysis is used often for drug or chemical studies where a
698 pathway is understood and the metabolites of that drug have been identified. The second is
699 metabolite profiling, which is the indiscriminate analysis of all metabolite compounds observable
700 using a particular analytical technique (85).

701 MS is useful for both targeted analysis and metabolite profiling. Targeted analysis of a
702 specific metabolite can be performed using the appropriate form of chromatography with the
703 proper MS instrumentation. However, metabolite profiling requires complex chromatography
704 and MS instrumentation that is suitable to observe a wide range of metabolites. FT-ICR MS is
705 popular for metabolite profiling because of its high resolution (86). Ultra-high resolution FT-
706 ICR MS can observe all ionized metabolites using direct infusion. Broad profiling by FT-ICR

707 MS can roughly identify metabolites using accurate mass measurements, but it does not have the
708 ability to discern isomers or isobaric ions. LC-TOF MS has recently grown into a technique
709 which can perform metabolite profiling (87). The draw to LC-TOF MS recently is due to the
710 increasingly high resolutions (~30,000) available and the fast scan speeds. By separating
711 metabolites and observing metabolites over time, the TOF MS is not hampered by its lower
712 resolution and can profile metabolites by accurate mass similar to FT-ICR MS. LC separation
713 can also be utilized to assist in accurate mass identification if retention times of known
714 metabolite standards are aligned with the retention times of the unknown sample metabolites.
715 GC-TOF MS is extremely useful for profiling derivatized or volatile metabolites (85). A major
716 benefit to GC is that it allows for the complete identification of the profiled metabolites through
717 the use of GC libraries.

718

719 Fourier Transform Infrared Spectroscopy

720 For comprehensive characterization of biological materials, such as proteins, lipids, and
721 carbohydrates it is amenable to utilize other analytical techniques that complement MS. MS
722 excels at inferring information from individual ions, techniques such as Fourier Transform
723 Infrared Spectroscopy (FTIR) analyze the entire sample simultaneously and infer information
724 from all of the analyte species.

725 The layout of the common double-beam interferometer, which most FTIR instruments
726 use today, was developed in 1891 by Michelson (88). For a detailed explanation of how the
727 Michelson interferometer is configured and produces an interferogram, please see Griffiths and
728 de Haseth (88). The interferogram produced by the two-beam instrument is transformed using
729 Fourier transform computation to produce an FTIR spectrum (88).

730 FTIR instrumentation has evolved greatly since the introduction of the Michelson
731 interferometer. After Michelson designed the interferometer and introduced the interferogram,
732 he showed using FT spectroscopy that they could discern the structures of atomic lines.
733 However, due to lack of computational resources, interferometry was not widely used for nearly
734 50 years. In the 1950's Fellgett showed that all spectral information was simultaneously
735 recorded by the interferogram. This was a huge informational advantage to the interferogram,
736 especially in IR (88). Soon after, Jacquinot determined that the maximum solid angle of
737 collimated light passed through an interferometer was greater than the same beam used with a
738 prism or grating in a monochromator (88). In the 1960's FTIR gained traction with the
739 introduction of compact computers and reliable lasers. The small lab-sized computers allowed
740 for computational processing of the interferogram just after analysis. The laser allowed for
741 precise measurements of the mirror position at equal time intervals, which produces an internal
742 standard for the wavenumber for all measurements (88).

743 As FTIR was able to take hold as a suitable lab technique, many other techniques that
744 utilize FTIR have been introduced to study biological samples. A common FTIR technique
745 employed is transmission FTIR. The technique measures the amount of IR radiation that is
746 absorbed by a sample as IR radiation is modulated over the spectral range of interest. The FT
747 transformed output describes the bulk properties of the sample material (89). Other sample
748 specific FTIR methods are specular reflection spectroscopy, attenuated total reflectance
749 spectroscopy, diffuse reflectance spectroscopy, and photoacoustic spectroscopy.

750 Due to its unique ability to be paired with nearly any sample type, photoacoustic
751 spectroscopy was utilized in Chapter 4 of this dissertation, and will be described more fully in
752 the next section.

753 *Fourier Transform Infrared-Photoacoustic Spectroscopy*

754 Fourier transform infrared-photoacoustic spectroscopy (FTIR-PAS) is an absorption
755 method. PAS is based on the photoacoustic effect, which was first described by Alexander
756 Graham Bell (90). He was able to successfully demonstrate the effect with his “spectrophone”
757 (91). It would take nearly a century until PAS would gain popularity again. In the 1980’s as
758 FTIR use increased, PAS proved to be a natural pairing with the innate IR modulation and
759 multiplex advantage.

760 FTIR-PAS can be applied to nearly any solid or semi-solid material (92). This gives
761 FTIR-PAS a large advantage over transmission spectroscopy and reflective spectroscopy
762 methods, which must be used with select sample types. FTIR-PAS also needs very little sample
763 preparation and is non-destructive, the sample must merely fit within the PA sample cell. It
764 performs well with opaque, dark, and highly scattering materials. This is possible because FTIR-
765 PAS does not detect IR radiation; rather it detects the heat produced by the absorption of the IR
766 radiation by the sample. PAS is performed generally with a PAS accessory, shown in Figure 1-
767 7. The PAS cell is placed within a suitable FTIR instrument. The accessory consists of a sealed
768 cell that has been purged with helium gas. The sample material is placed within the cell under a
769 salt window which passes IR radiation. The modulated IR radiation produced by the FTIR
770 passes through the window and impinges upon the sample material. As a discrete wavelength of
771 IR radiation illuminates the sample, the sample will heat if the respective IR radiation is
772 absorbed. Rapidly, the heat will evolve from the sample and produce a pressure wave within the
773 cell. The resultant sound waves are detected by a sensitive microphone and the FTIR and
774 microphone will produce an absorption spectrum usually in the IR range (93, 94). For a
775 thorough explanation of the PAS theory please see the article of Rosencwaig and Gersho (92).

776 *FTIR-PAS Utilized for Biological Materials*

777 Most FTIR techniques work well characterizing individual analyte compounds; however,
778 many fail when confronted with complex biological mixtures. FTIR-PAS works well with these
779 tough samples because tissues can be dried, ground, and then placed directly within the
780 accessory with little prep and can be reused for another methodology. For the analysis of these
781 complex biological mixtures, the pairing of FTIR-PAS and chemometrics is ideal to assist with
782 qualitative and quantitative analysis. Currently, FTIR-PAS is attracting the most attention as a
783 complement to magnetic resonance imaging (MRI) for microscopic imaging of tissues (95-97).

784 Mid-IR FTIR-PAS has become popular in the food science field. It has been employed to
785 analyze intact tissue samples of beef and pork (98). FTIR-PAS has been used to analyze cheddar
786 cheese and the packaging of the cheese (99). The analysis of the cheese using the depth profiling
787 properties of FTIR-PAS showed that moisture was lost near the surface of the cheese, also lipids
788 and proteins were found to migrate into the packaging itself. FTIR-PAS has been able to
789 differentiate between organic and conventional coffee varieties (100). The method has been
790 shown to quantitatively measure the amount of lipid in chocolate (101). FTIR-PAS can glean
791 viable information using an extremely small amount of sample. One study using peas was able
792 to determine total starch, total lipid, and total protein, while using such small amount of sample
793 that the peas were still viable (102). Chapter 4 of this dissertation expanded on the utilization of
794 FTIR-PAS for biological materials. It was used to quantitatively and qualitatively measure
795 resistant starch in unfractionated rat cecal contents for the first time.

796

797

798

799 **Dissertation Overview**

800 This dissertation focuses on the analysis of plant and animal extracts utilizing MS and
801 FTIR-PAS. Chapter 2 details the use of high resolution TOF MS to analyze metabolites
802 extracted from rat cecal and distal colon contents. The goal of the study is to determine whether
803 rats fed four different starch diets have metabolic profiles that could be considered significantly
804 different using partial least squares-discriminate analysis (PLS-DA) software. Chapter 3 delves
805 into a comprehensive identification of alpha-zein proteins using LC separation coupled to a high
806 resolution TOF MS. This is the first study to have comprehensively identified alpha-zein
807 proteins with accurate mass capabilities. The study aims at determining whether alpha-zein
808 protein extract profiles are different when extracted from corn gluten meal and dried distillers
809 grains with solubles in combination with varying extraction conditions. Chapter 4 revisits the
810 analysis of rat cecal and distal colon contents; however, the analysis focuses on starch
811 determination utilizing FTIR-PAS. Many starch analysis techniques are time consuming and
812 expensive, FTIR-PAS is explored to speed up analysis time and decrease cost on large sample
813 runs. FTIR-PAS spectra of the cecal and distal colon contents are processed using PLS to
814 determine quantitative starch values and principal component analysis (PCA) is applied to
815 determine qualitative starch differences.

816

817

818

819

820

821

822 **References**

- 823 1. Griffiths, I. W. J. J. Thomson-the centenary of his discovery of the electron and of his
824 invention of mass spectrometry. *Rapid Commun. Mass Sp.* **1997**, *11*, 2-16.
- 825 2. *Measuring mass: from positive rays to proteins*, Grayson, M. A., Ed.; Chemical Heritage
826 Press: Philadelphia, PA, **2002**.
- 827 3. Friedburg, H.; Paul, W. Optische abbildung mit neutralen atomen. *Naturwissenschaften*
828 **1951**, *38*, 159-160.
- 829 4. Bennewitz, H. G.; Paul, W. Eine method zur bestimmung von kernmomenten mit
830 fokussiertem atomstrahl. *Z. Phys.* **1954**, *139*, 489.
- 831 5. Bennewitz, H. G.; Paul, W. Fokussierung polarer molecule. *Z. Phys.* **1955**, *141*, 6.
- 832 6. Giese, C. F. Strong focusing ion source for mass spectrometry. *Rev. Sci. Instrum.* **1959**,
833 *30*, 260-261.
- 834 7. Paul, W. Electromagnetic traps for charged and neutral particles. *Rev. Mod. Phys.* **1990**,
835 *62*, 531-540.
- 836 8. Yost, R. A.; Enke, C. G. Triple quadrupole mass spectrometry for direct mixture analysis
837 and structure elucidation. *Anal. Chem.* **1979**, *51*, 1251A-1264A.
- 838 9. Douglas, D. J.; Aaron, J. F.; Dunmin, M. Linear ion trap in mass spectrometry. *Mass*
839 *Spectrom. Rev.* **2005**, *24*, 1-29.
- 840 10. Stephens, W. E. A pulsed mass spectrometer with time dispersion. *Phys. Rev.* **1946**, *69*,
841 691.
- 842 11. Cameron, A. E.; Eggers, D. F. An ion “velocitron”. *Rev. Sci. Instrum.* **1948**, *19*, 605-607.
- 843 12. Mamyrin, B. A.; Karataev, V. I.; Shmikk, D. V.; Zagulin V. A. The mass-reflectron, a
844 new nonmagnetic time-of-flight mass spectrometer with high resolution. *Sov. Phys. -*
845 *JETP*. **1973**, *37*, 45-48.
- 846 13. Chernushevich, I. V.; Loboda, A. V.; Thomson, B. A. An introduction to quadrupole-
847 time-of-flight mass spectrometry. *J. Mass Spectrom.* **2001**, *36*, 849-865.
- 848 14. Tito, M. A.; Tars, K.; Valegard, K.; Hajdu, J.; Robinson, C. V. Electrospray time-of-
849 flight mass spectrometry of the intact ms2 virus capsid. *J. Am. Chem. Soc.* **2000**, *122*,
850 3550-3551.
- 851 15. Wang, T.-I.; Chu, C.-W.; Hung, H.-M; Kuo, G.-S.; Han, C.-C. Design parameters of
852 dual-stage ion reflectrons. *Rev. Sci. Instrum.* **1994**, *65*, 1585-1589.
- 853 16. Dodonov, A. F.; Kozlovski, V. I.; Soulimenkov, I. V.; Raznikov, V. V.; Loboda, A. V.;
854 Zhen, Z.; Horwath, T.; Wollnik, H. High-resolution electrospray ionization orthogonal-
855 injection time-of-flight mass spectrometry. *Eur. J. Mass Spectrom.* **2000**, *6*, 481-490.
- 856 17. Marshall, A. G. Fourier transform ion cyclotron resonance mass spectrometry. *Acc.*
857 *Chem. Res.* **1985**, *18*, 316-322.
- 858 18. Comisarow, M. B.; Marshall, A. G. Fourier transform ion cyclotron resonance
859 spectroscopy. *Chem. Phys. Lett.* **1974**, *25*, 282-283.
- 860 19. Marshall, A. G.; Hendrickson, C. L.; Jackson, G. S. Fourier transform ion cyclotron
861 resonance mass spectrometry: a primer. *Mass Spectrom. Rev.* **1998**, *17*, 1-35.
- 862 20. Kingdon, K. H. A method for the neutralization of electron space charge by positive
863 ionization at very low gas pressures. *Phys. Rev.* **1923**, *21*, 408-418.
- 864 21. Knight, R. D. Storage of ions from laser-produced plasmas. *Appl. Phys. Lett.* **1981**, *38*,
865 221-223.
- 866 22. Makarov, A. Electrostatic axially harmonic orbital trapping: a high-performance
867 technique of mass analysis. *Anal. Chem.* **2000**, *72*, 1156-1162.

868 23. Hardman, M.; Makarov, A. A. Interfacing the orbitrap mass analyzer to an electrospray
869 ion source. *Anal. Chem.* **2003**, *75*, 1699-1705.

870 24. Hu, Q.; Noll, R. J.; Li, H.; Makarov, A.; Hardman, M.; Cooks, R. G. The orbitrap: a new
871 mass spectrometer. *J. Mass. Spectrom.* **2005**, *40*, 430-443.

872 25. Koppenaal, D. W.; Barinaga, C. J.; Denton, M. B.; Sperline, R. P.; Hieftje, G. M.;
873 Schilling, G. D.; Andrade, F. J.; Barnes, J. H. MS detectors. *Anal. Chem.* **2005**, *77*, 419A-
874 427A.

875 26. Westman-Brinkmalm, A.; Brinkmalm, G. A mass spectrometer's building blocks. In
876 *Mass spectrometry: instrumentation, interpretation, and applications*, Elkman, R.;
877 Silberring, J.; Westman-Brinkmalm, A.; Kraj, A., Eds.; John Wiley & Sons: Hoboken, NJ,
878 **2009**; pp 15-71.

879 27. Wenzel, R. J.; Matter, U.; Schultheis, L.; Zenobi, R. Analysis of megadalton ions using
880 cryodetection MALDI time-of-flight mass spectrometry. *Anal. Chem.* **2005**, *77*, 4329-
881 4337.

882 28. Gohlke, R. S.; McLafferty, F. W. Early gas chromatography/mass spectrometry. *J. Am. Soc. Mass Spectrom.* **1993**, *4*, 367-371.

883 29. *Handbook of instrumental techniques for analytical chemistry*, Settle, F. A. Ed.; Prentice
884 Hall: Upper Saddle River, NJ, **1997**.

885 30. McNair, H. M.; Miller, J. M. *Basic gas chromatography*, 2nd ed.; Wiley-Interscience:
886 Hoboken, NJ, **2009**.

887 31. Snyder, L. R.; Kirkland, J. J.; Dolan, J. W. *Introduction to modern liquid chromatography*, 3rd ed.; Wiley: Hoboken, NJ, **2010**.

888 32. Coutinho, F. M. B.; Carvalho, D. L.; La Torre Aponte, M. L.; Barbosa, C. C. R.
889 Pellicular ion exchange resins based on divinylbenzene and 2-vinylpyridine. *Polymer*
890 **2001**, *42*, 43-48.

891 33. Pirkle, W. H.; Pochapsky, T. C. Consideration of chiral recognition relevant to the liquid
892 chromatographic separations of enantiomers. *Chem. Rev.* **1989**, *89*, 347-362.

893 34. Janson, J.-C.; Jönsson, J. Å. Introduction to chromatography. In *Protein purification: principles, high resolution methods, and applications*, 3rd ed.; Janson, J.-C., Ed.; John
894 Wiley & Sons: Hoboken, NJ, **2011**; pp 25-50.

895 35. Wu, C.; Siems, W. F.; Klasmeier, J.; Hill, H. H. Separation of isomeric peptides using
896 electrospray ionization/high-resolution ion mobility spectrometry. *Anal. Chem.* **2000**, *72*,
897 391-395.

898 36. Shelimov, K. B.; Clemmer, D. E.; Hudgins, R. R.; Jarrold M. F. Protein structure *in*
899 *vacuo*: gas-phase conformation of BPTI and cytochrome *c*. *J. Am. Chem. Soc.* **1997**, *119*,
900 2240-2248.

901 37. Ruotolo, B. T.; Benesch, J. L. P.; Sandercock, A. M.; Hyung, S.-J.; Robinson, C. V. Ion
902 mobility-mass spectrometry analysis of large protein complexes. *Nat. Protoc.* **2008**, *3*,
903 1139-1152.

904 38. Wu, C.; Siems, W. F.; Asbury, G. R.; Hill, H. H. Electrospray ionization high-resolution
905 ion mobility spectrometry-mass spectrometry. *Anal. Chem.* **1998**, *70*, 4929-4938.

906 39. Henderson, S. C.; Valentine, S. J.; Counterman, A. E.; Clemmer, D. E. ESI/ion trap/ion
907 mobility/time-of-flight mass spectrometry for rapid and sensitive analysis of
908 biomolecular mixtures. *Anal. Chem.* **1999**, *71*, 291-301.

909

910

911

912 40. Mesleh, M. F.; Hunter, J. M.; Shvartsburg, A. A.; Schatz, G. C.; Jarrold, M. F. Structural
 913 information from ion mobility measurements: effects of the long-range potential. *J. Phys.*
 914 *Chem.* **1996**, *100*, 16082-16086.

915 41. Chen, Y.-L.; Collings, B. A.; Douglas, D. J. Collision cross sections of myoglobin and
 916 cytochrome c ions with Ne, Ar, and Kr. *J. Am. Soc. Mass Spectrom.* **1997**, *8*, 681-687.

917 42. Clemmer, D. E.; Jarrold, M. F. Ion mobility measurements and their applications to
 918 clusters and biomolecules. *J. Mass. Spectrom.* **1997**, *32*, 577-592.

919 43. Hudgins, R. R.; Woenckhaus, J.; Jarrold, M. F. High resolution ion mobility
 920 measurements for gas phase proteins: correlation between solution phase and gas phase
 921 conformations. *Int. J. Mass Spectrom.* **1997**, *165*, 497-507.

922 44. Clemmer, D. E.; Liu, Y. Characterizing oligosaccharides using injected-ion
 923 mobility/mass spectrometry. *Anal. Chem.* **1997**, *69*, 2504-2509.

924 45. Liu, Y.; Valentine, S. J.; Counterman, A. E.; Hoaglund, C. S.; Clemmer, D. E. Injected-
 925 ion mobility analysis of biomolecules. *Anal. Chem.* **1997**, *69*, 728A-735A.

926 46. Shelimov, K. B.; Jarrold, M. F. Conformations, unfolding, and refolding of
 927 apomyoglobin in vacuum: an activation barrier for gas-phase protein folding. *J. Am.*
 928 *Chem. Soc.* **1997**, *119*, 2987-2994.

929 47. Hoaglund, C. S.; Valentine, S. J.; Sporleder, C. R.; Reilly, J. P.; Clemmer, D. E. Three-
 930 dimensional ion mobility/TOFMS analysis of electrosprayed biomolecules. *Anal. Chem.*
 931 **1998**, *70*, 2236-2242.

932 48. *Transport properties of ions in gases*, Mason, E. A.; McDaniel, E. W., Eds.; Wiley: New
 933 York, NY, **1988**.

934 49. Shvartsburg, A. A.; Smith, R. D. Fundamentals of travelling wave ion mobility
 935 spectrometry. *Anal. Chem.* **2008**, *80*, 9689-9699.

936 50. *Practical organic mass spectrometry: a guide for chemical and biochemical analysis*, 2nd
 937 ed.; Chapman, J. R., Ed.; Wiley: New York, NY, **1993**.

938 51. Dempster, A. J. Positive ray analysis of lithium and magnesium. *Phys. Rev.* **1921**, *18*,
 939 415.

940 52. Nier, A. O. A mass spectrometer for isotope and gas analysis. *Rev. Sci. Instrum.* **1947**, *18*,
 941 398.

942 53. Gohlke, R. S. Time-of-flight mass spectrometry and gas-liquid partition chromatography.
 943 *Anal. Chem.* **1959**, *31*, 525-541.

944 54. *Interpretation of mass spectra*, 2nd ed.; McLafferty, F. W., Ed.; University Science
 945 Books: Mill Valley, CA, **1980**.

946 55. Peterkop, R. K. *Theory of ionization of atoms by electron impact*, Translation by
 947 Aronson, E.; Hummer, D. G., Ed.; Colorado Associated University Press: Boulder, CO,
 948 **1977**.

949 56. Taylor, G. Disintegration of water drops in an electric field. *P. R. Soc. London* **1964**, *280*,
 950 383-397.

951 57. Wilm, M.; Mann, M.; Analytical properties of the nanoelectrospray ion source. *Anal.*
 952 *Chem.* **1996**, *68*, 1-8.

953 58. Beavis, R. C.; Chaudhary, T.; Chait, B. T. α -Cyano-4-hydroxycinnamic acid as a matrix
 954 for matrix assisted laser desorption mass spectrometry. *Org. Mass Spectrom.* **1992**, *27*,
 955 156-158.

956 59. Kampmeier, J.; Dreisewerd, K.; Schürenberg, M.; Strupat, K. Investigations of 2,5-DHB
 957 and succinic acid as matrices for IR and UV MALDI. Part: I UV and IR laser ablation in
 958 the MALDI process. *Int. J. Mass Spectrom.* **1997**, *169*, 31-41.

959 60. Karas, M.; Glückmann, M.; Schäfer, J. Ionization in matrix-assisted laser
 960 desorption/ionization: singly charged molecular ions are the lucky survivors. *J. Mass*
 961 *Spectrom.* **2000**, *35*, 1-12.

962 61. Karas, M.; Krüger, R. Ion formation in MALDI: the cluster ionization mechanism. *Chem.*
 963 *Rev.* **2003**, *103*, 427-439.

964 62. Glückmann, M.; Pfenninger, A.; Krüger, R.; Thierolf, M.; Karas, M.; Horneffer, V.;
 965 Hillenkamp, F.; Strupat, K. Mechanisms in MALDI analysis: surface interaction or
 966 incorporation of analytes? *Int. J. Mass Spectrom.* **2001**, *210*, 121-132.

967 63. Knochenmuss, R. Ion formation mechanisms in UV-MALDI. *Analyst*, **2006**, *131*, 966-
 968 986.

969 64. Weston, D. J. Ambient ionization mass spectrometry: current understanding of
 970 mechanistic theory; analytical performance and application areas. *Analyst*, **2010**, *135*,
 971 661-668.

972 65. Cooks, R. G.; Ouyang, Z.; Takats, Z.; Wiseman, J. M. Ambient mass spectrometry.
 973 *Science*, **2006**, *311*, 1566-1570.

974 66. Wiseman, J. M.; Ifa, D. R.; Zhu, Y.; Kissinger, C. B.; Manicke, N. E.; Kissinger, P. T.;
 975 Cooks, R. G. Desorption electrospray ionization mass spectrometry: imaging drugs and
 976 metabolites in tissues. *Proc. Natl. Acad. Sci.* **2008**, *105*, 18120-18125.

977 67. Esquenazi, E.; Yang, Y.-L.; Watrous, J.; Gerwick, W. H.; Dorrestein, P. C. Imaging mass
 978 spectrometry of natural products. *Nat. Prod. Rep.* **2009**, *26*, 1521-1534.

979 68. Zimmerman, T. A.; Monroe, E. B.; Tucker, K. R.; Rubakhin, S. S.; Sweedler, J. V.
 980 Imaging of cells and tissues with mass spectrometry: adding chemical information to
 981 imaging. *Method Cell Biol.* **2008**, *89*, 361-390.

982 69. Vickerman, J. C. Molecular imaging and depth profiling by mass spectrometry-SIMS,
 983 MALDI or DESI? *Analyst*, **2011**, *136*, 2199-2217.

984 70. Wiseman, J. M.; Ifa, D. R.; Song, Q.; Cooks, R. G. Tissue imaging at atmospheric
 985 pressure using desorption electrospray ionization (DESI) mass spectrometry. *Angew.*
 986 *Chem. Int. Ed.* **2006**, *45*, 7188-7192.

987 71. Shrestha, B.; Nemes, P.; Nazarian, J.; Hathout, Y.; Hoffman, E. P.; Vertes, A. Direct
 988 analysis of lipids and small metabolites in mouse brain tissue by AP IR-MALDI and
 989 reactive LAESI mass spectrometry. *Analyst*, **2010**, *135*, 751-758.

990 72. Nemes, P.; Vertes, A. Laser ablation electrospray ionization for atmospheric pressure, in
 991 vivo, and imaging mass spectrometry. *Anal. Chem.* **2007**, *79*, 8098-8106.

992 73. Shiea, J.; Huang, M.-Z.; Hsu, H.-J.; Lee, C.-Y.; Yuan, C.-H.; Beech, I.; Sunner, J.
 993 Electrospray-assisted laser desorption/ionization mass spectrometry for direct ambient
 994 analysis of solids. *Rapid Commun. Mass Spectrom.* **2005**, *19*, 3701-3704.

995 74. Vaikkinen, A.; Shrestha, B.; Kauppila, T. J.; Vertes, A.; Kostiainen, R. Infrared laser
 996 ablation atmospheric pressure photoionization mass spectrometry. *Anal. Chem.* **2012**, *84*,
 997 1630-1636.

998 75. Claassen, M. Inference and validation of protein identifications. *Mol. Cell Proteomics*
 999 **2012**, *11*, 1097-1104.

1000 76. Roepstorff, P. Proposal for a common nomenclature for sequence ions in mass spectra of
 1001 peptides. *Biomed. Mass Spectrom.* **1984**, *11*, 601.

1002 77. Dančík, V.; Addona, T. A.; Clauser, K. R.; Vath, J. E.; Pevzner, P. A. *De novo* peptide
1003 sequencing via tandem mass spectrometry. *J. Comput. Biol.* **1999**, *6*, 327-342.

1004 78. Dahiyat, B. I.; Mayo, S. L. De novo protein design: fully automated sequence selection.
1005 *Science* **1997**, *278*, 82-87.

1006 79. Shevchenko, A.; Chernushevich, I.; Ens, W.; Standing, K. G.; Thomson, B.; Wilm, M.;
1007 Mann, M. Rapid '*de novo*' peptide sequencing by a combination of nanoelectrospray,
1008 isotopic labelling and a quadrupole/time-of-flight mass spectrometer. *Rapid Commun.*
1009 *Mass Sp.* **1997**, *11*, 1015-1024.

1010 80. Kelleher, N. L.; Lin, H. Y.; Valaskovic, G. A.; Aaserud, D. J.; Fridriksson, E. K.;
1011 McLafferty, F. W. Top down versus bottom up protein characterization by tandem high-
1012 resolution mass spectrometry. *J. Am. Chem. Soc.* **1999**, *121*, 806-812.

1013 81. Syka, J. E. P.; Coon, J. J.; Schroeder, M. J.; Shabanowitz, J.; Hunt, D. F. Peptide and
1014 protein sequence analysis by electron transfer dissociation mass spectrometry. *Proc. Natl.*
1015 *Acad. Sci.* **2004**, *101*, 9528-9533.

1016 82. Zubarev, R. A.; Horn, D. M.; Fridriksson, E. K.; Kelleher, N. L.; Kruger, N. A.; Lewis,
1017 M. A.; Carpenter, B. K.; McLafferty, F. W. Electron capture dissociation for structural
1018 characterization of multiply charged protein cations. *Anal. Chem.* **2000**, *72*, 563-573.

1019 83. Zubarev, R. A.; Kruger, N. A.; Fridriksson, E. K.; Lewis, M. A.; Horn, D. M.; Carpenter,
1020 B. K.; McLafferty, F. W. Electron capture dissociation and gaseous multiply-charged
1021 proteins is favored at disulfide bonds and other sites of high hydrogen atom affinity. *J.*
1022 *Am. Chem. Soc.* **1999**, *121*, 2857-2862.

1023 84. Zubarev, R. A.; Kelleher, N. L.; McLafferty, F. W. Electron capture dissociation of
1024 multiply charged protein cations. A nonergodic process. *J. Am. Chem. Soc.* **1998**, *120*,
1025 3265-3266.

1026 85. Villas-Bôas, S. G.; Mas, S.; Åkesson, M.; Smedsgaard, J.; Nielsen, J. Mass spectrometry
1027 in metabolome analysis. *Mass Spectrom. Rev.* **2005**, *24*, 613-646.

1028 86. Asharoni, A.; Ric de Vos, C. H.; Verhoeven, H. A.; Maliepaard, C. A.; Kruppa, G.; Bino,
1029 R. Goodenowe, D. B. Nontargeted metabolome analysis by use of Fourier transform ion
1030 cyclotron mass spectrometry. *Omics* **2002**, *6*, 217-234.

1031 87. Ric de Vos C. H.; Moco, S.; Lommen, A.; Keurentjes, J. J. B.; Bino, R. J.; Hall R. D.
1032 Untargeted large-scale plant metabolomics using liquid chromatography coupled to mass
1033 spectrometry. *Nat. Protoc.* **2007**, *2*, 778-791.

1034 88. Griffiths, P. R.; de Haseth, J. A. *Fourier transform infrared spectroscopy*, Elving, P. J.;
1035 Winefordner, J. D.; Kolthoff, I. M., Eds.; John Wiley & Sons: New York, NY, **1986**.

1036 89. Mirabella, F. M. Introduction. In *Modern techniques in applied molecular spectroscopy*,
1037 Mirabella, F. M., Ed.; John Wiley & Sons: New York, **1998**, pp 1-10.

1038 90. Bell, A. G. On the production and reproduction of sound by light. *Am. J. Sci. (Series 3)*
1039 **1880**, *20*, 305-324.

1040 91. Bell, A. G. Upon the production of sound by radiant energy. *Phil. Mag. (Series 5)* **1881**,
1041 *11*, 510-528.

1042 92. Rosencwaig, A.; Gersho, A. Theory of the photoacoustic effect with solids. *J. Appl. Phys.*
1043 **1976**, *47*, 64-69.

1044 93. McClelland, J. F.; Jones, R. W.; Luo, S.; Seaverson, L. M. A Practical Guide to FT-IR
1045 Photoacoustic Spectroscopy. In *Practical Sampling Techniques for Infrared Analysis*,
1046 Coleman, P. B., Ed.; CRC Press: Boca Raton, FL, **1993**; pp 107-144.

1047 94. McClelland, J. F.; Bajic, S. J.; Jones, R. W.; Seaverson, L. M. Photoacoustic
1048 spectroscopy. In *Modern Techniques in Applied Molecular Spectroscopy*, Mirabella, F.
1049 M., Ed.; Wiley-Interscience: New York, NY, **1998**; pp 221-265.

1050 95. *Photoacoustic imaging and spectroscopy*, Wang, L. V., Ed.; CRC Press: Boca Raton, FL,
1051 **2009**.

1052 96. Cox, B.; Laufer, J. G.; Arridge, S. R.; Beard, P. C. Quantitative spectroscopic
1053 photoacoustic imaging: A Review. *J. Biomed. Opt.* **2012**, *17*, No. 061202.

1054 97. Hu, S.; Wang, L. V. Optical-resolution photoacoustic microscopy: auscultation of
1055 biological systems at the cellular level. *Biophys. J.* **2013**, *105*, 841-847.

1056 98. Yang, H.; Irudayaraj, J. Characterization of beef and pork using Fourier-transform
1057 infrared photoacoustic spectroscopy. *Lebensm.-Wiss. Technol.* **2001**, *34*, 402-409.

1058 99. Irudayaraj, J.; Yang, H. Analysis of cheese using step-scan Fourier transform infrared
1059 photoacoustic spectroscopy. *Appl. Spectrosc.* **2000**, *54*, 595-600.

1060 100. Gordillo-Delgado, F.; Marín, E.; Cortés-Hernández, D. M.; Mejía-Morales, C.; García-
1061 Salcedo, A. J. Discrimination of organic coffee via Fourier transform infrared-
1062 photoacoustic spectroscopy. *J. Sci. Food Agric.* **2012**, *92*, 2316-2319.

1063 101. Belton, P. S.; Saffa, A. M.; Wilson, R. H. The potential of Fourier transform infrared
1064 spectroscopy for the analysis of confectionery products. *Food Chem.* **1988**, *28*, 53-61.

1065 102. Letzelter, N. S.; Wilson, R. H.; Jones, A. D.; Sinnaeve, G. Quantitative determination of
1066 the composition of individual pea seeds by Fourier transform infrared photoacoustic
1067 spectroscopy. *J. Sci. Food Agric.* **1995**, *67*, 239-245.

1068 103. Soyk, M. W. Instrumentation development for coupling ion/ion reactions and ion
1069 mobility in biological mass spectrometry. PhD Dissertation. Iowa State University:
1070 Ames, IA, **2008**.

1071 104. Olsen, J. V.; de Godoy, L. M. F.; Li G.; Macek, B.; Mortensen, P.; Pesch, R.; Makarov,
1072 A.; Lange, O.; Horning, S.; Mann, M. Parts per million mass accuracy on an Orbitrap
1073 mass spectrometer via lock mass injection into a C-trap. *Mol. Cell Proteomics* **2005**, *4*,
1074 2010-2021.

1075 105. Giles, K.; Pringle, S. D.; Worthington, K. R.; Little, D.; Wildgoose, J. L.; Bateman, R. H.
1076 Applications of a travelling wave-based radio-frequency-only stacked ring ion guide.
1077 *Rapid Commun. Mass Spectrom.* **2004**, *18*, 2401-2414.

1078

1079

1080

1081

1082

1083

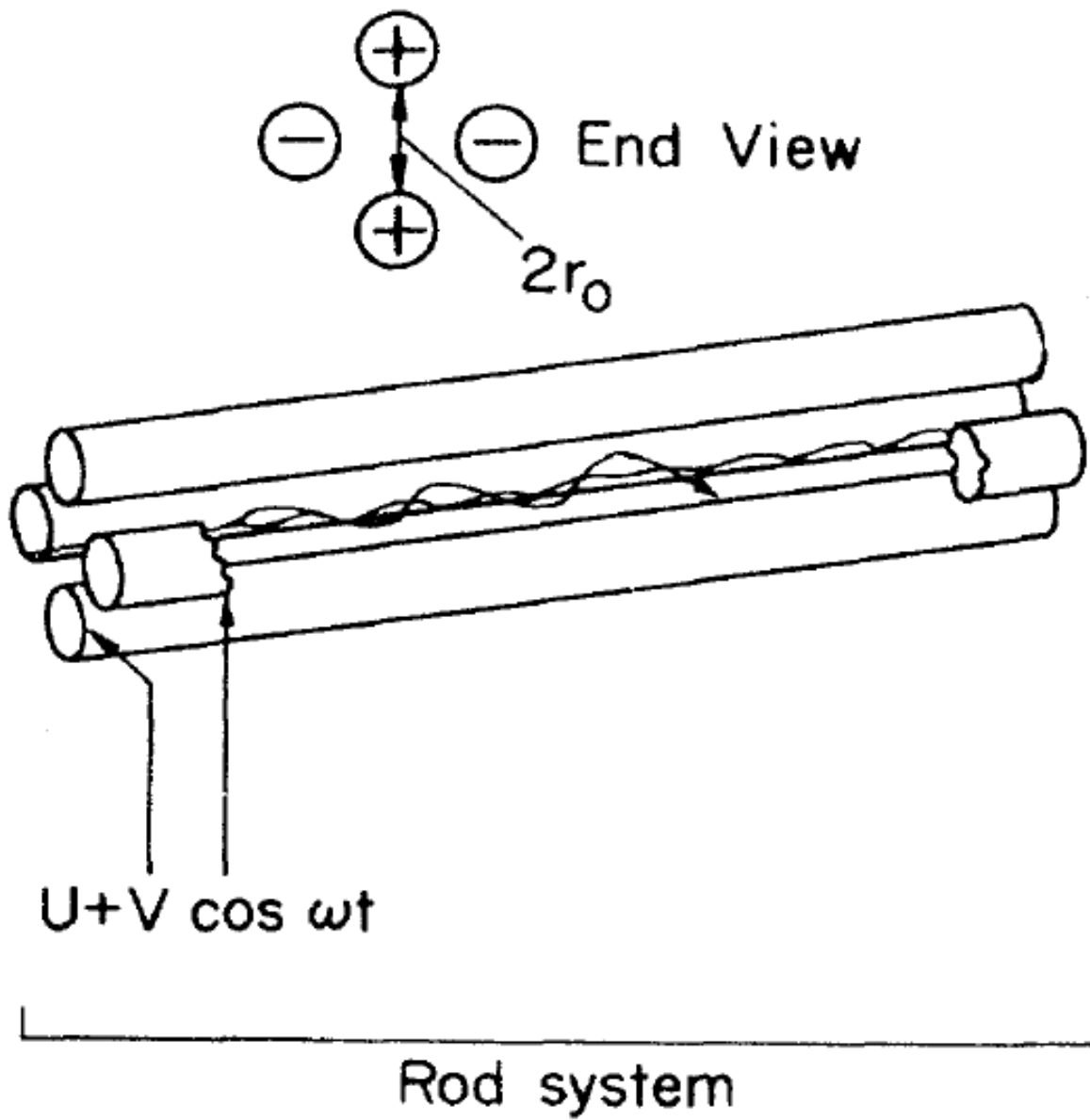
1084

1085

1086

1087

1088



1089

1090

Figure 1-1 Side and end view of quadrupole rod system (7).

1091

1092

1093

1094

1095

1096

1097

1098

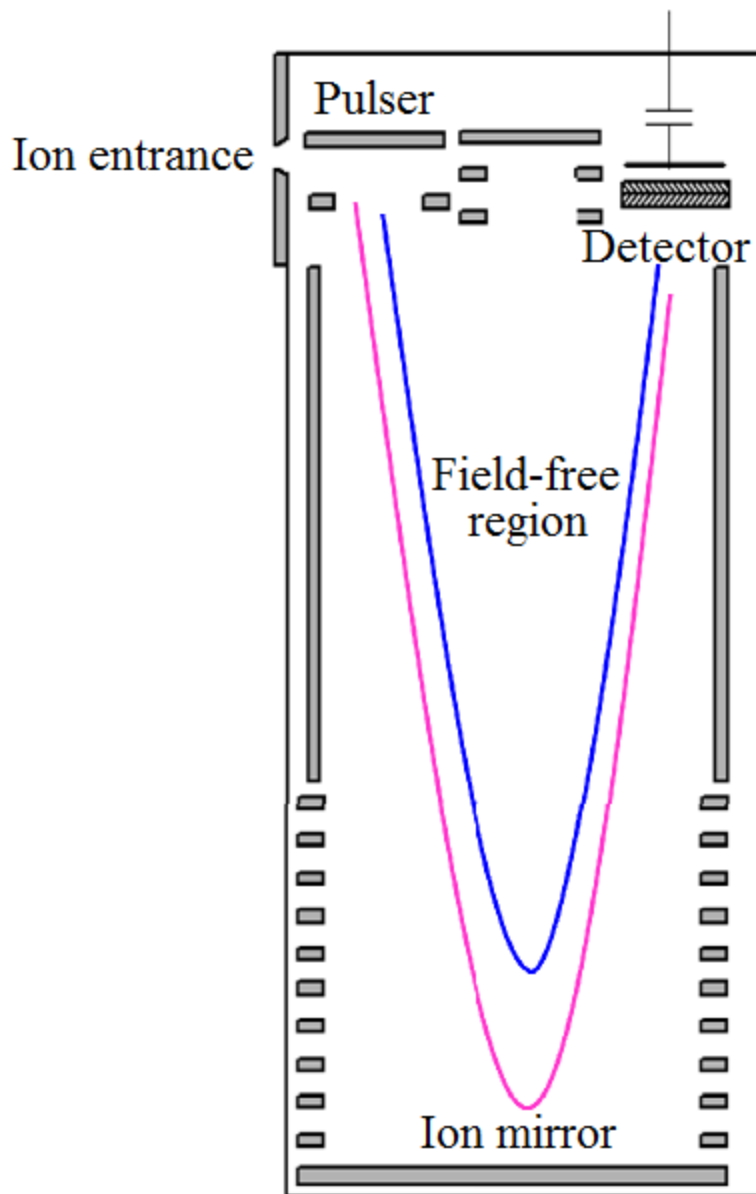
1099

1100

1101

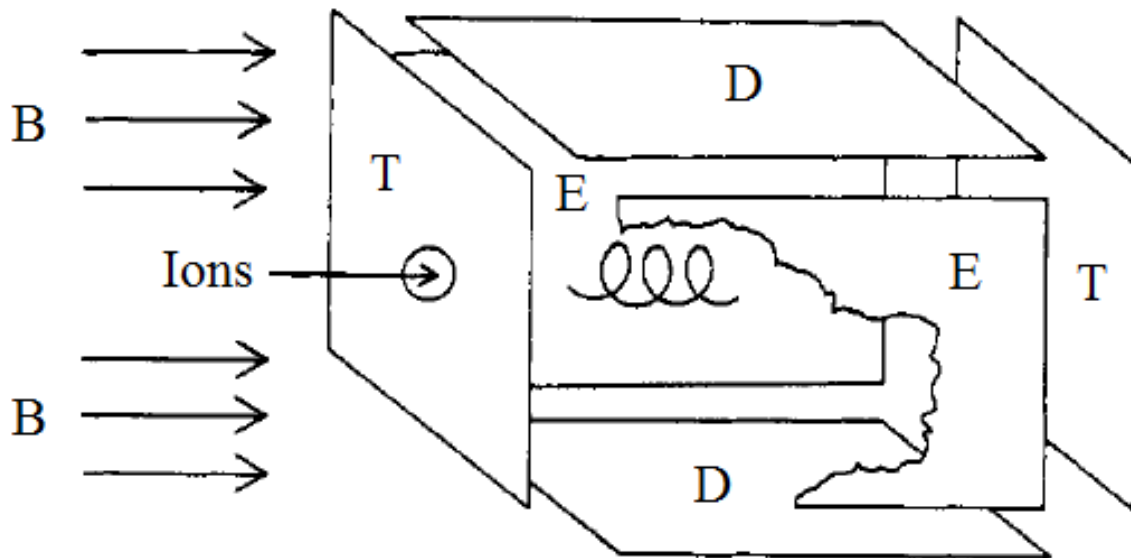
1102

V-Reflectron time-of flight mass spectrometer



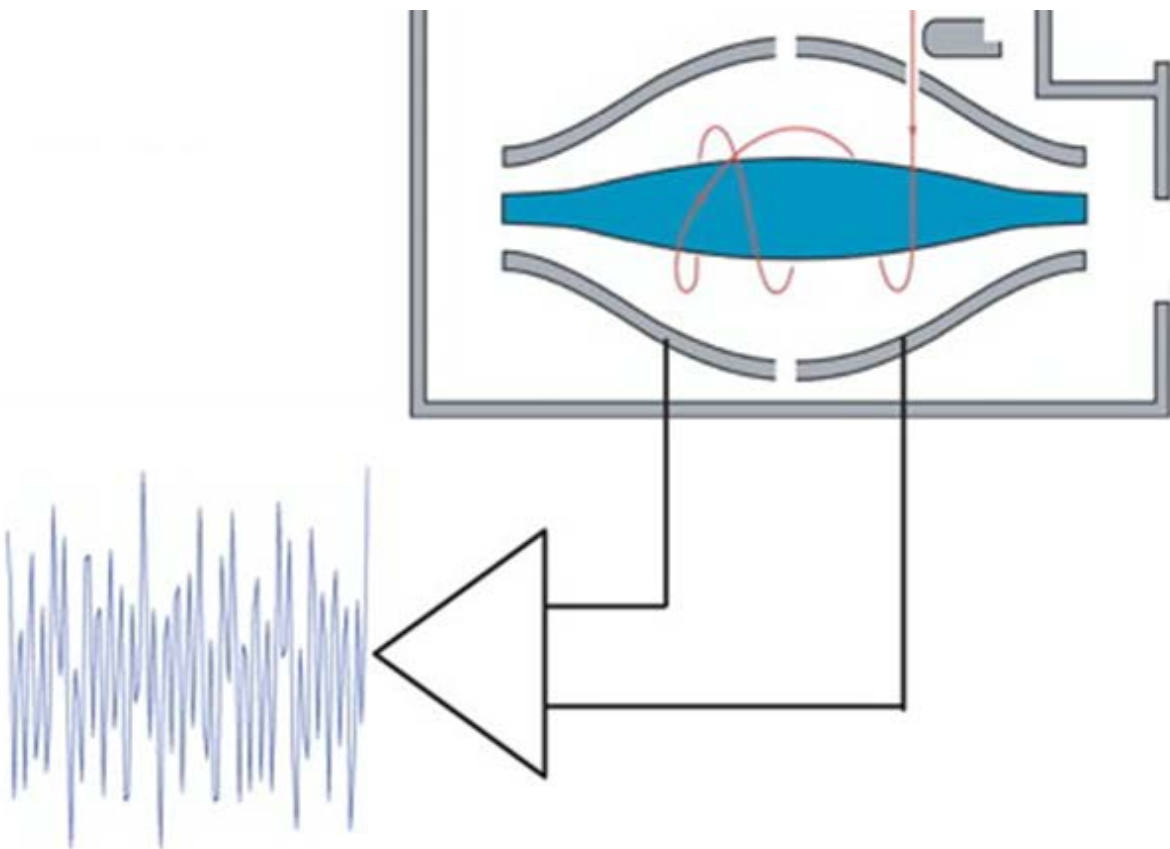
1103
1104 **Figure 1-2** Time of flight reflectron, the blue and pink lines detail the flight path of two ions
1105 with different kinetic energy profiles traveling from the pulser to the detector (103).

1106
1107



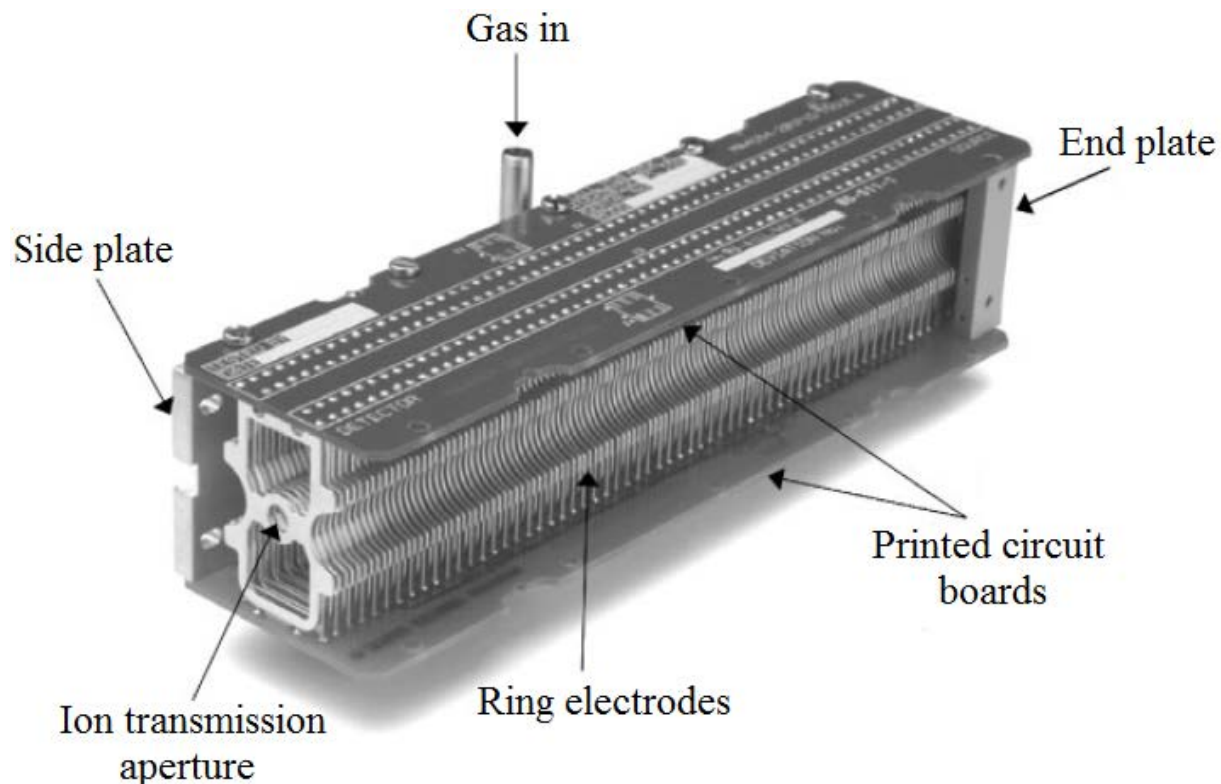
1108
1109 **Figure 1-3** Diagram of FT-ICR cell. The first trapping plate (T) contains a hole for the ions to
1110 enter the cell. The excitation plates (E) modulate the radii of the trapped ions. The detection
1111 plates (D) measure the image-current of the ions as they oscillate in within the trap. The whole
1112 time a magnetic field (B) is applied axially to the trapped ion flight path (17).

1113
1114
1115
1116
1117
1118
1119
1120
1121
1122
1123
1124
1125
1126
1127
1128
1129
1130
1131
1132
1133

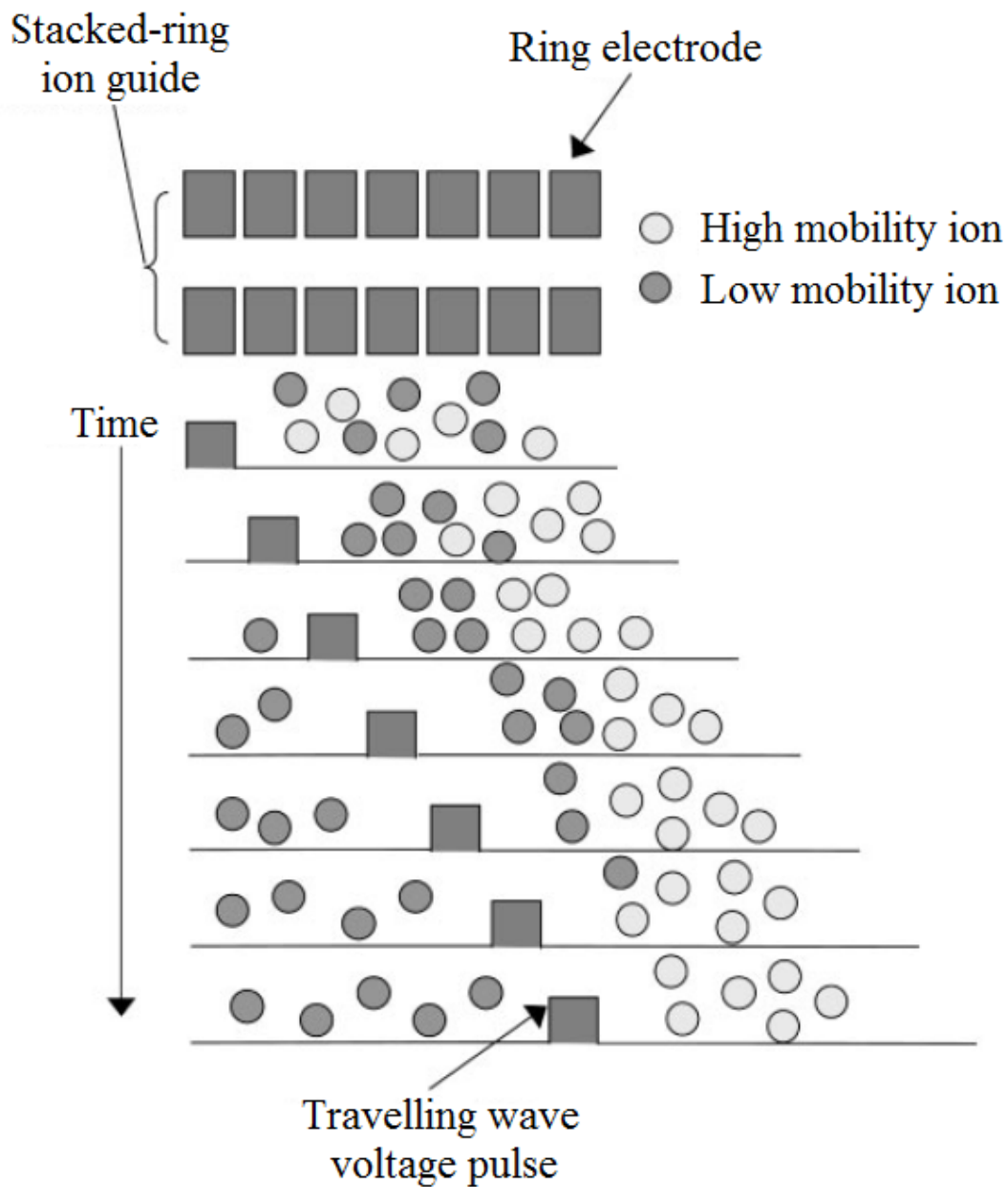


1134
1135 **Figure 1-4** Schematic of Orbitrap detector detailing the entrance of the ions into the detector,
1136 orbit about the center electrode, and subsequent image-current frequency detected by the
1137 symmetric exterior electrodes (104).

1138
1139
1140
1141
1142
1143
1144
1145
1146
1147

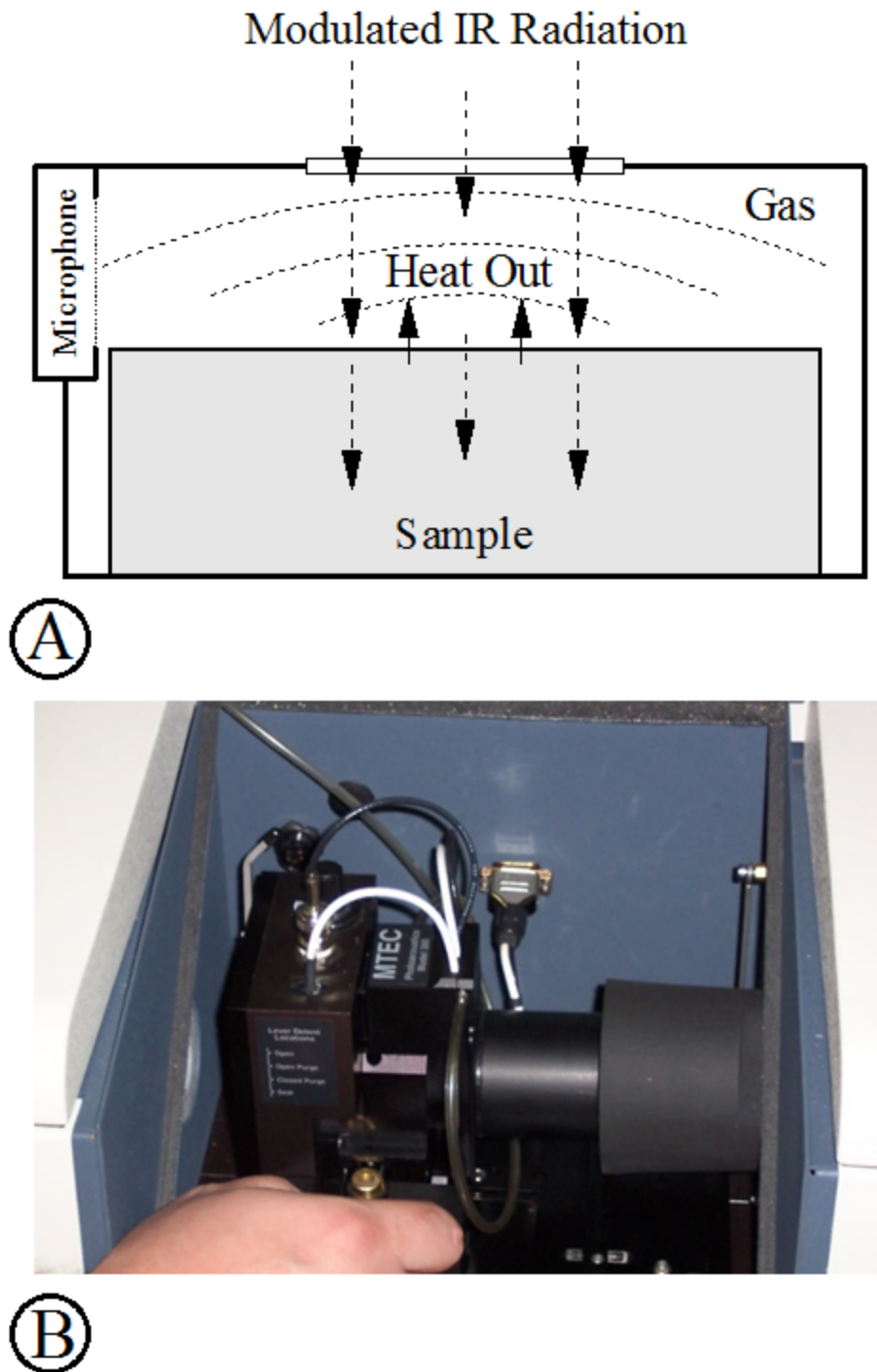


1148
1149 **Figure 1-5** Photograph of the travelling wave ion mobility device (105).
1150
1151
1152
1153
1154
1155
1156
1157
1158
1159
1160
1161
1162
1163
1164
1165
1166
1167
1168
1169
1170
1171



1172
1173
1174
1175
1176
1177
1178
1179
1180
1181

Figure 1-6 Diagram of the separation performed within a travelling wave ion mobility cell (105).



1182
1183
1184
1185

Figure 1-7 Diagram A shows how the PAS cell functions in the presence of modulated IR radiation (not to scale). Picture B is an exterior view of a functioning PAS cell nestled within a FTIR instrument. Diagram and photograph courtesy of the McClelland group.

1186 **CHAPTER 2**
1187
1188
1189
1190 **HIGH RESOLUTION TIME-OF-FLIGHT MASS SPECTROMETRY**
1191 **FINGERPRINTING OF METABOLITES FROM CECUM AND DISTAL COLON**
1192 **CONTENTS OF RATS FED RESISTANT STARCH**
1193
1194 Modified from a paper published in *Analytical and Bioanalytical Chemistry*¹
1195
1196 By
1197 Timothy J. Anderson,^{2,3*} Roger W. Jones,² Yongfeng Ai,⁴ Robert S. Houk,^{2,3} Jay-lin Jane,⁴
1198 Yinsheng Zhao,⁴ Diane F. Birt,⁴ John F. McClelland^{2,5}
1199
1200 ¹Reprinted with permission of *Analytical and Bioanalytical Chemistry* 406(3):745-756
1201 ²Ames Laboratory-USDOE, Iowa State University, Ames, Iowa 50011
1202 ³Department of Chemistry, Iowa State University, Ames, Iowa 50011
1203 ⁴Department of Food Science and Human Nutrition, Iowa State University, Ames, Iowa 50011
1204 ⁵Department of Mechanical Engineering, Iowa State University, Ames, Iowa 50011
1205
1206
1207
1208
1209
1210
1211
1212
1213
1214
1215
1216
1217 *Corresponding Author, Email timma@iastate.edu, Phone 515-294-4285

1218 **Abstract**

1219 Time-of-flight mass spectrometry along with statistical analysis was utilized to study metabolic
1220 profiles among rats fed resistant starch (RS) diets. Fischer 344 rats were fed four starch diets
1221 consisting of 55% (w/w, dbs) starch. A control starch diet consisting of corn starch was
1222 compared against three RS diets. The RS diets were high-amylose corn starch (HA7), HA7
1223 chemically modified with octenyl succinic anhydride, and stearic-acid-complexed HA7 starch.
1224 A subgroup received antibiotic treatment to determine if perturbations in the gut microbiome
1225 were long lasting. A second subgroup was treated with azoxymethane (AOM), a carcinogen. At
1226 the end of the eight week study, cecal and distal-colon contents samples were collected from the
1227 sacrificed rats. Metabolites were extracted from cecal and distal colon samples into acetonitrile.
1228 The extracts were then analyzed on an accurate-mass time-of-flight mass spectrometer to obtain
1229 their metabolic profile. The data were analyzed using partial least-squares discriminant analysis
1230 (PLS-DA). The PLS-DA analysis utilized a training set and verification set to classify samples
1231 within diet and treatment groups. PLS-DA could reliably differentiate the diet treatments for
1232 both cecal and distal colon samples. The PLS-DA analyses of the antibiotic and no antibiotic
1233 treated subgroups were well classified for cecal samples and modestly separated for distal-colon
1234 samples. PLS-DA analysis had limited success separating distal colon samples for rats given
1235 AOM from those not treated; the cecal samples from AOM had very poor classification. Mass
1236 spectrometry profiling coupled with PLS-DA can readily classify metabolite differences among
1237 rats given RS diets.

1238

1239

1240 **Keywords** Resistant Starch, Mass Spectrometry, Metabolites, PLS-DA

1241 **Introduction**

1242 Food is composed of three main components, which are protein, lipid and starch. Cereal
1243 grains are one of the world's most important food sources; of these, its most abundant
1244 component is typically starch. Amylopectin and amylose make up the bulk of starch granules;
1245 their relative concentration can vary depending on source material. Amylopectin comprises
1246 typically about 70% of the starch granule but can reach 100% for waxy corn varieties. Amylose
1247 levels are typically about 15 to 30% of the starch granule (1-3).

1248 Both amylopectin and amylose are comprised of polymeric glucose. Recent studies have
1249 shown that amylose forms double helical structures, and the hydroxyl groups of the individual
1250 glucose units may be esterified with a variety of lipid-like compounds (3). Amylose can also
1251 form single helical complexes with free fatty acids and iodine. These modified amylose structures
1252 along with food materials that contain up to 85% amylose are examples of resistant starch (RS)
1253 (3), which effectively resist digestion in the stomach and small intestine, and thus are processed
1254 farther along the gut (4).

1255 RS has been studied for a variety of health benefits. RS may aid diabetics, decrease
1256 energy density, and also act as a prebiotic (5-10). Prebiotics are materials which resist digestion
1257 by the host and are metabolized in the gut by microorganisms (10). The microorganisms release
1258 compounds, such as short chain fatty acids, which are believed to be beneficial to the host
1259 organism (11, 12). The interplay between microorganisms and host is complex; the
1260 microorganisms may even interact with host diet to increase deleterious conditions such as
1261 intestinal inflammation (13). Some materials, such as oligofructose, lactulose, and transgalacto-
1262 oligosaccharides are well characterized and known to be prebiotics, but only recently has RS
1263 been classified as a prebiotic (14-20).

1264 The catabolism of prebiotics by microorganisms produces a vast array of chemical
1265 components, which are classified as metabolites (21). Metabolites from gut microorganisms can
1266 be obtained from blood, urine or feces (22-24). Blood and urine reflect metabolic changes that
1267 occur in the gut from direct absorption through the intestinal lining (25, 26). Feces are complex
1268 media from which a direct interplay between microorganism and host can be observed (27).

1269 There are five RS categories. Whole grains and ground legumes contain type 1 RS.
1270 Type 1 RS is amylose protected by cell wall material and other plant materials that are difficult
1271 to digest. Type 2 RS retains a crystalline structure, which resists enzyme hydrolysis, and is
1272 found primarily in banana and potato starch. Type 3 RS is retrograded starch; this occurs when
1273 the starch granule has gelatinized and reformed a crystalline structure (28). Type 4 RS is a
1274 chemically modified starch molecule. To produce the type 4 RS, a lipid compound such as
1275 octenyl succinic anhydride is generally bound to the various hydroxyl groups of glucose within
1276 the starch amylose molecule (14, 29). Type 5 RS is formed from a physical interaction of
1277 debranched helical starch amylose and a long chain fatty acid, such as palmitic or stearic acid
1278 (30).

1279 Mass spectrometry has emerged as one of the most important platforms for metabolite
1280 analysis due to improvements in ionization methodology and high resolution instruments. A
1281 variety of metabolite separation methods can be coupled with mass spectrometers. The coupling
1282 allows comprehensive analysis through fingerprinting or profiling of metabolites (31, 32). Gas
1283 chromatography-mass spectrometry (GC-MS) is useful for the analysis of thermally stable
1284 volatile compounds. GC-MS often utilizes electron impact (EI) ionization. The GC separation
1285 and subsequent EI fragmentation often allow metabolite identification through database
1286 searching (27, 33-35). Liquid chromatography-mass spectrometry (LC-MS) is very useful for

1287 metabolite analysis because specialized columns can be used to separate either polar or non-polar
1288 compounds (25, 26, 36). LC-MS can also be coupled with collision induced dissociation (CID)
1289 that provides fragment ions for potential metabolite identification (28, 37). Capillary
1290 electrophoresis (CE) is another separation technique that can be used prior to mass spectrometry
1291 analysis (38, 39). Work performed with CE and LC-MS has attempted to identify metabolites
1292 using standard retention time libraries and elemental formulas from accurate mass measurements
1293 (40). Ultra-high resolution mass spectrometry using Fourier transform ion cyclotron resonance
1294 (FT-ICR) instruments has been used for metabolite analysis (41, 42). Even matrix assisted laser
1295 desorption ionization (MALDI) imaging has recently been coupled with mass spectrometry to
1296 obtain metabolite insight (43).

1297 Statistical tools have become important in the post examination of metabolites analyzed
1298 using mass spectrometry. Tools such as principal component analysis (PCA), soft independent
1299 modeling of class analogy (SIMCA), partial least-squares discriminant analysis (PLS-DA), linear
1300 discriminant analysis (LDA), and artificial neural networks all allow differentiation and group
1301 prediction (26, 27, 34, 35, 39, 44-46). Using these tools, difficult and complex analyses of large
1302 amounts of data can be more easily graphed and visualized.

1303 The current study describes such methods for profiling the metabolites from rat cecal and
1304 distal colon contents to deduce differences among RS diets. Three different RS and a control
1305 corn starch were fed to rats. The first RS was a type 2 RS that consisted of high amylose corn
1306 starch (HA7). The second RS was a type 4 RS that was HA7 corn starch modified with octenyl
1307 succinic anhydride (OS-HA7). The last RS was a type 5 RS that was produced by complexing
1308 HA7 with stearic acid (StA-HA7). The main goal of this study was to determine whether
1309 statistical tools, such as PLS-DA, could observe differences among RS starch diets from rat cecal

1310 and distal colon contents using mass spectrometry. Another goal was to understand whether
1311 statistical tools could accurately group diets and target their individual biomarkers that vary the
1312 most among the diets.

1313

1314 **Materials and Methods**

1315 *Animal Study*

1316 Male Fischer 344 rats were housed and fed according to the procedure of Zhao et al. (47).
1317 The study initially used 90 rats (two died before sacrifice) that were obtained at five weeks old,
1318 and were placed on specific feeding regimens for eight weeks, as shown in the flow diagram in
1319 Figure 2-1. The animals were randomly separated into four starch diet groups: Control, HA7,
1320 OS-HA7, and StA-HA7. The control and StA-HA7 starch diet groups each had 29 rats, and both
1321 diets contained four further subgroup treatments. Rats fed HA7 and OS-HA7 starch diets had 15
1322 rats each, and both diets contained only two further subgroup treatments. All four starch diet
1323 groups were divided into two treatment subgroups, which consisted of 9 to 10 rats given either
1324 two injections of the carcinogen azoxymethane (AOM, Midwest Research Institute, Kansas City,
1325 MO) at a dose of 20 mg AOM/kg rat body weight and 4 to 5 rats given two injections of saline
1326 administered eight weeks prior to sample collection, following the method of Zhao et al. (47). In
1327 the control and StA-HA7 diet groups, both of the injection subgroups were further split into two
1328 more subgroups consisting of rats either administered an antibiotic consisting of a combination
1329 of imipenem and vancomycin at a dose of 50 μ g/mL each in the drinking water or not
1330 administered any antibiotic in week 2 (Figure 2-1).

1331

1332

1333 *Starch Diet Materials*

1334 Normal corn starch (NCS, Cargill Gel TM) and HA7 (AmyloGel TM) were purchased from
1335 Cargill Inc. (Minneapolis, MN), 2-Octen-1-ylsuccinic anhydride (OSA), pullulanase
1336 from *Bacillus acidopullulyticus* and stearic acid (SA) were purchased from Sigma-Aldrich Co.
1337 (St. Louis, MO). All starch was cooked prior to addition to the rat diets, in accordance with the
1338 procedure of Zhao et al. (47). The non-starch component of the rat diet was prepared in
1339 compliance with the standards of the American Society for Nutritional Sciences for mature rats
1340 (AIN-93M) (48). The diets were prepared every other day and served fresh to the rats.

1341

1342 *Preparation of OS-HA7 Starch Diet*

1343 OS-HA7 was produced from the HA7 through modification with OSA (49). The HA7
1344 was suspended in water at a concentration of 35% (w/w, dsb). The pH of the starch slurry was
1345 adjusted to 8.0 by adding a sodium hydroxide aqueous solution (3%, w/w), and the temperature
1346 was maintained at 35 °C. OSA (10%, w/w, dsb) was added to the slurry dropwise while
1347 maintaining the pH at 8.0 and 35 °C. After the reaction was completed, the pH of the starch
1348 slurry became stable and was then adjusted to 6.5 by adding 1.0 M hydrochloric acid. The starch
1349 was recovered using filtration, washed with distilled water and 100% ethanol, dried at 37 °C, and
1350 then ground to fine powder.

1351

1352 *Preparation of StA-HA7 Starch Diet*

1353 StA-HA7 was prepared from the HA7 following the method of Hasjim et al. (30) with
1354 modifications. The HA7 was suspended in water at a concentration of 10% (w/w, dsb). The
1355 starch slurry was pre-heated to 80 °C, and the temperature maintained for 1 h with stirring.

1356 Pullulanase (5 units/g starch, dsb) was added to the slurry to hydrolyze α 1-6 branch linkages of
1357 the starch at 60 °C for 24 h. Stearic acid (SA, 10%, w/w, dsb) was added, and the mixture was
1358 kept at 80 °C for 1 h with vigorous stirring for amylose-SA complex formation. After cooling to
1359 room temperature, the StA-HA7 was recovered using centrifugation, washed with 50% (v/v)
1360 aqueous ethanol solution, dried at 37 °C, and then ground.

1361

1362 *Rat Cecal Samples*

1363 The rat cecum was removed just after sacrifice. The cecum contents were placed in 15-
1364 mL centrifuge tubes (Corning, Tewksbury, MA) and stored on dry ice until placed in long term
1365 storage at -80 °C. Of the 88 rats sampled, 81 cecal samples were analyzed. For control, HA7,
1366 OS-HA7, and StA-HA7 diets, 24, 15, 14, and 28 samples were analyzed, respectively. The
1367 lower number of samples analyzed for the control diet was due to reduced sample volume. All
1368 RS fed rats had ceca of substantial size; on average they were nearly four times the mass of the
1369 control.

1370

1371 *Rat Distal Colon Samples*

1372 After sacrifice, the rat colon was opened. Fecal pellets were collected from the large
1373 intestine starting from the anus to 5 cm up the colon and were placed in 15-mL centrifuge tubes
1374 containing phosphate buffer. The samples were placed on dry ice, and then stored long term at
1375 -80 °C. Seventy-two distal colon samples were analyzed from the original 88 rats. From control,
1376 HA7, OS-HA7, and StA-HA7 diets, 22, 13, 11, and 26 samples were analyzed, respectively. The
1377 drop in samples analyzed in respect to cecum samples was due to random amounts of fecal

1378 pellets in the colon. Some rats contained many pellets, while some had none at the time of
1379 sacrifice.

1380

1381 *Metabolite Extraction for Cecal and Distal Colon Samples*

1382 The metabolite extraction was an adaption of the method of Antunes et al. (42). Frozen
1383 cecal and distal colon samples were thawed and approximately 150 mg of sample was placed in a
1384 2.0-mL microcentrifuge tube (Eppendorf, Hamburg, Germany). The tube was then half-filled
1385 with 1 mm zirconia/silica beads (Biospec Products, Bartlesville, OK) and 1 mL of HPLC grade
1386 acetonitrile (Fischer Scientific, Fair Lawn, NJ) was introduced. The microcentrifuge tubes were
1387 placed on a vortex apparatus (Fisherbrand, Bohemia, NY) with an orbital bead homogenizing
1388 adaptor (Mo Bio Laboratories Inc., Carlsbad, CA). The samples were vortexed until
1389 homogenized. The liquid portion of each sample was then pipetted into a clean microcentrifuge
1390 tube. The samples were placed in a centrifuge (Model 5415C, Eppendorf, Westbury, NY) for 5
1391 minutes at 12,000 rpm. From the centrifuge tube, 500 μ L of supernatant was placed in a clean
1392 centrifuge tube, then vacuum centrifuged (Labconco Corporation, Kansas City, MO) at 50 °C
1393 and depressurized with a dry vacuum pump (Welch Rietchle Thomas, Skokie, IL). The dried
1394 metabolite extracts were stored at -20 °C.

1395 The dried metabolite extracts were reconstituted for mass spectrometry analysis by
1396 adding 500 μ L of a 60% (v/v) aqueous acetonitrile solution. The extract was vigorously
1397 vortexed and then centrifuged for 2 minutes at 12,000 rpm. 100 μ L of supernatant was removed
1398 and placed in a clean microcentrifuge tube. An additional 500 μ L of 60% (v/v) aqueous
1399 acetonitrile was added to dilute the sample. Formic acid was added to produce a 0.2% formic
1400 acid sample solution to aid in positive ion production by electrospray ionization (ESI). Lastly,

1401 the solution was vortexed and transferred into 12x35 mm clear glass vials to be placed in an LC
1402 autosampler.

1403

1404 *Mass Spectrometry*

1405 From the reconstituted cecal and distal colon metabolite extracts, 20 μ L of sample was
1406 injected into an Agilent 1260 Infinity LC system (Agilent Technologies, Inc., Santa Clara, CA),
1407 which was used as an autosampler. The samples were direct-infused from the LC and ionized
1408 using ESI in positive mode on an Agilent 6224 time-of-flight mass spectrometer operated at an
1409 acquisition rate of 4 GHz. A sample run lasted 5 minutes with a mobile phase of 60% (v/v)
1410 aqueous acetonitrile. A second mobile phase of 60% (v/v) aqueous acetonitrile with 20 ppm of a
1411 50/50 mixture of polyethylene glycol (PEG) 200 and 600 standards (Hampton Research, Aliso
1412 Viejo, CA) was used for calibration. At 48 seconds into a sample run, the PEG-containing
1413 mobile phase was used for 12 seconds. At 1 minute the primary mobile phase was switched
1414 inline and flushed the PEG calibrant from the system prior to the next sample.

1415 The software used was Agilent MassHunter Qualitative Analysis. Each spectrum was
1416 background subtracted, and the m/z scale was recalibrated using 17 ammoniated PEG-adduct
1417 peaks ranging from m/z 168.1236 to 872.5430. The calibrated spectra were centroided and
1418 exported as text files. The text files for each diet and subgroup were averaged using custom
1419 software. The averaged text files were then uploaded to the MassTRIX website, and accurate
1420 mass data were compared to rat metabolites in the KEGG database (50).

1421

1422

1423

1424 *Statistical Analysis*

1425 Separate PLS-DA classification models were developed using commercial software
1426 (Pirouette Version 4.5; Infometrix, Inc.; Bothell, WA) for diet, AOM treatment, and antibiotic
1427 treatment. The cecal and distal fecal datasets were modeled separately. The cecal and distal
1428 fecal datasets consisted of spectra from 81 and 72 rats, respectively. These sets included data
1429 from AOM-treated and antibiotic-treated rats, as well as untreated ones. The verification set
1430 consisted of 25% of the total number of samples and the remaining 75% of samples were placed in the
1431 training set. The verification set was comprised of as close to one quarter of diet, AOM, and antibiotic
1432 treated samples as possible to ensure equal weighting during classification. The appropriate number of
1433 rats from each treatment was randomly selected for the verification set without previous knowledge of the
1434 spectral results. Each spectrum was normalized so that the base peak had an intensity of 100.
1435 Small peaks with intensities below one were then eliminated. The data were aligned using a
1436 mass tolerance of 0.005 m/z so that peaks in different spectra within a range of m/z ~ 0.010 were
1437 assigned the same (average) mass. In PLS-DA, each training-set spectrum is assigned a class-fit
1438 value of one for any class to which its sample belongs and a class-fit value of zero for classes to
1439 which its sample does not belong. When the verification set is analyzed, the resulting model
1440 determines the class-fit values of each spectrum for every class. Each verification-set spectrum
1441 is then assigned to the class for which its class-fit value is closest to one, which usually means
1442 the one class for which its class-fit value is above 0.5.

1443 Prior to modeling, the spectra were always mean centered and for some models one-
1444 component orthogonal signal correction was used (51). The resulting regression vectors for the
1445 classes (e.g., diets) were used to identify those peaks that most strongly differentiate the classes,
1446 and the corresponding species were examined as possible biomarkers.

1447 **Results and Discussion**1448 *Mass Spectrometry*

1449 Even without the mass spectrometry analysis, there were obvious differences in the
1450 digestive-tract contents of rats fed different diets. As described previously, the RS fed rats had
1451 ceca which were as much as four times greater in mass than the rats on the control diet. The
1452 increased mass may have been due to increased fermentation time in the cecum to obtain
1453 nutrients from resilient RS components. The color, consistency, and aroma of the cecal contents
1454 were much different for the control compared to the RS diets. These differences may be linked
1455 to the amount of the starch fermented, and thus tied to the gut microorganisms and metabolites.
1456 The primary difference among distal colon contents was that the various diets had distinct colors.

1457 Mass spectra of metabolites from the cecal contents of rats that were fed with different
1458 diets and received no AOM or antibiotic were averaged and are compared in Figure 2-2. The
1459 main emphasis of the study was to determine differences among diets in respect to their
1460 metabolite profiles. A metabolite peak was considered specific to a diet group if the peak was
1461 approximately three times the intensity of the same peak in the other diets. The peaks are given
1462 letter labels in the figure, and Table 2-1 lists their m/z values and the diets in which they were
1463 found. First, the peaks that were specific to only one diet group were inspected. The control
1464 group had four specific peaks labeled *y*, *z*, *aa*, and *ai*. The HA7 group had no specific peaks.
1465 The OS-HA7 group contained six specific peaks marked *c*, *p*, *w*, *ad*, *ag*, and *aj*. The last group,
1466 StA-HA7, had four specific peaks labeled *t*, *u*, *ah*, and *ak*. Far fewer metabolite peaks were
1467 shared between any two of the groups. The *ab* peak was shared by the control and HA7 groups.
1468 Another peak, labeled *f*, was in both the control and StA-HA7 groups. The HA7 and StA-HA7
1469 groups had five mutual peaks marked *e*, *i*, *j*, *n* and *r*. Fewer peaks were observed among three

1470 common groups. The control, HA7, and StA-HA7 diets shared the *g* peak. The control, OS-
1471 HA7, and StA-HA7 diets contained a single peak in common, labeled *h*. The HA7, OS-HA7 and
1472 StA-HA7 diet groups shared the three peaks *b*, *k* and *s*. Only one prominent metabolite was
1473 observed in all groups; it was the *d* peak.

1474 Mass spectra of the diet treatment metabolites in the distal colon contents are compared
1475 in Figure 2-3. Similarly to the cecal contents, the mass spectra for the distal colon contents were
1476 averaged from rats that received no AOM or antibiotic. The peaks were also classified as
1477 specific to diet groups if they were approximately three times the intensity of the other diet
1478 groups. Like the labeled cecal-contents peaks in Figure 2-2, further information about the
1479 lettered peaks in Fig 2-3 can be found in Table 2-1. No peaks were observed to be specific to the
1480 control group. The HA7 group had only one exclusive peak, labeled *af*. The OS-HA7 group had
1481 seven peaks—*m*, *p*, *q*, *w*, *ad*, *ae*, and *aj*. Lastly, StA-HA7 had the six peaks *k*, *l*, *o*, *t*, *ac*, and *ak*.
1482 Fewer metabolite peaks were shared between any two groups than the peaks specific to a single
1483 group. The control and StA-HA7 diet groups shared the four peaks *a*, *g*, *x* and *ah*. The HA7 and
1484 StA-HA7 diets contained five common peaks—*j*, *n*, *r*, *s*, and *v*. Only the metabolite *h* was shared
1485 among the control, OS-HA7, and StA-HA7 diet groups. The two peaks *b* and *d* were shared
1486 among all four diet groups.

1487 Analysis of the mass spectra in Figure 2-1 and 2-2 highlighted modest differences
1488 between the cecal and distal colon contents. Spectra for the control and StA-HA7 diet group for
1489 both digestive locations have been placed in Figure 2-4 for comparison. Specific peaks across
1490 digestive locations for a diet group were chosen with the same rule as described above for Figure
1491 2-2, and Figure 2-3, and the peaks are again identified in Table 2-1. The control group for the
1492 cecal contents contained peaks labeled *y*, *z*, *aa*, *ab*, and *ai*, which were more intense than the

1493 same peaks in the distal colon contents. The distal colon contents contained the four peaks
1494 labeled *g*, *l*, *x*, and *ac*, which were more intense than those same peaks observed in the cecal
1495 contents. Both digestive locations shared the peaks *a*, *b*, *d*, *f*, *h*, and *ah* with similar intensities.
1496 The StA-HA7 group for both cecal and distal colon digestive locations was more complex than
1497 the control group. The cecal contents contained only one peak, labeled *ah*, that was more intense
1498 than in the distal colon contents. Peaks *g*, *l*, *o*, and *ac* had higher intensities in the distal colon
1499 contents than in the cecal contents. Peaks labeled *a*, *b*, *d*, *f*, *h*, *j*, *k*, *n*, *r*, *s*, *t*, *u* and *ak* were at
1500 similar intensities in the cecal and distal colon contents.

1501 From this scrutiny of the mass spectra of the cecal contents and distal colon contents for
1502 the diets, it is apparent that RS diets altered the metabolism of the rats. In Table 2-1 the cecal
1503 contents from each diet had a distinct metabolite profile. Of the 27 labeled metabolites, 52%
1504 were specific to only one diet group. These differences among diets persisted into the distal
1505 colon contents, for which 54% of the 26 labeled metabolites in Table 2-1 were exclusive to
1506 individual diet groups. Figure 2-4 compared the cecal and the distal colon contents of the control
1507 diet, Table 2-1 described that 77% of the 13 labeled metabolites are specific to one or the other
1508 digestive location. Figure 2-4 also compared spectra of cecal and distal colon contents of the
1509 StA-HA7 diet, and 22 metabolites from Table 2-1 were specific to only 45% of either digestive
1510 location. For the control, there appears to be substantial change to the metabolite profile.
1511 However, for RS, such as StA-HA7, there was less variability in the metabolite profile from
1512 cecum to distal colon.

1513 In a companion study to this one that used the same samples, Anderson et al. (52)
1514 determined through enzymatic assay that the average cecal starch content (dsb) for the control,
1515 HA7, OS-HA7, and StA-HA7 diets were 0.7%, 18.3%, 48.8%, and 21.9%, respectively. The

1516 residual starch differences are most likely attributed to the ability of each starch to be fermented
1517 in the cecum. The control and OS-HA7, which were the most and least fermented diets,
1518 respectively, had more diet-specific metabolites for both cecal and distal contents. The HA7 and
1519 StA-HA7 RS diets had nearly the same degree of fermentation and also shared many metabolites
1520 in the cecal and distal colon contents. The HA7 and StA-HA7 similarities also could be due to
1521 the relationship between the diets; StA-HA7 was produced from a complex of HA7 and stearic
1522 acid, and StA-HA7 may share some of the fermentation products of its parent RS. Regardless,
1523 the degree of fermentation and the nature of the starch source are probably the largest factors
1524 regarding the divergence of the metabolite profiles.

1525

1526 *Statistical Analysis of Cecal Contents*

1527 Classification analysis of the mass spectra for the RS diet groups was performed with
1528 PLS-DA for the cecal extracts. PLS-DA modeling was done for the cecal contents with a 61
1529 sample training set, and a 20 sample verification set. The verification set contained 6, 4, 3, and 7
1530 samples from the control, HA7, OS-HA7, and StA-HA7 diets, respectively. The PLS-DA
1531 analysis of cecal contents for diet correctly classified all training-set samples; all verification-set
1532 samples were classified properly. Figure 2-5 displays the PLS-DA results and the quality of
1533 separation for the cecal contents RS diet groups. The closed and open symbols correspond to
1534 verification-set samples that do and do not belong to the indicated diet, respectively. For the
1535 control and OS-HA7 diets, all samples were spaced well away from the 0.5 nominal threshold
1536 for class differentiation. StA-HA7 had nearly all closed symbols positioned well above the 0.5
1537 line, but one sample appeared slightly above the nominal threshold. HA7 had three of its
1538 samples positioned above the 0.5 line, but one sample appeared below the threshold line.

1539 Nevertheless, it is readily classified as HA7 because its class-fit values for all of the other diets
1540 were even lower.

1541 PLS-DA fingerprint analysis for the cecal contents was also carried out for the antibiotic
1542 subgroup treatments. The cecal contents PLS-DA antibiotic analysis had no training-set
1543 misclassifications. In Figure 2-6 only two verification-set samples were misclassified. Thus, the
1544 PLS-DA statistical classification separated the cecal contents antibiotic and saline treatments
1545 well.

1546 Classifying the cecal-content samples by AOM subgroup treatment was much less
1547 successful (data not shown). PLS-DA was able to produce a model for AOM treatment
1548 classification that properly predicted all of the training-set samples, but its analysis yielded 13
1549 misclassifications among the 20 verification-set samples. Clearly, at the time the animals were
1550 sacrificed and the samples taken, eight weeks after the last AOM injection, the AOM treatment
1551 had too little effect on the cecal contents to be observed via mass spectrometry.

1552

1553 *Statistical Analysis of Distal Colon Contents*

1554 Classification analysis was also performed for the spectra of the distal colon contents RS
1555 groups. PLS-DA was performed with a 54-sample training set and 18-member verification set.
1556 The verification set contained 6, 3, 3, and 6 samples from the control, HA7, OS-HA7, and StA-
1557 HA7 diets, respectively. The PLS-DA diet group analysis of the distal colon contents
1558 misclassified only one verification-set sample. Figure 2-7 shows the PLS-DA verification-set
1559 analysis of the distal colon contents. The distal-colon-contents categorization for the diet
1560 samples was not as clean as it was for the cecal contents. The HA7, OS-HA7, and StA-HA7
1561 diets have all of their markers in the correct region above or below the 0.5 class-fit threshold, but

1562 many markers occur very close to the threshold. The control diet classification clearly shows all
1563 of the errant samples. In the control diet classification, one control sample fell below the 0.5
1564 class-fit threshold, but it still correctly classified due to its class-fit value being closest to one for
1565 the control group. The other errant sample in the control-diet classification is the open, inverted
1566 triangle (StA-HA7 sample) at a control-diet class-fit value of 0.76. This same sample
1567 corresponds to the highest filled triangle in the StA-HA7 classification (class-fit value 1.45).
1568 Because the class-fit value for the sample in the control diet class is closer to one, the sample
1569 was misclassified as belonging to the control diet.

1570 PLS-DA analysis of the distal-colon-contents training set for antibiotic treatment had no
1571 misclassified samples. The PLS-DA verification set in Figure 2-6 contained four misclassified
1572 samples. The PLS-DA classification was able only to modestly separate distal colon antibiotic
1573 and saline subgroup treatments. It has been observed that antibiotics have a profound effect on
1574 the microbial gut community and metabolic processes in mice (42). A cultured gut microbial
1575 community can return to pre-antibiotic treatment levels approximately three weeks after
1576 treatment (53, 54). A metabolic study also determined that urinary and fecal metabolites of mice
1577 return to near control conditions three weeks after antibiotic treatment (55). However, a
1578 comprehensive pyrosequencing study of the gut microbiome found that antibiotic recovery did
1579 not return to the initial conditions, even after six weeks (56).

1580 Our findings are consistent with long-term antibiotic perturbations to the gut microbiome.
1581 Eight weeks after the antibiotic treatment, the cecal contents antibiotic treatment was still well
1582 separated from the saline treatment, and distal colon antibiotic treatment was modestly different
1583 from the saline treatment (Figure 2-6).

1584 The distal colon PLS-DA modeling of the training set for AOM treatment had no
1585 misclassifications. The verification set for the PLS-DA analysis had four misclassifications (data
1586 not shown). AOM is a carcinogen and promotes the growth of preneoplastic lesions in the colon.
1587 Previous work had suggested that a RS diet decreased the levels of preneoplastic lesions in rats
1588 given AOM (47) but preneoplastic lesions in the animals used for this study were not appreciably
1589 different among the four diet treatments (unpublished data). As described above, the cecum
1590 metabolite profile was not greatly affected by the AOM treatment. The PLS-DA distal colon
1591 analysis does appear to show that AOM may have had a minor effect on the metabolite profile in
1592 the distal colon. This could be attributed to the possibility that lesions would appear in the colon,
1593 rather than the cecum. These lesions thus would most likely not have a large effect upstream on
1594 the cecal metabolites.

1595

1596 *Biomarkers from Resistant Starch Diets*

1597 An effort was made to locate a small group of distinctive metabolites from the cecal and
1598 distal colon contents diet treatments as indicators or biomarkers for the diets. The statistical
1599 analysis of the cecal and distal colon contents yielded a vector regression plot for each diet (data
1600 not shown). The regression vectors indicated how strongly each m/z peak contributed to the
1601 PLS-DA classification of the parent diet in relation to the three diets by assigning each m/z peak
1602 a relative intensity. Mass spectral peaks that contributed a substantial weight to the variation and
1603 classification of the diets gave a strong, positive vector intensity for that diet. The absolute
1604 normalized intensity of a m/z peak within a specific diet in relation to the other diets did not
1605 necessarily predict a large vector regression coefficient. In many cases, m/z peaks had analogous
1606 intensities among multiple groups, but was considered a biomarker for only a single group. That

1607 biomarker had a high regression coefficient because the m/z peak was a key component in
1608 classifying that diet group from the others.

1609 For both cecal and distal colon contents analysis, the five or six metabolites with the
1610 strongest positive regression-vector values were examined as potential biomarkers. The accurate
1611 m/z values of these potential biomarkers were compared against the KEGG database using
1612 MassTRIX (50). The accurate mass of the biomarkers matched within an accuracy of ± 0.005
1613 Da.

1614 The potential biomarkers from each RS diet for cecal and distal colon contents are shown
1615 in Table 2-2. The biomarkers comprise a variety of compound classes ranging from amino acids
1616 and glucose to various steroids. Amino acids appear often among many of the diet categories;
1617 proline, leucine, isoleucine, valine, methionine, and phenylalanine are all present. In many cases
1618 the amino acid biomarkers that are prevalent in the cecal contents are not prevalent enough to be
1619 chosen as biomarkers for the distal colon contents. The control diet was the only diet to retain an
1620 amino acid biomarker, proline, between cecal and distal colon contents. By contrast, the control
1621 diet has leucine or isoleucine only in the cecum, while methionine appears only in the distal
1622 colon contents list. It is not apparent why the RS diets would have such variations in the
1623 prevalence of amino acid biomarkers, but the large differences between the cecum and the distal
1624 colon could be due to host absorption or differences in the bacterial community induced by the
1625 different diets. Table 2-2 also shows that many biomarkers are conserved in both the cecal and
1626 distal colon contents. Biomarkers with the m/z of 116.071, 148.134, 251.128, 321.240, 336.228,
1627 357.239, and 595.352 were observed in the cecal and distal contents in their respective diet
1628 groups. The similarity in the biomarkers between the cecal and distal colon contents correspond
1629 well with Figure 2-4. The Figure 2-4 control and StA-HA7 diets contained many of the same

1630 cecal and distal-colon contents m/z peaks. Thus, many of the most prominent biomarkers could
1631 transit the large intestine.

1632

1633 **Conclusions**

1634 Metabolite extracts of rat cecal and distal colon contents from the starch diets could be
1635 accurately fingerprinted using PLS-DA. The PLS-DA verification-set plots showed that the diet
1636 groups for the cecal and distal colon contents could be distinguished from each other. Utilizing
1637 PLS-DA, the antibiotic subgroup treatments were divided well for the cecal contents and
1638 modestly separated for the distal colon contents. Thus, the digestive system of the rats had most
1639 likely regained normal function following antibiotic treatment, but had different microbial
1640 communities. The AOM and saline treated rats partially separated based on the distal colon
1641 contents, but failed to separate for the cecal contents. The AOM treatment may not have had an
1642 effect on the cecum due to AOM targeting the colon or the time frame of AOM induced
1643 carcinogenesis may not have been reached.

1644 Future proposed work will involve studying changes in metabolites over time within the
1645 period immediately following administration of the diet. Compounds which appear to change
1646 over time will be compared to biomarkers in this study in an attempt to improve understanding of
1647 RS digestion. Also due to the variety of biomarker compounds, parallel companion studies will
1648 be run to observe polar or non-polar metabolites and to definitely identify observed compounds
1649 using MS/MS or GC/MS.

1650

1651

1652

1653 **Acknowledgement**

1654 We would like to thank Dr. Gregory J. Phillips for the use of his lab to extract the fecal
1655 metabolites (Department of Veterinary Science and Medicine, Iowa State University). We would
1656 also like to give our appreciation to Herman S. Sahota for the use of custom software to average
1657 mass spectra (Department of Computer Science, Iowa State University). This project was
1658 supported by the Iowa State University Plant Sciences Institute and supported in part by the
1659 Department of Agriculture, CSREES award number 2009-65503-05798. This research was
1660 performed in part at the Ames Laboratory. Ames Laboratory is operated for the U.S. Department
1661 of Energy by Iowa State University under contract no. DE-AC02-07CH11358.

1662

1663

1664

1665

1666

1667

1668

1669

1670

1671

1672

1673

1674 **References**

1. Sajilata, M. G.; Singhal, R. S.; Kulkarni, P. R. Resistant starch-a review. *Compr. Rev. Food Sci. Food Saf.* **2006**, *5*, 1-17.
2. Atkin, N. J.; Cheng, S. L.; Abeysekera, R. M.; Robards, A. W. Localisation of amylose and amylopectin in starch granules using enzyme-gold labelling. *Starch-Stärke* **1999**, *51*, 163-172.
3. Jane, J. Structural Features of Starch Granules II. In: *Starch: Chemistry and Technology*; 3rd Edn. BeMiller J. N.; Whistler, R. L., Eds. Academic Press Inc.: Orlando, **2009**; pp 193-227.
4. Champ, M.; Langkilde, A-M.; Brouns, F.; Kettlitz, B.; Le Bail-Collet, Y. Advances in dietary fibre characterisation. 2. Consumption, chemistry, physiology and measurement of resistant starch; implications for health and food labeling. *Nutr. Res. Rev.* **2003**, *16*, 143-161.
5. Robertson, M. D. Dietary-resistant starch and glucose metabolism. *Curr. Opin. Clin. Nutr. Metab. Care* **2012**, *15*, 362-367.
6. Saltiel, A. R.; Kahn, C. R. Insulin signalling and the regulation of glucose and lipid metabolism. *Nature* **2001**, *414*, 799-806.
7. Ranganathan, S.; Champ, M.; Pechard, C.; Blanchard, P.; Nguyen, M.; Colonna, P.; Krempf, M. Comparative study of the acute effects of resistant starch and dietary fibers on metabolic indexes in men. *Am. J. Clin. Nutr.* **1994**, *59*, 879-883.
8. Eckel, R. H.; Grundy, S. M.; Zimmet, P. Z. The metabolic syndrome. *Lancet* **2005**, *365*, 1415-1428.
9. Bodinham, C. L.; Frost, G. S.; Robertson, M. D. Acute ingestion of resistant starch reduces food intake in healthy adults. *Brit. J. Nutr.* **2010**, *103*, 917-922.
10. Gibson, G. R.; Probert, H. M.; Van Loo, J.; Rastall, R. A.; Roberfroid, M. B. Dietary modulation of the human colonic microbiota: updating the concept of prebiotics. *Nutr. Res. Rev.* **2004**, *17*, 259-275.
11. Jenkins, D. J. A.; Vuksan, V.; Kendall, C. W. C.; Würsch, P.; Jeffcoat, R.; Waring, S.; Mehling, C. C.; Vidgen, E.; Augustin, L. S. A.; Wong, E. Physiological effects of resistant starches on fecal bulk, short chain fatty acids, blood lipids and glycemic index. *J. Am. Coll. Nutr.* **1998**, *17*, 609-616.
12. Nilsson, A. C.; Östman, E. M.; Knudsen, K. E. B.; Holst, J. J.; Björck, I. M. E. A cereal-based evening meal rich in indigestible carbohydrates increases plasma butyrate the next morning. *J. Nutr.* **2010**, *140*, 1932-1936.
13. Ding, S.; Chi, M. M.; Scull, B. P.; Rigby, R.; Schwerbrock, N. M. J.; Magness, S.; Jobin, C.; Lund, P. K. High-fat diet: bacteria interactions promote intestinal inflammation which precedes and correlates with obesity and insulin resistance in mouse. *PLOS One* **2010**, *5*, e12191.
14. Brown, I. L.; Wang, X.; Topping, D. L.; Playne, M. J.; Conway, P. L. High amylose maize starch as a versatile prebiotic for use with probiotic bacteria. *Food Aust.* **1998**, *50*, 603-610.
15. Roberfroid, M. B. Functional foods: concepts and applications to inulin and oligofructose. *Brit. J. Nutr.* **2002**, *87*, S139-S143.
16. Tuohy, K. M.; Ziemer, C. J.; Klinder, A.; Knöbel, Y.; Pool-Zobel, B. L.; Gibson, G. R. A human volunteer study to determine the prebiotic effects of lactulose powder on human colonic microbiota. *Microb. Ecol. Health Dis.* **2002**, *14*, 165-173.

1720 17. Ito, M.; Kimura, M.; Deguchi, Y.; Miyamori-Watabe, A.; Yajima, T.; Kan, T. Effects of
 1721 transgalactosylated disaccharides on the human intestinal microflora and their
 1722 metabolism. *J. Nutr. Sci. Vitaminol.* **1993**, *39*, 279-288.

1723 18. Marotti, I.; Bregola, V.; Aloisio, I.; Di Gioia, D.; Bosi, S.; Di Silvestro, R.; Quinn, R.;
 1724 Dinelli, G. Prebiotic effect of soluble fibres from modern and old durum-type wheat
 1725 varieties on *Lactobacillus* and *Bifidobacterium* strains. *J. Sci. Food Agric.* **2012**, *92*,
 1726 2133-2140.

1727 19. Kritchevsky, D. (1995) Epidemiology of fibre, resistant starch and colorectal cancer. *Eur.*
 1728 *J. Cancer Prev.* **1995**, *4*, 345-352.

1729 20. van Munster, I. P.; Tangeman, A.; Nagengast, F. M. Effect of resistant starch on colonic
 1730 fermentation, bile acid metabolism, and mucosal proliferation. *Digest Dis. Sci.* **1994**, *39*,
 1731 834-842.

1732 21. Hamer, H. M.; De Preter, V.; Windey, K.; Verbeke, K. Functional analysis of colonic
 1733 bacterial metabolism: relevant to health? *Am. J. Physiol. Gastrointest. Liver Physiol.*
 1734 **2012**, *302*, G1-G9.

1735 22. Yin, P.; Zhao, X.; Li, Q.; Wang, J.; Li, J.; Xu, G. Metabonomics study of intestinal
 1736 fistulas based on ultraperformance liquid chromatography coupled with Q-TOF mass
 1737 spectrometry (UPLC/Q-TOF MS). *J. Proteome Res.* **2006**, *5*, 2135-2143.

1738 23. Williams, R. E.; Lenz, E. M.; Evans, J. A.; Wilson, I. D.; Granger, J. H.; Plumb, R. S.;
 1739 Stumpf, C. L. A combined ¹H NMR and HPLC-MS-based metabonomic study of urine
 1740 from obese (fa/fa) Zucker and normal Wistar-derived rats. *J. Pharm. Biomed. Anal.* **2005**,
 1741 *38*, 465-471.

1742 24. Poroyko, V.; Morowitz, M.; Bell, T.; Ulanov, A.; Wang, M.; Donovan, S.; Bao, N.; Gu,
 1743 S.; Hong, L.; Alverdy, J. C.; Bergelson, J.; Liu, D. C. Diet creates metabolic niches in the
 1744 "immature gut" that shape microbial communities. *Nutr. Hosp.* **2011**, *26*, 1283-1295.

1745 25. Mellert, W.; Kapp, M.; Strauss, V.; Wiemer, J.; Kamp, H.; Walk, T.; Looser, R.;
 1746 Prokoudine, A.; Fabian, E.; Krennrich, G.; Herold, M.; van Ravenzwaay, B. Nutritional
 1747 impact on the plasma metabolome of rats. *Toxicol. Lett.* **2011**, *207*, 173-181.

1748 26. Legido-Quigley, C.; Stella, C.; Perez-Jimenez, F.; Lopez-Miranda, J.; Ordovas, J.;
 1749 Powell, J.; van-der-Ouderaa, F.; Ware, L.; Lindon, J. C.; Nicholson, J. K.; Holmes, E.
 1750 Liquid chromatography-mass spectrometry methods for urinary biomarker detection in
 1751 metabonomic studies with application to nutritional studies. *Biomed. Chromatogr.* **2010**,
 1752 *24*, 737-743.

1753 27. Ventura, M.; Turroni, F.; Canchaya, C.; Vaughan, E. E.; O'Toole, P. W.; van Sinderen,
 1754 D. Microbial diversity in the human intestine and novel insights from metagenomics.
 1755 *Front Biosci.* **2009**, *14*, 3214-3221.

1756 28. Englyst, H. N.; Kingman, S. M.; Cumming, J. H. Classification and measurement of
 1757 nutritionally important starch fractions. *Eur. J. Clin. Nutr.* **1992**, *46*, S33-S50.

1758 29. Baghurst, P. A.; Baghurst, K. I.; Record, S. J. Dietary fibre, non-starch polysaccharides
 1759 and resistant starch-a review. *Food Aust.* **1996**, *48*, S3-S35.

1760 30. Hasjim, J.; Lee, S-O.; Hendrich, S.; Setiawan, S.; Ai, Y.; Jane, J. Characterization of
 1761 novel resistant-starch and its effects on postprandial plasma-glucose and insulin
 1762 responses. *Cereal Chem.* **2010**, *87*, 257-262.

1763 31. Dettmer, K.; Aronov, P. A.; Hammock, B. D. Mass spectrometry-based metabolomics.
 1764 *Mass Spectrom. Rev.* **2007**, *26*, 51-78.

1765 32. Scalbert, A.; Brennan, L.; Fiehn, O.; Hankemeier, T.; Kristal, B. S.; van Ommen, B.;
 1766 Pujos-Guillot, E.; Verheij, E.; Wishart, D.; Wopereis, S. Mass-spectrometry-based
 1767 metabolomics: limitations and recommendations for future progress with particular focus
 1768 on nutrition research. *Metabolomics* **2009**, *5*, 435-458.

1769 33. Vitali, B.; Ndagijimana, M.; Maccaferri, S.; Biagi, E.; Guerzoni, M. E.; Brigidi, P. An *in*
 1770 *vitro* evaluation of the effect of probiotics and prebiotics on the metabolic profile of
 1771 human microbiota. *Anaerobe* **2012**, *18*, 386-391.

1772 34. Blokland, M. H.; Van Tricht, E. F.; Van Rossum, H. J.; Sterk, S. S.; Nielen, M. W. F.
 1773 Endogenous steroid profiling by gas chromatography-tandem mass spectrometry and
 1774 multivariate statistics for the detection of natural hormone abuse in cattle. *Food Addit.*
 1775 *Contam. A.* **2012**, *29*, 1030-1045.

1776 35. Tsugawa, H.; Tsujimoto, Y.; Arita, M.; Bamba, T.; Fukusaki, E.; GC/MS based
 1777 metabolomics: development of a data mining system for metabolite identification by
 1778 using soft independent modeling of class analogy (SIMCA). *BMC Bioinformatics* **2011**,
 1779 *12*, 131.

1780 36. Plumb, R. S.; Granger, J. H.; Stumpf, C. L.; Johnson, K. A.; Smith, B. W.; Gaulitz, S.;
 1781 Wilson, I. D., Castro-Perez, J. A rapid screening approach to metabonomics using UPLC
 1782 and oa-TOF mass spectrometry: application to age, gender and diurnal variation in
 1783 normal/Zucker obese rats and black, white and nude mice. *Analyst* **2005**, *130*, 844-849.

1784 37. Mateos-Martín, M. L.; Pérez-Jiménez, J.; Fuguet, E.; Torres, J. L. Non-extractable
 1785 proanthocyanidins from grapes are a source of bioavailable (epi)catechin and derived
 1786 metabolites in rats. *Br. J. Nutr.* **2012**, *108*, 290-297.

1787 38. Ohashi, Y.; Hirayama, A.; Ishikawa, T.; Nakamura, S.; Shimizu, K.; Ueno, Y.; Tomita,
 1788 M.; Soga, T. Depiction of metabolome changes in histidine-starved *Escherichia coli* by
 1789 CE-TOFMS. *Mol. Biosyst.* **2008**, *4*, 135-147.

1790 39. Matsumoto, M.; Kibe, R.; Ooga, T.; Aiba, Y.; Kurihara, S.; Sawaki, E.; Koga, Y.; Benno,
 1791 Y.; Impact of intestinal microbiota on intestinal luminal metabolome. *Scientific Reports*
 1792 **2012**, *2*, 233.

1793 40. Ooga, T.; Sato, H.; Nagashima, A.; Sasaki, K.; Tomita, M.; Soga, T.; Ohashi, Y.
 1794 Metabolomic anatomy of an animal model revealing homeostatic imbalances in
 1795 dyslipidaemia. *Mol. Biosyst.* **2011**, *7*, 1217-1223.

1796 41. Hasegawa, M.; Ide, M.; Kuwamura, M.; Yamate, J.; Takenaka, S. Metabolic
 1797 fingerprinting in toxicological assessment using FT-ICR MS. *J. Toxicol. Pathol.* **2010**,
 1798 *23*, 67-74.

1799 42. Antunes, L. C. M.; Han, J.; Ferreira, R. B. R.; Lolić, P.; Borchers, C. H.; Finlay, B. B.
 1800 Effect of antibiotic treatment on the intestinal metabolome. *Antimicrob. Agents*
 1801 *Chemother.* **2011**, *55*, 1494-1503.

1802 43. Rath, C. M.; Alexandrov, T.; Higginbottom, S. K.; Song, J.; Milla, M. E.; Fischbach, M.
 1803 A.; Sonnenburg, J. L.; Dorrestein, P. C. Molecular analysis of model gut microbiotas by
 1804 imaging mass spectrometry and nanodesorption electrospray ionization reveals dietary
 1805 metabolite transformations. *Anal. Chem.* **2012**, *84*, 9259-9267.

1806 44. Chen, Y.; Zhu, S. B.; Xie, M. Y.; Nie, S. P.; Liu, W.; Li, C.; Gong, X. F.; Wang, Y. X.
 1807 Quality control and original discrimination of *Ganoderma lucidum* based on high-
 1808 performance liquid chromatographic fingerprints and combined chemometrics methods.
 1809 *Anal. Chim. Acta* **2008**, *623*, 146-156.

1810 45. Fremout, W.; Kuckova, S.; Crhova, M.; Sanyova, J.; Saverwyns, S.; Hynek, R.; Kodicek,
1811 M.; Vandenabeele, P.; Moens, L. Classification of protein binders in artist's paints by
1812 matrix-assisted laser desorption/ionisation time-of-flight mass spectrometry: an
1813 evaluation of principal component analysis (PCA) and soft independent modeling of class
1814 analogy (SIMCA). *Rapid Commun. Mass Spectrom.* **2011**, *25*, 1631-1640.

1815 46. Benabdelkamel, H.; Di Donna, L.; Mazzotti, F.; Naccarato, A.; Sindona, G.; Tagarelli,
1816 A.; Taverna, D. (2012) Authenticity of PGI "Clementine of Calabria" by multielement
1817 fingerprint. *J. Agric. Food Chem.* **2012**, *60*, 3717-3726.

1818 47. Zhao, Y.; Hasjim, J.; Li, L.; Jane, J.; Hendrich, S.; Birt, D. F. Inhibition of
1819 azoxymethane-induced preneoplastic lesions in the rat colon by a cooked stearic acid
1820 complexed high-amylose cornstarch. *J. Agric. Food Chem.* **2011**, *59*, 9700-9708.

1821 48. Reeves, P. G. Components of the AIN-93 diets as improvements in the AIN-76A diet. *J.*
1822 *Nutr.* **1997**, *127*, 838S-841S.

1823 49. Zhang, B.; Huang, Q.; Luo, F.; Fu, X.; Jiang, H.; Jane, J. Effects of octenylsuccinylation
1824 on the structure and properties of high-amylose maize starch. *Carbohydr. Polym.* **2011**,
1825 *84*, 1276-1281.

1826 50. Suhre, K.; Schmitt-Kopplin, P. MassTRIX: mass translator into pathways. *Nucleic Acids*
1827 *Res.* **2008**, *36*, W481-W484 (Web Server Issue).

1828 51. Westerhuis, J. A.; de Jong, S.; Smilde, A. K. Direct orthogonal signal correction.
1829 *Chemometr. Intell. Lab. Sys.* **2001**, *56*, 13-25.

1830 52. Anderson, T. J.; Ai, Y.; Jones, R. W.; Houk, R. S.; Jane, J.; Zhao, Y.; Birt, D. F.;
1831 McClelland, J. F. Analysis of resistant starches in rat cecal contents using Fourier
1832 transform infrared photoacoustic spectroscopy. *J. Agric. Food Chem.* **2013**, *61*, 1818-
1833 1822.

1834 53. Croswell, A.; Amir, E.; Teggatz, P.; Barman, M.; Salzman, N. H. Prolonged impact of
1835 antibiotics on intestinal microbial ecology and susceptibility to enteric *Salmonella*
1836 infection. *Infect. Immun.* **2009**, *77*, 2741-2753.

1837 54. Manichanh, C.; Reeder, J.; Gibert, P.; Varela, E.; Llopis, M.; Antolin, M.; Guigo, R.;
1838 Knight, R.; Guarner, F. Reshaping the gut microbiome with bacterial transplantation and
1839 antibiotic intake. *Genome Res.* **2010**, *20*, 1411-1419.

1840 55. Zhung, X.; Xie, G.; Zhao, A.; Zhao, L.; Yao, C.; Chiu, N. H. L.; Zhou, Z.; Bao, Y.; Jia,
1841 W.; Nicholson, J. K.; Jia, W. The footprints of gut microbial-mammalian co-metabolism.
1842 *J. Proteome Res.* **2011**, *10*, 5512-5522.

1843 56. Antonopoulos, D. A.; Huse, S. M.; Morrison, H. G.; Schmidt, T. M.; Sogin, M. L.;
1844 Young, V. B. Reproducible community dynamics of the gastrointestinal microbiota
1845 following antibiotic perturbation. *Infect. Immun.* **2009**, *77*, 2367-2375.

1846

1847

1848

1849

1850

1851

1852 **Table 2-1**

1853 Metabolite Peaks Found in (C) Cecal and (D) Distal Colon Samples as Shown in Figures 2-1 through 2-3

Peak	m/z	Control	HA7	OS-HA7	StA-HA7
a	116.071	D			D
b	118.087	D	C D	C D	C D
c	121.065			C	
d	132.102	C D	C D	C D	C D
e	141.066		C		C
f	141.112	C			C
g	148.134	C D	C		C D
h	166.087	C D		C D	C D
i	173.129		C		C
j	195.113		C D		C D
k	212.14		C	C	C D
l	217.104				D
m	229.151			D	
n	230.187		C D		C D
o	242.187				D
p	251.128			C D	
q	273.108			D	
r	276.134		C D		C D
s	277.129		C D	C	C D
t	321.240				C D
u	335.219				C
v	336.228		D		D
w	357.239			C D	
x	373.274	D			D
y	377.265	C			
z	378.269	C			
aa	379.280	C			
ab	393.242	C	C		
ac	409.164				D
ad	479.263			C D	
ae	501.246			D	
af	563.268		D		
ag	591.322			C	
ah	595.352	D			C D
ai	733.559	C			
aj	737.286			C D	
ak	839.565				C D

1854

1855 **Table 2-2**

Biomarkers with Substantial Contribution to Class Differentiation Matched to KEGG Database for Cecal Contents

Cecal Contents	m/z	Compound ^a	Molecular Formula
Control	116.071	Proline [M+H] ⁺	C ₅ H ₉ NO ₂
	132.102	Leucine [M+H] ⁺	C ₆ H ₁₃ NO ₂
	132.102	Isoleucine [M+H] ⁺	C ₆ H ₁₃ NO ₂
	148.134	No Database Match	Unknown
	377.265	3-Acetyl-5alpha-androstane-3beta,17beta-diol 3-acetate [M+H] ⁺	C ₂₃ H ₃₆ O ₄
	595.350	L-Stercobilin [M+H] ⁺	C ₃₃ H ₄₆ N ₄ O ₆
HA7 Diet	118.087	Valine [M+H] ⁺	C ₅ H ₁₁ NO ₂
	141.113	No Database Match	Unknown
	161.093	Alanyl-alanine [M+H] ⁺	C ₆ H ₁₂ N ₂ O ₃
	161.093	Nonadienal [M+Na] ⁺	C ₉ H ₁₄ O
	203.053	Glucose [M+Na] ⁺	C ₆ H ₁₂ O ₆
	336.228	12-hydroxyicosa-trienoic acid [M+H] ⁺	C ₂₀ H ₃₁ O ₄
OS-HA7	251.129	Methylripariochromene A [M+H] ⁺	C ₁₄ H ₁₈ O ₄
	294.157	No Database Match	Unknown
	357.238	Allotetrahydrodeoxycorticosterone [M+Na] ⁺	C ₂₁ H ₃₄ O ₃
	479.263	No Database Match	Unknown
	591.322	Urobilin [M+H] ⁺	C ₃₃ H ₄₂ N ₄ O ₆
	591.322	Deoxycholic acid 3-glucuronide [M+Na] ⁺	C ₃₀ H ₄₈ O ₁₀
StA-HA7	242.187	No Database Match	Unknown
	276.134	Alanyltryptophan [M+H] ⁺	C ₁₄ H ₁₇ N ₃ O ₃
	277.129	Homoanserine [M+Na] ⁺	C ₁₁ H ₁₈ N ₄ O ₃
	321.240	Oxoctadecanoic acid [M+Na] ⁺	C ₁₈ H ₃₄ O ₃
	321.240	hydroxy-Eicosatetraenoic acid [M+H] ⁺	C ₂₀ H ₃₂ O ₃
	335.219	hydroperoxy, octadecadienoic acid [M+Na] ⁺	C ₁₈ H ₃₂ O ₄

1856 ^aNotation refers to the stated molecule (M) and the observed adduct bracketed with the positive charge

1857

1858

1859

1860

1861

1862

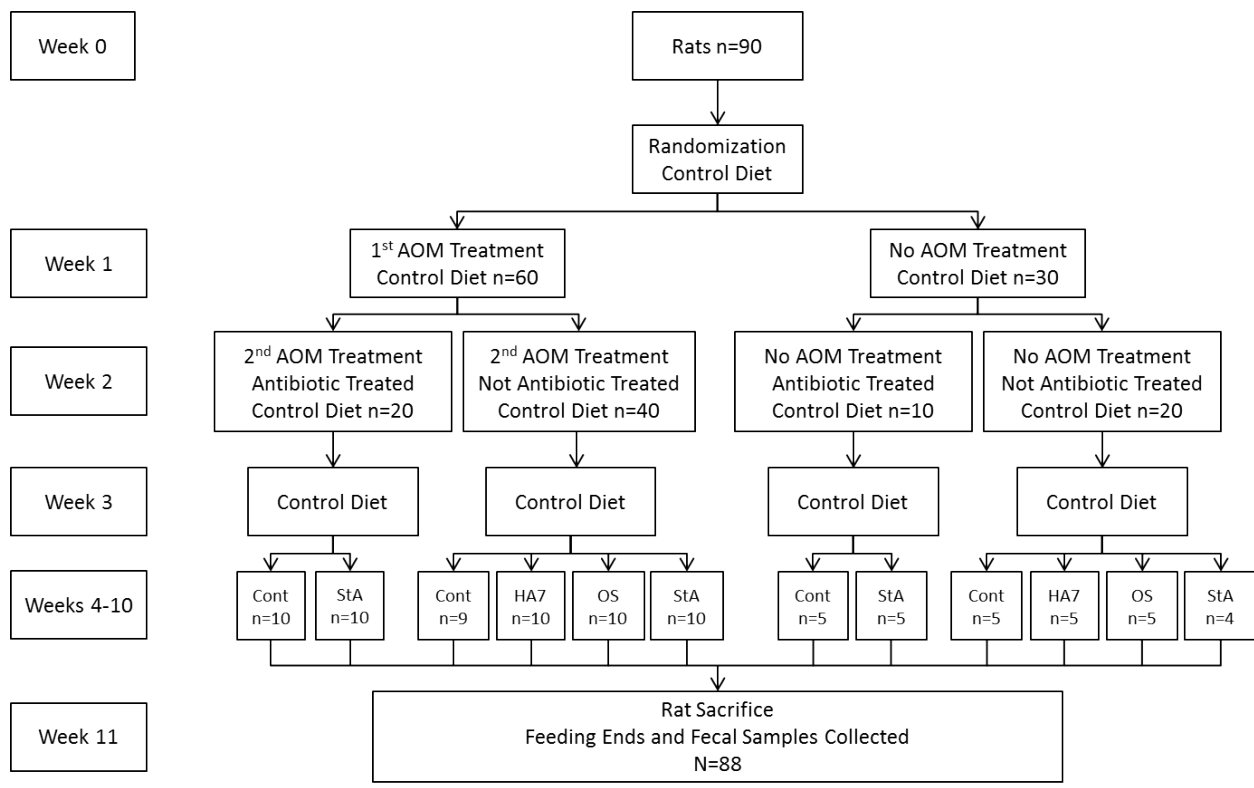
1863 **Table 2-3**

Biomarkers with Substantial Contribution to Class Differentiation Matched to KEGG Database for Distal Colon Contents

Distal Contents	m/z	Compound ^a	Molecular Formula
Control	116.071	Proline [M+H] ⁺	C ₅ H ₉ NO ₂
	141.111	No Database Match	Unknown
	148.134	No Database Match	Unknown
	150.059	Methionine [M+H] ⁺	C ₅ H ₁₁ NO ₂ S
	595.353	L-Stercobilin [M+H] ⁺	C ₃₃ H ₄₆ N ₄ O ₆
HA7 Diet	230.187	No Database Match	Unknown
	254.155	Gamma-Aminobutyryl-lysine [M+Na] ⁺	C ₁₀ H ₂₁ N ₃ O ₃
	255.147	Homoanserine [M+H] ⁺	C ₁₁ H ₁₈ N ₄ O ₃
	336.228	12-hydroxyicosa-trienoic acid [M+H] ⁺	C ₂₀ H ₃₁ O ₄
	563.268	Protoporphyrin [M+Na] ⁺	C ₃₄ H ₃₄ N ₄ O ₄
OS-HA7	118.087	Valine [M+H] ⁺	C ₅ H ₁₁ NO ₂
	212.140	No Database Match	Unknown
	251.127	Methylripariochromene A [M+H] ⁺	C ₁₄ H ₁₈ O ₄
	294.162	No Database Match	Unknown
	357.240	Allotetrahydrodeoxycorticosterone [M+Na] ⁺	C ₂₁ H ₃₄ O ₃
StA-HA7	737.286	No Database Match	Unknown
	116.071	Proline [M+H] ⁺	C ₅ H ₉ NO ₂
	124.039	Picolinic acid [M+H] ⁺	C ₆ H ₅ NO ₂
	166.087	Phenylalanine [M+H] ⁺	C ₉ H ₁₁ NO ₂
	166.087	Stachydrine [M+Na] ⁺	C ₇ H ₁₃ NO ₂
	212.140	No Database Match	Unknown
	321.240	Oxoctadecanoic acid [M+Na] ⁺	C ₁₈ H ₃₄ O ₃
	321.240	hydroxy-Eicosatetraenoic acid [M+H] ⁺	C ₂₀ H ₃₂ O ₃
	409.164	Burseran [M+Na] ⁺	C ₂₂ H ₂₆ O ₆
	409.164	1,2-Dihydro-5-hydroxy-2-(1-hydroxy-1-methylethyl)-4-(isobutyryl)-6-phenylfuran-8-one [M+H] ⁺	C ₂₄ H ₂₄ O ₆

1864 ^aNotation refers to the stated molecule (M) and the observed adduct bracketed with the positive charge

1865



1866

1867 **Figure 2-1** Flow diagram of the animal study detailing the treatment schedule for AOM,
1868 antibiotic, and diet up until sacrifice. The diets that were given for weeks 4-10 are represented as
1869 the abbreviations cont (Control), HA7 (HA7), OS (OS-HA7), and StA (StA-HA7). The amount
1870 of rats in each group of the flow chart are represented by the letter “n”

1871

1872

1873

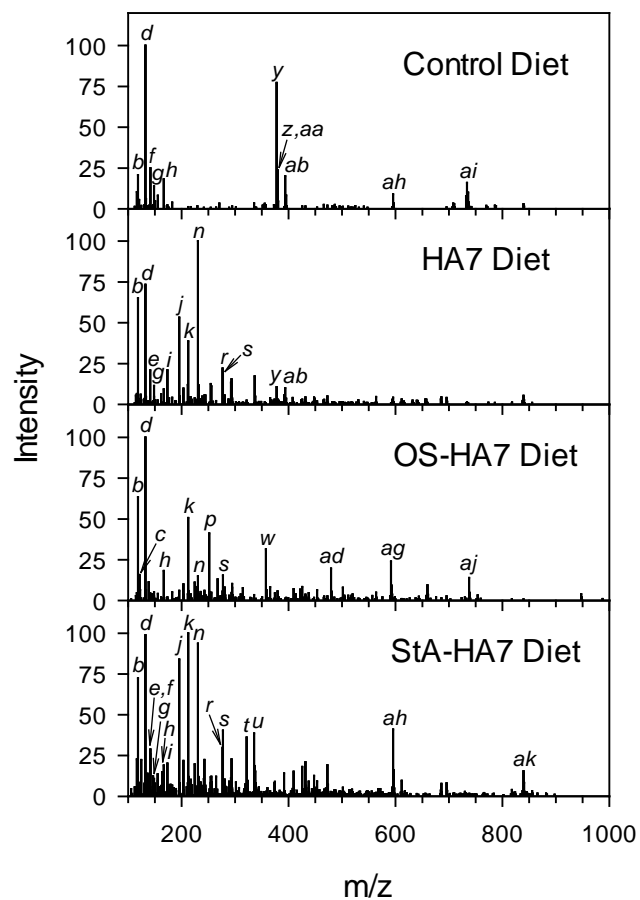
1874

1875

1876

1877

1878



1879

1880 **Figure 2-2** Averaged mass spectra of cecal content samples from each diet group with no AOM
 1881 or antibiotic treatments. The peak intensities have been normalized against the strongest peak in
 1882 the spectrum for each diet. The most prominent metabolite peaks in each diet have been labeled
 1883 and can be matched to their respective m/z in Table 2-1

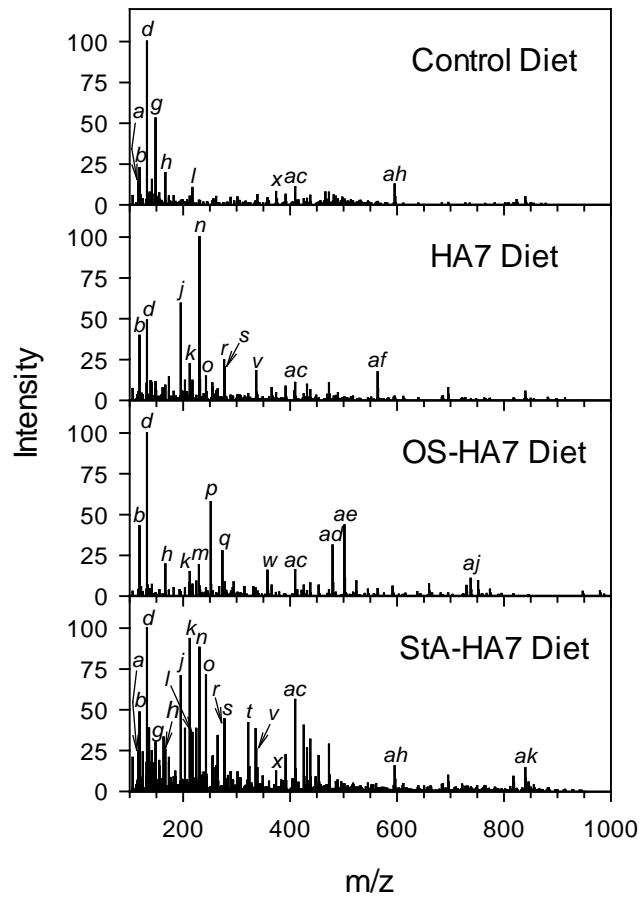
1884

1885

1886

1887

1888



1889

1890 **Figure 2-3** Averaged mass spectra of distal colon content samples from each diet group with no
 1891 AOM or antibiotic treatments. The peak intensities have been normalized against the strongest
 1892 peak in the spectrum for each diet. The most prominent metabolite peaks in each diet have been
 1893 labeled and can be matched to their respective m/z in Table 2-1

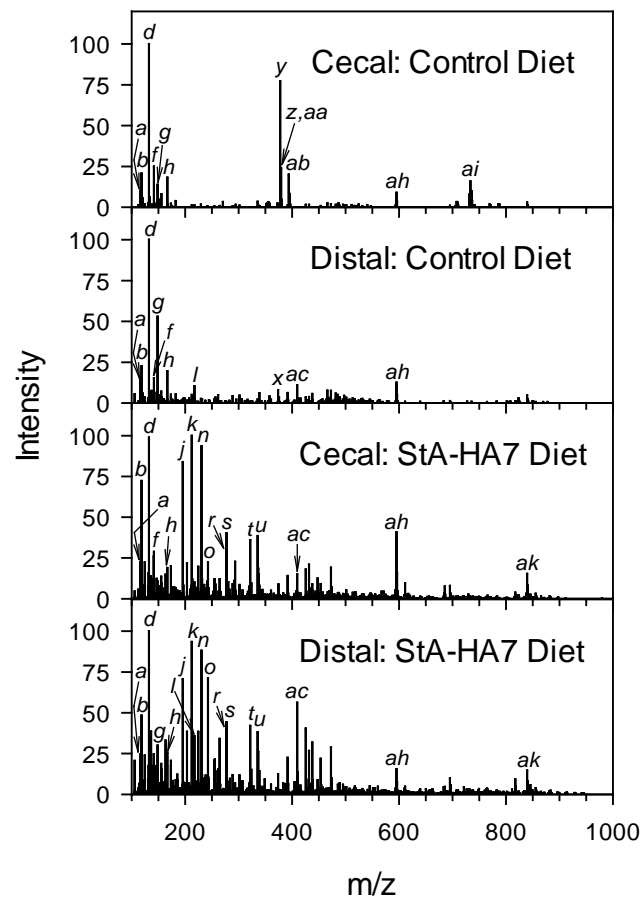
1894

1895

1896

1897

1898



1899

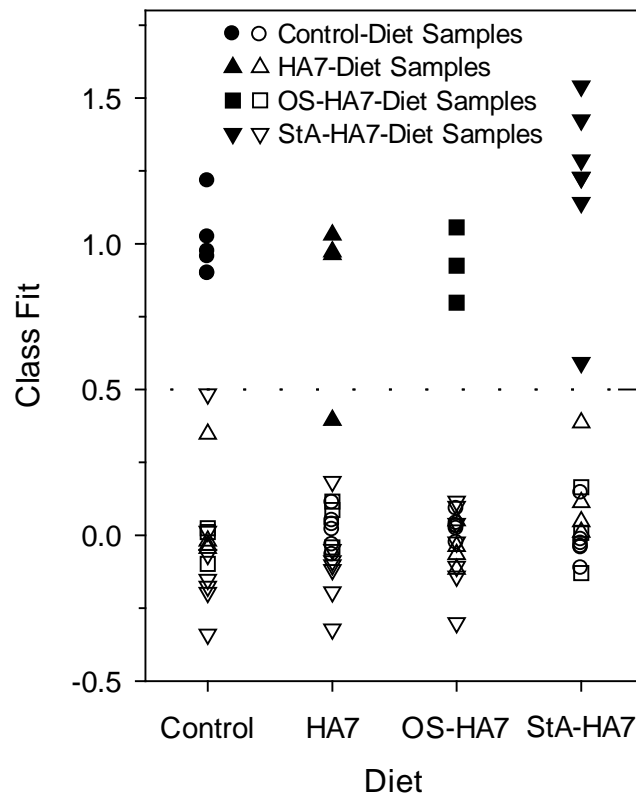
1900 **Figure 2-4** Averaged mass spectra comparison of cecal and distal colon content samples from
 1901 two example diets with no AOM or antibiotic treatments. The peak intensities have been
 1902 normalized against the strongest peak in the spectrum for each diet. The most prominent
 1903 metabolite peaks in the spectra have been labeled and can be matched to their respective m/z in
 1904 Table 2-1

1905

1906

1907

1908



1909

1910 **Figure 2-5** PLS-DA analysis of cecal-content verification-set samples for diet treatments,
 1911 including AOM and antibiotic treated samples. The solid markers represent the samples that
 1912 belong to the tested class and should ideally have a class fit value of 1.0. The open markers
 1913 correspond to samples which do not belong to the tested class and ideally have a class fit of 0

1914

1915

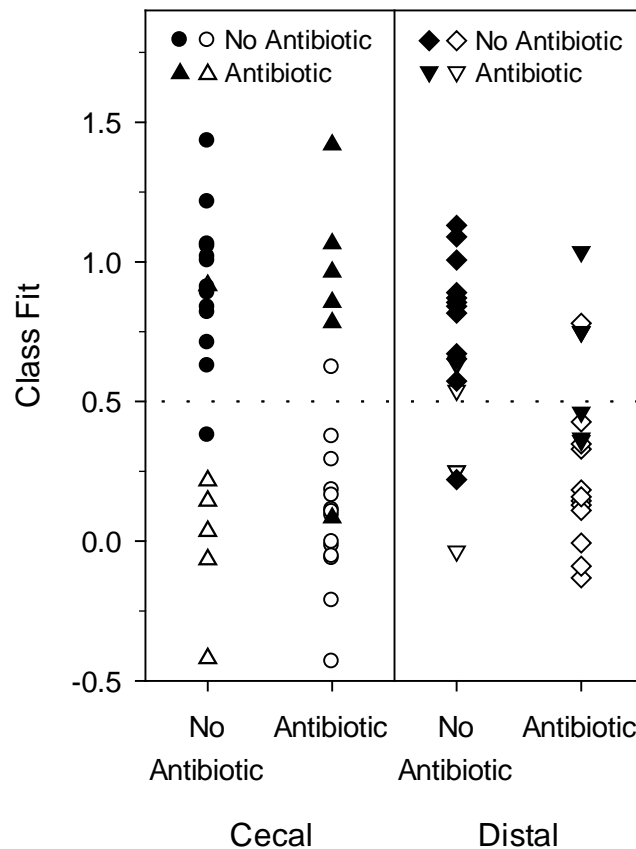
1916

1917

1918

1919

1920



1921

1922 **Figure 2-6** PLS-DA analysis of cecal-content and distal-colon-content verification-set samples
 1923 for antibiotic treatment, including diets and AOM treated samples. The solid markers represent
 1924 the samples that belong to the tested class and should ideally have a class fit value of 1.0. The
 1925 open markers correspond to sample which do not belong to the tested class and ideally have a
 1926 class fit of 0

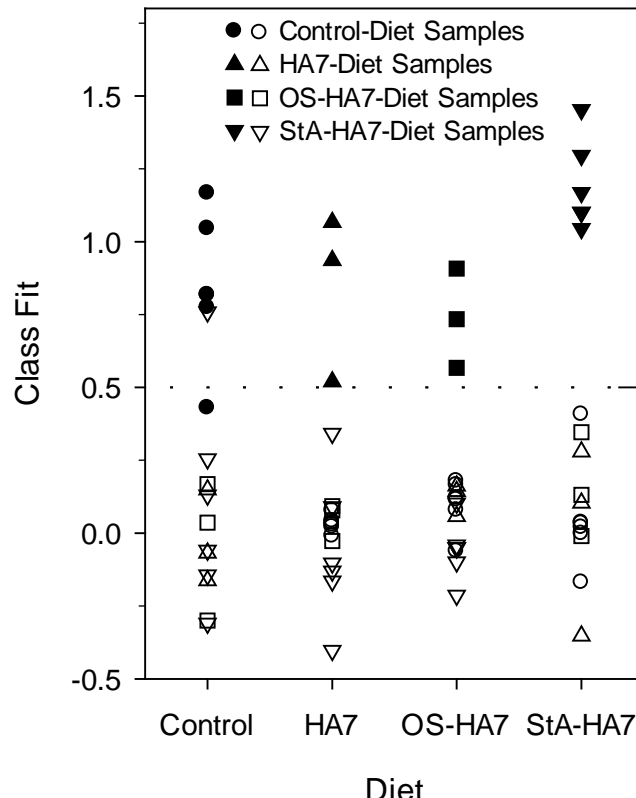
1927

1928

1929

1930

1931



1932

1933 **Figure 2-7** PLS-DA analysis of distal-colon-content verification-set samples for diet treatments,
 1934 including AOM and antibiotic treated samples. The solid markers represent the samples that
 1935 belong to the tested class and should ideally have a class fit value of 1.0. The open markers
 1936 correspond to samples which do not belong to the tested class and ideally have a class fit of 0

1937

1938

1939

1940

1941

1942

1943

1944

1945

1946

1947 **CHAPTER 3**

1948

1949

1950

1951 **COMPREHENSIVE IDENTIFICATION OF ALPHA-ZEIN PROTEINS BY HIGH -**
1952 **PERFORMANCE LIQUID CHROMATOGRAPHY ACCURATE MASS TIME-OF-**
1953 **FLIGHT MASS SPECTROMETRY**

1954

1955 Paper submitted to *The Journal of Agricultural and Food Chemistry*.

1956

1957 By

1958

1959 Derrick L. Morast,^{1,2,3,4} Timothy J. Anderson,^{1,2,4} R. S. Houk^{1,2*}

1960

1961 ¹Ames Laboratory-USDOE, Iowa State University, Ames, Iowa 500111962 ²Department of Chemistry, Iowa State University, Ames, Iowa 500111963 ³Present address: Exxon Mobil Refining & Supply, Baytown TX 77520 USA1964 ⁴These authors contributed equally to this work

1965

1966

1967

1968

1969

1970

1971

1972

1973

1974

1975

1976 * Corresponding Author. Tel: 1-515-294-9462 Fax -0050 rshouk@iastate.edu

1977 **Abstract**

1978 High-resolution mass spectrometry (HRMS) was used to detect many proteins in α -zein samples
1979 extracted from corn gluten meal (CGM) and distillers' dried grains with solubles (DDGS).
1980 High-performance liquid chromatography (LC) was utilized for the separation of the complex
1981 protein samples. Proteins were introduced into the mass spectrometer via electrospray ionization
1982 (ESI). Measured molecular weights (M_r) were compared with protein database values and
1983 previous mass spectrometric α -zein analyses. Overall, 95 α -zein proteins were identified; 49 of
1984 these had M_r values similar to those of previously reported proteins. The remaining 46 proteins
1985 are identified for the first time. Interestingly, the α -zein extracted from DDGS contained many
1986 of the same intact proteins observed in the CGM extract, despite the fermentation and thermal
1987 processes used to convert dry milled corn to DDGS.

1988

1989

1990

1991

1992

1993

1994

1995

1996

1997

1998 **Keywords** Zein, corn gluten meal, CGM, distillers dried grains with solubles, DDGS, high-
1999 resolution mass spectrometry, high-performance liquid chromatography

2000 **Introduction**

2001 Zeins, also known as corn prolamines, are alcohol-soluble storage proteins. Their main function
2002 is to provide nitrogen during germination. Zein proteins have a high content of glutamine and
2003 proline and are insoluble in water. There are currently many commercial applications for zeins,
2004 especially in adhesives and plastics. There is considerable interest in utilizing zein as a polymeric
2005 material for films, coatings, and plastics since it is both biodegradable and renewable (1-4).

2006 Several methods have been reported for the extraction of zeins from maize endosperm (5-
2007 8), along with corresponding nomenclature systems. The most widely used nomenclature,
2008 described by Esen and used herein, classifies zein fractions as α -, β -, γ -, and δ -zeins based on
2009 differences in solubility and amino acid sequence (9, 10). Of the four fractions, α -zein is the
2010 most abundant, containing 75 to 85% of total zein proteins. They range in size from 210 to 245
2011 amino acids and are commonly divided into two groups, $M_r \sim 22$ kDa and $M_r \sim 19$ kDa, based
2012 on relative SDS-PAGE migration. The protein sequences are $\sim 90\%$ homologous within each
2013 group and $\sim 60\%$ homologous between the two groups (11). The α -zein proteins contain high
2014 levels of glutamine ($\sim 25\%$), leucine ($\sim 20\%$), alanine ($\sim 15\%$), and proline ($\sim 11\%$) (12).

2015 Zein is produced from corn using four different methods, two of which will be discussed
2016 further. Corn wet-milling and the dry-grind ethanol process both generate coproducts which
2017 contain α -zein proteins. CGM, a coproduct of the corn wet-milling process, can contain between
2018 62 to 74% protein (13). Many commercially useful applications have been found for CGM and
2019 most commercial zein extraction methods remove mainly α -zein proteins from CGM (14, 15).
2020 For this reason, CGM is fairly valuable and currently sells for around \$550/ton.

2021 The dry-grind ethanol process used for the production of ethanol from corn generates
2022 DDGS as a coproduct. Protein content in DDGS is about 28 to 30% (16). During the ethanol

2023 process, a high-temperature cooking step (90 to 105 °C for 1 to 3 hrs) is used, which may alter
2024 the α -zein proteins. Only small scale extractions of α -zein proteins from DDGS have been
2025 reported (17). DDGS has found little commercial application outside of use as livestock feed
2026 and currently sells for only \$100/ton or less.

2027 These α -zein extraction procedures yield complex mixtures of many proteins. Mass
2028 spectrometry (MS) is a powerful tool for the analysis of such protein mixtures. When ionized by
2029 electrospray ionization (ESI), protein cations are highly charged and are observed in a wide
2030 variety of charge states. This charge state distribution allows for the molecular weight of the
2031 protein to be calculated from many measured values of mass-to-charge ratio (m/z). A high-
2032 resolution mass spectrometer (HRMS) measures m/z values more accurately than lower
2033 resolution instruments. In favorable cases, individual proteins can often be identified in complex
2034 mixtures by HRMS alone (18, 19), especially if isotope peaks within individual charge states can
2035 be resolved, and protein extracts can be sufficiently purified for a predicted protein class.

2036 High-performance liquid chromatography (LC) is very useful for separation of protein
2037 mixtures. However, the complexity of the α -zein sample and the sequence homology of the α -
2038 zein proteins make it difficult to get complete separation with LC alone. A previous 2-
2039 dimensional electrophoresis study identified 41 α -zein proteins and it was noted that this number
2040 was well below the estimated number of α -zein genes in the genome (20). One benefit of using
2041 HRMS is that baseline LC separation of the proteins is often not necessary. Also, deconvolution
2042 software can classify most co-eluting proteins.

2043 To our knowledge, all previous maize protein separations by LC used UV absorbance
2044 detection instead of MS. Although LC/UV has many useful applications, the lack of mass
2045 information limits its ability to identify proteins in such complex mixtures. In particular, it is

2046 difficult to identify proteins from retention time alone unless the analytes are almost baseline
2047 resolved and retention time is compared against purified reference standards of each protein of
2048 interest. Given the inability of LC to baseline separate each α -zein protein and the lack of
2049 standards, identification of coeluting compounds in very complex mixtures by UV absorbance
2050 detection alone is difficult.

2051 Capillary electrophoresis (CE) has been coupled to a mass spectrometer via ESI for the
2052 analysis of maize proteins (21, 22). CE generally provides a faster separation with higher
2053 resolution than LC, however coupling CE to a mass spectrometer is not as straightforward. For
2054 that reason, LC is a more widely used technique with MS detection.

2055 The present work compares LC-MS results for zeins to those reported by others using
2056 CE-MS and MALDI-MS. Many new zein proteins are reported here.

2057

2058 **Materials and Methods**

2059 *Alpha-Zein Protein Extraction*

2060 CGM was obtained from Cargill, Inc. (Eddyville, IA) and DDGS was obtained from
2061 Lincolnway Energy (Nevada, IA). The CGM and DDGS extraction methods were reported
2062 previously (23, 24). A variety of solvent systems were employed. For CGM, a total of ten
2063 samples were extracted using five different solvent systems: 88% aqueous 2-propanol (IPA),
2064 70% aqueous IPA, 55% aqueous IPA, 70% aqueous IPA with 22.5% glycerol, and 70% aqueous
2065 ethanol (EtOH). Each extraction was done with or without sodium hydroxide (NaOH) and a
2066 reductant (sodium bisulfite). For DDGS, a total of 6 samples were extracted using three different
2067 solvent systems: 88% aqueous IPA, 70% aqueous IPA, and 70% aqueous EtOH. These solvents
2068 were chosen based on performance results from previous CGM extractions (23). Half of the 6

2069 samples were pretreated with a combination of the enzyme mixtures Multifect GX GC (0.4%)
2070 and Multifect pectinase FE (0.1%) (Genencor International, New York, NY), while the other half
2071 had no enzyme pretreatment. These enzyme mixtures were employed to remove any crystalline
2072 cellulose matrix which may have impeded extraction of zeins.

2073 After extraction with the solvent of interest, the solution was centrifuged for 15 min at
2074 room temperature and 8000 x g (Beckman, Palo Alto, CA). The supernatant was cold
2075 precipitated at -20 °C overnight. The suspended precipitate was centrifuged at -20 °C and 8000
2076 x g to remove excess solvent and impurities, leaving a purified zein protein pellet. This pellet
2077 was dissolved in 88% IPA in water and dried in a vacuum oven at 50 °C at 0.6 bar. Dried
2078 samples were kept at 4 °C until use.

2079 Figure 3-1 shows two representative SDS-PAGE gels of CGM and DDGS extraction
2080 products. The two bands observed for each sample correspond to the 19 and 22 kDa α -zein
2081 protein fractions. All five CGM samples were extracted without sodium hydroxide or a reducing
2082 agent. A similar band pattern was observed for the five corresponding extractions with sodium
2083 hydroxide and the reducing agent. For DDGS, samples 1-3 had no enzyme pretreatment prior to
2084 extraction while samples 4-6 were pretreated.

2085

2086 *HPLC-TOF MS*

2087 Fifty milligrams of α -zein protein extract were dissolved in 55% aqueous IPA with 5%
2088 (v/v) 2-mercaptoethanol. A 5 μ L sample was injected onto a reversed phase LC column (3.0 x
2089 150 mm, 3.5 μ m Agilent Zorbax 300 Å Stable Bond-C3). Proteins were eluted using a 60 min
2090 linear gradient from 50% to 60% acetonitrile, with 0.1% trifluoroacetic acid (TFA), on an
2091 Agilent 1260 Infinity LC system (Agilent Technologies). The accurate-mass Agilent 6224 time-

2092 of-flight mass spectrometer was operated at a data acquisition rate of 4 GHz. Mass spectra were
2093 deconvoluted using Agilent MassHunter BioConfirm software. Protein molecular weights were
2094 measured using a minimum of ten consecutive charge states, a signal-to-noise ratio (S/N) of
2095 thirty or more, and a protein fit score of at least 9 (out of 10).

2096

2097 **Results and Discussion**

2098 *Previous MS Studies of Zein Proteins*

2099 Previous zein protein studies utilizing mass spectrometry involved low resolution
2100 instruments and relied on either matrix-assisted laser desorption/ionization (MALDI) or CE
2101 coupled to ESI-MS (21, 22, 25, 26). There are several potential issues with each of these
2102 techniques, especially when coupled to a low resolution mass spectrometer. First, some α -zein
2103 proteins differ in molecular weight by only 2 Da. With MALDI, each laser shot has the potential
2104 to ionize all proteins present in the sample. Without the separating power of a high resolution
2105 mass spectrometer, the direct analysis of every protein in the complex zein sample would be very
2106 difficult. This is evident when referring to mass spectra generated via MALDI-MS by Wang et
2107 al. and Adams et al (25, 26). They saw broad mass spectral peaks spanning ~100 Da that are
2108 probably the sum of peaks from 10 or more α -zein proteins instead of individual proteins. A
2109 second concern when using MALDI directly on complex samples is the ability to detect low
2110 concentration proteins within the mixture of α -zein proteins. Since no analytical separation is
2111 performed prior to ionization, most of the signal generated will be from proteins at higher
2112 concentrations.

2113 Third, there could be issues with the proteins co-crystallizing with the matrix when using
2114 MALDI. Alpha-zein proteins have peculiar properties, especially their solubility characteristics.

2115 As solvent is removed, they tend to aggregate into spherical structures or arrange into ordered
2116 films (27). It is possible that during solvent evaporation, some α -zein proteins aggregate rather
2117 than co-crystallize with the matrix. These proteins would not be ionized or detected efficiently
2118 by MALDI.

2119 CE-ESI is a better alternative than MALDI when using a low resolution mass
2120 spectrometer. One advantage of CE over MALDI is the ability to separate proteins in the
2121 complex mixture prior to analysis. However, CE-ESI-MS has lower sensitivity than LC-ESI-
2122 MS. The number of charge states generated for each α -zein protein via CE-ESI appears to be
2123 lower as well, perhaps because of the buffers and background electrolyte used during CE. Erny
2124 et al. had to use as few as three charge states for protein identification, whereas with LC-ESI we
2125 require at least ten observable peaks from consecutive charge states in the present work (21).
2126 For many proteins, over 20 charge states were observed. Signal-to-noise ratio appears to be
2127 much lower for the previous CE studies than our current LC study as well.

2128

2129 *Measured Mass Spectra and M_r Values*

2130 As an example of our results, Figure 3-2a shows a typical mass spectrum obtained during
2131 an eluting fraction that lasted \sim 60 s. The resulting deconvoluted spectrum for protein M_r
2132 24,137.61 Da is also shown. At least three other proteins co-eluted during this timeframe.
2133 However, the deconvolution software recognizes the peaks corresponding to each protein of
2134 interest (bottom panel). The inset displays a zoomed in view of the area around the 17+ peak
2135 showing that the peaks from other proteins are almost baseline resolved by the MS.

2136 Using M_r data from the LC-ESI-MS measurements, GenBank and UniProt were searched
2137 for amino acid sequences corresponding to zein proteins expected from *zea mays*. Molecular

2138 weights of each protein, without the signal peptide, were calculated. The signal peptide for α -
2139 zein proteins is typically 21 amino acids in length. This signal peptide is cleaved off naturally
2140 before the zeins are extracted and is therefore absent from the mature protein (28).

2141

2142 *Comparison of Observed Alpha-Zein Proteins with Database Entries*

2143 Table 3-1 lists the observed molecular weights of those α -zein proteins, measured via
2144 high-resolution mass spectrometry, which closely match database search results. In several
2145 cases, the amino acid sequence of different database entries vary only due to the loss of the
2146 signal peptide. This resulted in multiple “matches” for the mature protein. For that reason, the
2147 literature column lists the reference cited for each entry (21, 22, 25-44). The CGM and DDGS
2148 columns list the number of samples (out of 10 and 6, respectively) in which each protein was
2149 identified.

2150 For the proteins listed in Table 3-1, 71% (24 of 34) were in at least one CGM and DDGS
2151 sample. However, of those 24 proteins, 18 of them were in at least half of all CGM and DDGS
2152 samples. Four of the proteins were found only in CGM while six were only found in DDGS.
2153 Most of the proteins (85%) have observed molecular weights which are within 2 Da of the
2154 calculated values. Fourteen of the proteins listed in Table 3-1 were identified in a previous mass
2155 spectrometry analysis of zein (21, 22, 25, 26). The remaining 18 proteins are identified and
2156 reported here for the first time and are italicized in Table 3-1.

2157 The results in Table 3-1 lead to the following key points. First, this and subsequent tables
2158 report only M_r values, not actual sequences. The absolute sequence of a protein cannot be
2159 established via mass spectrometry without either digesting the protein and sequencing the
2160 resulting peptides (bottom-up proteomics) or fragmenting the intact protein using dissociation

2161 techniques, usually electron-capture/electron-transfer (top-down proteomics). Neither of these
2162 techniques was utilized for the present study. Digestion and CID of LC α -zein protein fractions
2163 would potentially provide more definitive assignments. However typical enzyme digestions
2164 occur in aqueous solutions and α -zein proteins are not soluble in water.

2165 The mass spectrometry studies cited above definitively match many specific database
2166 entries, namely those from Woo et al (29). In some cases, our experimental M_r values vary by
2167 10s to 100s of Da from supposedly matched or identified proteins. Note that each protein listed
2168 in the present work was observed in at least ten MS peaks from consecutive charge states with a
2169 minimum protein fit score of nine and a signal-to-noise ratio of at least thirty.

2170 Thus, we are confident that each protein identified represents an actual protein in a CGM
2171 sample, a DDGS sample, or both. However, we cannot definitively say each protein listed is the
2172 exact protein cited from the database.

2173 One special case is the two possible assignments for the 26,752.24 Da protein, noted with
2174 asterisks in Table 3-1. This predicted protein was near two observed ones, 1.26 Da from
2175 26,750.98 and 0.65 Da from 26,752.89. Although these two α -zein proteins share ~85% of their
2176 sequence, they also have 37 different amino acids. Of the many proteins found, this is the only
2177 case in which an observed protein closely matches two database proteins. Without at least partial
2178 digestion and sequence analysis, we cannot match the sequence in the observed peaks to those in
2179 the database, so both are listed.

2180 Second, there are a few cases in which a database protein was found in only one sample.
2181 These proteins tended to be lower abundance components of the total sample. As such, they only
2182 met the rigorous deconvolution criteria in one (or a few) sample(s). When the criteria were

2183 lowered to a S/N of 10 and only 5 consecutive charge states, many of the low-abundance
2184 proteins were observed in multiple samples (data not shown).

2185 For those proteins which were found in only some of the CGM or DDGS samples, the
2186 sodium bisulfite and NaOH treatments did affect whether a protein was observed or not. In other
2187 words, one protein might not be observed in CGM extracted with 70% aqueous IPA treated with
2188 NaOH and sodium bisulfite, while that same protein would be present in CGM treated the same
2189 way. This observation was found for the DDGS samples with or without enzyme treatment (data
2190 not shown). A more detailed analysis of each sample extraction procedure, including protein
2191 purity, yield, and recovery assessments, can be found in previous publications (23, 24).

2192 There were 15 proteins from Table 3-1 which were also identified in one of the previous
2193 mass spectrometry publications. These proteins are listed in Table 3-2. All but two of the
2194 proteins listed in Table 3-2 were identified in over half of our CGM and DDGS samples. In
2195 addition, 12 of the 15 proteins were identified in 8 or more CGM samples while 13 of the 15
2196 proteins were found in 4 or more of the DDGS samples. We consider this reasonable agreement
2197 with previous work.

2198 Some proteins have been reported in multiple publications. For those proteins, both the
2199 observed molecular weights are listed. In some cases the original publication did not directly
2200 cite the specific database entry shown in Table 3-1. In other cases, the original publication does
2201 cite the database entry listed in Table 3-1, even though their observed molecular weights
2202 sometimes deviate from the calculated value by a large margin. For these entries, we simply
2203 report the previous data and do not imply that both groups actually identify the same protein.

2204 As an extreme example, Adams et al. report GenBank accession number AF371268, with
2205 a calculated M_r of 24,705.60 Da (25). Their observed M_r was 24,515 Da. Our data, taken on an

2206 instrument with much higher resolution and mass accuracy, measured an α -zein protein with M_r
2207 24,706.84 Da. We did not observe a protein fitting our acceptance criteria with M_r 24,515 Da, as
2208 discussed below.

2209 For the data listed in Table 3-2, previous analysis via CE-ESI-MS generated data with
2210 observed molecular weights within ~1.4 Da of the calculated values, much closer than previous
2211 MALDI-MS experiments (~43.6 Da) (21, 22). Of course the deviation from the calculated value
2212 for MALDI analysis is skewed by the small sample size and the 191 Da deviation listed above.
2213 If that single aberrant value is removed, the deviation drops to 14.2 Da. Although this value is
2214 better, it is still much larger than that for the data generated via HRMS (1.2 Da, present work)
2215 and CE-MS (21-22). We believe this point illustrates the previous stated concerns regarding the
2216 analyses of a complex mixture of very similar proteins, such as α -zein proteins, via MALDI.

2217

2218 *Alpha-Zein Proteins without Database Entries*

2219 Table 3-3 compares molecular weights of α -zein proteins measured via HRMS with M_r
2220 values similar to those found in previous MS studies, but which were not in the database. Nine
2221 of the 15 proteins listed in Table 3-3 were found in over half of the CGM and DDGS samples.
2222 Moreover, 10 of the 15 were found in 9 or more of the CGM samples and 11 of 15 were found in
2223 four or more of the DDGS samples. One protein, M_r 23,217.76, was found in all 10 of the CGM
2224 samples but none of the DDGS samples. Of the α -zein proteins which were compared to
2225 database entries or previous mass spectrometry studies (Tables 3-1 and 3-3), 27 of the 49 (55%)
2226 proteins were found in over half of the CGM and DDGS samples. Twenty-nine proteins were
2227 identified in 8 or more of the CGM samples and thirty-four were found in four or more of the
2228 DDGS samples.

2229 It is interesting to compare our list of proteins in Tables 3-1 to 3-3 to previous data. In
2230 some previous studies a protein is assigned to a specific GenBank accession number, implying
2231 that the protein observed has the same sequence as that given in the database. For example,
2232 Adams et al. observed (25), via MALDI, an α -zein protein with M_r 24,069 Da. They assigned it
2233 to GenBank accession number AF371271 with a calculated M_r 24,087 Da. However, our study
2234 shows two proteins with slightly different M_r values (24,071.90 Da and 24,087.90 Da), both of
2235 which were present in every CGM and DDGS sample. Wang et al (26). report an α -zein protein
2236 with M_r 24,097 Da, also via MALDI, and assign it to the same protein (AF371271, M_r 24,087
2237 Da). We find an α -zein protein having a mass of 24,096.55 Da. Erny et al (21). also reported an
2238 α -zein protein of mass 24,695 Da, observed via CE-ESI-MS. This protein is compared to
2239 GenBank accession number AF371268 from Woo et al (29). having a calculated M_r 24,706 Da.
2240 It is also compared to a protein found by Adams et al (25). of mass 24,644 Da. Adams, however,
2241 actually compared their observed 24,644 Da protein to GenBank accession number AF371267,
2242 with a calculated mass of 24,818 Da. Our study found α -zein proteins having a mass of
2243 24,694.62 Da and 24,096.55 Da. We did not observe an α -zein protein having a mass of 24,818
2244 Da.

2245 Table 3-4 contains a list of 47 observed proteins observed in the present work that fit the
2246 deconvolution criteria. These proteins did not match proteins from either the database or
2247 previous mass spectrometry studies. It is possible that some of these “new” proteins are Na^+ or
2248 K^+ salt adducts of expected proteins (45). Overall, only 10 of these 47 proteins were found in
2249 over half of the CGM and DDGS samples. Fifteen of the 47 “new” proteins were found in 7 or
2250 more of the CGM samples and 18 of the 47 were found in 4 or more of the DDGS samples.
2251 Twelve of the 47 proteins were found only in a single CGM or DDGS sample; two of these, M_r

2252 26,375 and 26,419.76, were identified in one CGM and one DDGS sample. Three of the
2253 proteins were identified in every DDGS sample but none of the CGM samples. Only one
2254 protein was found in every CGM sample but none of the DDGS samples.

2255

2256 *Comparison of Proteins from CGM and DDGS*

2257 One goal of the present work was to compare the individual α -zein proteins extracted
2258 from both CGM and DDGS. Most commercial zein is produced from CGM and as such, CGM
2259 commands a higher market price. Heating during the fermentation process is thought to
2260 adulterate α -zein proteins in DDGS. However, previous studies have shown the ability to extract
2261 a high purity zein protein fraction from the much cheaper DDGS, although no molecular weight
2262 information has been described other than that provided by SDS-PAGE (24, 46, 47).

2263 Of the α -zein proteins previously reported (Tables 1-3), about 71% (34 of 48) were found
2264 in both CGM and DDGS. Overall, 56 of the 95 (59%) α -zein proteins that fit our deconvolution
2265 criteria were found in both CGM and DDGS. Also, 22 proteins were found only in DDGS
2266 samples and 17 proteins were found only in CGM samples.

2267 Based solely on these results, there is no simple answer to the question of whether α -zein
2268 proteins are adulterated during conversion of dry milled corn to DDGS. However, we believe
2269 our findings, in support with the information from previous publications, suggest conventional
2270 DDGS contains many viable α -zein proteins.

2271 **Acknowledgements**

2272 The authors would like to thank Professor Buddhi Lamsal (Iowa State University) for his
2273 guidance in the alpha zein protein extractions. We also thank Kamel Harrata, Instrument
2274 Services group, Department of Chemistry, Iowa State University for providing access to the
2275 instrumentation. Derrick Morast and Timothy Anderson would like to acknowledge the
2276 GAANN Fellowship (Iowa State University, 2009) for financial support.

2277 **References**

1. Lawton, J. W. Zein: A history of processing and use. *Cereal Chem.* **2002**, *79*, 1-18.
2. Wu, Q. X.; Sakabe, H.; Isobe, S. Studies on the toughness and water resistance of zein-based polymers by modification. *Polymer* **2003**, *44*, 3901-3908.
3. Wang, Y.; Padua, G. W. Tensile properties of extruded Zein sheets and extrusion blown films. *Macromol. Mater. Eng.* **2003**, *288*, 886-893.
4. Lawton, J. W. Plasticizers for zein: Their effect on tensile properties and water absorption of zein films. *Cereal Chem.* **2004**, *81*, 1-5.
5. Wilson, C. M. A nomenclature for zein polypeptides based on isoelectric focusing and sodium dodecyl sulfate polyacrylamide gel electrophoresis. *Cereal Chem.* **1985**, *62*, 361-365.
6. Wilson, C. M. Serial analysis of zein by isoelectric focusing and sodium dodecyl sulfate gel electrophoresis. *Plant Physiol.* **1986**, *82*, 196-202.
7. Hastings, H.; Bonanomi, S.; Soave, C.; Di Fonzo, N.; Salamini, F. Mapping of genes for minor zein sodium dodecylsulfate subunits and revision of zein gene nomenclature. *Genet. Agrar.* **1984**, *38*, 447-464.
8. Esen, A. Separation of alcohol-soluble proteins (zeins) from maize into three fractions by differential solubility. *Plant Physiol.* **1986**, *80*, 623-627.
9. Thompson, G. A.; Larkins, B. A. Structural elements regulating zein gene expression. *Bioessays* **1989**, *10*, 108-113.
10. Esen, A. A proposed nomenclature for the alcohol-soluble proteins (zeins) of maize (*Zea mays* L.). *J. Cereal Sci.* **1987**, *5*, 117-128.
11. Coleman, C. E.; Larkins, B. A. The prolamins of maize. In *Seed Proteins*, Shewry, P. R.; Casey, R., Eds. Kluwer: Dordrecht, Netherlands, **1999**; pp 109-139.
12. Thompson, G. A.; Larkins, B. A. Characterization of zein genes and their regulation in maize endosperm. In *The Maize Handbook*, Freeling, M.; Walbot, V., Eds. Springer-Verlag: New York, **1994**; pp 639-647.
13. Wu, S. W.; Myers, D. J.; Johnson, L. A. Factors affecting yield and composition of zein extracted from commercial corn gluten meal. *Cereal Chem.* **1997**, *74*, 258-263.
14. Carter, R.; Reck, D. R. Low temperature solvent extraction process for producing high purity zein. U.S. Patent 3,535,305, Oct. 20, 1970.
15. Takahashi, H.; Yanai, N. Process for refining zein. U.S. Patent 5,342,923, Aug. 30, 1994.
16. Singh, V.; Moreau, R. A.; Hicks, K. B.; Belyea, R. L.; Staff, C. H. Removal of fiber from distillers dried grains with solubles (DDGS) to increase value. *Trans. ASAE* **2002**, *45*, 389-392.
17. Anderson, T. J.; Lamsal, B. P. Zein extraction from corn, corn products, and coproducts and modifications for various applications: A review. *Cereal Chem.* **2011**, *88*, 159-173.
18. Jensen, P. K.; Paša-Tolić, L.; Anderson, G. A.; Horner, J. A.; Lipton, M. S.; Bruce, J. E.; Smith, R. D. Probing proteomes using capillary isoelectric focusing-electrospray ionization Fourier transform ion cyclotron resonance mass spectrometry. *Anal. Chem.* **1999**, *71*, 2076-2084.
19. Mann, M.; Hendrickson, R. C.; Pandey, A. Analysis of proteins and proteomes by mass spectrometry. *Annu. Rev. Biochem.* **2001**, *70*, 437-473.

2322 20. Consoli, L.; Damerval, C. Quantification of individual zein isoforms resolved by two-
 2323 dimensional electrophoresis: Genetic variability in 45 maize inbred lines. *Electrophoresis*
 2324 **2001**, 2983-2989.(21) Erny, G. L.; Marina, M. L.; Cifuentes, A. Capillary-electrophoresis
 2325 mass spectrometry of zein proteins from conventional and transgenic maize.
 2326 *Electrophoresis* **2007**, 28, 4192-4201.

2327 22. Erny, G. L.; Leon, C.; Marina, M. L.; Cifuentes, A. Time of flight versus ion trap mass
 2328 spectrometry coupled to capillary electrophoresis to analyse intact proteins. *J. Sep. Sci.*
 2329 **2008**, 31, 1810-1818.

2330 23. Anderson, T. J.; Lamsal, B. P. Development of new method for extraction of α -zein from
 2331 corn gluten meal using different solvents. *Cereal Chem.* **2011**, 88, 356-362.

2332 24. Anderson, T. J.; Ilankovan, P.; Lamsal, B. P. Two fraction extraction of alpha-zein from
 2333 DDGS and its characterization. *Ind. Crops Prod.* **2012**, 37, 466-472.

2334 25. Adams, W. R.; Huang, S. S.; Kriz, A. L.; Luethy, M. H. Matrix-assisted laser desorption
 2335 ionization time-of-flight mass spectrometry analysis of zeins in mature maize kernels. *J.*
 2336 *Agric. Food Chem.* **2004**, 52, 1842-1849.

2337 26. Wang, J. F.; Geil, P. H.; Kolling, D. R. J.; Padua, G. W. Analysis of zein by matrix-
 2338 assisted laser desorption/ionization mass spectrometry. *J. Agric. Food Chem.* **2003**, 51,
 2339 5849-5854.

2340 27. Guo, Y.; Liu, Z.; An, H.; Li, M.; Hu, J. Nano-structure and properties of maize zein
 2341 studied by atomic force microscopy. *J. Cereal Sci.* **2005**, 41, 277-281.

2342 28. Pedersen, K.; Devereux, J.; Wilson, D. R.; Sheldon, E.; Larkins, B. A. Cloning and
 2343 sequence analysis reveal structural variation among related zein genes in maize. *Cell*
 2344 **1982**, 29, 1015-1026.

2345 29. Woo, Y. M.; Hu, D. W. N.; Larkins, B. A.; Jung, R. Genomics analysis of genes
 2346 expressed in maize endosperm identifies novel seed proteins and clarifies patterns of zein
 2347 gene expression. *Plant Cell* **2001**, 13, 2297-2317.

2348 30. Alexandrov, N. N.; Brover, V. V.; Freidin, S.; Troukhan, M. E.; Tatarinova, T. V.;
 2349 Zhang, H.; Swaller, T. J.; Lu, Y.-P.; Bouck, J.; Flavell, R. B.; Feldmann, K. A. Insights
 2350 into corn genes derived from large-scale cDNA sequencing. *Plant Mol. Biol.* **2009**, 69,
 2351 179-194.

2352 31. Soderlund, C.; Descour, A.; Kudrna, D.; Bomhoff, M.; Boyd, L.; Currie, J.; Angelova,
 2353 A.; Collura, K.; Wissotski, M.; Ashley, E.; Morrow, D.; Fernandes, J.; Walbot, V.; Yu,
 2354 Y. Sequencing, mapping, and analysis of 27,455 maize full-length cDNAs. *Plos Genetics*
 2355 **2009**, 5.

2356 32. Geraghty, D.; Peifer, M. A.; Rubenstein, I.; Messing, J. The primary structure of a plant
 2357 storage protein: Zein. *Nucleic Acids Res.* **1981**, 9, 5163-5174.

2358 33. Marks, M. D.; Lindell, J. S.; Larkins, B. A. Nucleotide sequence analysis of zein
 2359 messenger RNAs from maize endosperm. *J. Biol. Chem.* **1985**, 260, 6451-6459.

2360 34. Kriz, A. L.; Boston, R. S.; Larkins, B. A. Structural and transcriptional analysis of DNA
 2361 sequences flanking genes that encode 19 kDa zeins. *Mol. Gen. Genet.* **1987**, 207, 90-98.

2362 35. Marks, M. D.; Larkins, B. A. Analysis of sequence microheterogeneity among zein
 2363 messenger RNAs. *Journal of Biological Chemistry* **1982**, 257, 9976-9983.

2364 36. Kim, C. S.; Hunter, B. G.; Kraft, J.; Boston, R. S.; Yans, S.; Jung, R.; Larkins, B. A. A
 2365 defective signal peptide in a 19-kD alpha-zein protein causes the unfolded protein
 2366 response and an opaque endosperm phenotype in the maize De*-B30 mutant. *Plant*
 2367 *Physiol.* **2004**, 134, 380-387.

2368 37. Viotti, A.; Cairo, G.; Vitale, A.; Sala, E. Each zein gene class can produce polypeptides
2369 of different sizes. *EMBO J.* **1985**, *4*, 1103-1110. (38) Geraghty, D. E.; Messing, J.;
2370 Rubenstein, I. Sequence analysis and comparison of cDNAs of the zein multigene
2371 family. *EMBO J.* **1982**, *1*, 1329-1335.

2372 39. Song, R. T.; Llaca, V.; Linton, E.; Messing, J. Sequence, regulation, and evolution of the
2373 maize 22-kD alpha zein in gene family. *Genome Res.* **2001**, *11*, 1817-1825.

2374 40. Thompson, G. A.; Siemieniak, D. R.; Sieu, L. C.; Slightom, J. L.; Larkins, B. A.
2375 Sequence analysis of linked maize 22 kDa alpha-zein genes. *Plant Mol. Biol.* **1992**, *18*,
2376 827-833.

2377 41. Liu, C. N.; Rubenstein, I. Molecular characterization of two types of 22-kDa alpha-zein
2378 genes in a gene cluster in maize. *Mol. Gen. Genet.* **1992**, *234*, 244-253.

2379 42. Spena, A.; Viotti, A.; Pirrotta, V. A homologous repetitive block structure underlies the
2380 heterogeneity of heavy and light chain zein genes. *EMBO J.* **1982**, *1*, 1589-1594.

2381 43. Hu, N. T.; Peifer, M. A.; Heidecker, G.; Messing, J.; Rubenstein, I. Primary structure of a
2382 genomic zein sequence of maize. *EMBO J.* **1982**, *1*, 1337-1342.

2383 44. Coleman, C. E.; Lopes, M. A.; Gillikin, J. W.; Boston, R. S.; Larkins, B. A. A defective
2384 signal peptide in the maize high lysine mutant Flory-2. *Proc. Natl. Acad. Sci. U. S. A.*
2385 **1995**, *92*, 6828-6831.

2386 45. Tong, H.; Bell, D.; Tabei, K.; Siegel, M. M. Automated data massaging, interpretation,
2387 and E-mailing modules for high throughput open access mass spectrometry. *J. Am. Soc.*
2388 *Mass Spectrom.* **1999**, *10*, 1174-1187.

2389 46. Xu, W.; Reddy, N.; Yang, Y. An acidic method of zein extraction from DDGS. *J. Agric.*
2390 *Food Chem.* **2007**, *55*, 6279-6284.

2391 47. Lawton, J. W. Isolation of zein using 100% ethanol. *Cereal Chem.* **2006**, *83*, 565-568.

2392

2393

2394

2395

2396

2397

2398

2399

2400

2401

2402

Table 3-1

A Comparison of Molecular Weights of α -Zein Proteins Measured via High-Resolution Mass Spectrometry to Protein Database Search Results

Molecular weight (obs., HRMS)	Molecular weight (GenBank)	Difference	CGM samples	DDGS samples	Literature
23231.84	23230.87	0.97	8/10	6/6	(20, 26, 27)
23327.99	23324.99	3.00	0	6	(28)
23344.93	23346.09	-1.17	9	6	(19, 26, 29)
23358.33	23358.96	-0.63	9	6	(20, 23, 25, 26)
23361.24	23360.04	1.20	9	6	(19, 20, 24, 26, 30)
23366.54	23367.03	-0.49	3	2	(20, 26, 30)
23420.76	23419.06	1.70	9	6	(40)
23493.78	23496.30	-2.52	0	6	(31, 32)
23527.20	23527.33	-0.12	0	6	(36)
23568.96	23567.33	1.64	0	1	direct submission
24020.97	24019.79	1.18	10	6	(33)
24032.98	24036.82	-3.84	10	5	(34)
24077.73	24076.84	0.89	0	4	(35)
24087.90	24086.86	1.04	10	6	(19, 20, 23, 25, 26)
24137.61	24135.91	1.70	10	6	(20, 26)
24326.40	24325.13	1.27	1	0	direct submission
24375.20	24377.15	-1.95	1	0	direct submission
24424.43	24423.12	1.31	10	6	(19, 20, 26)
24706.84	24705.60	1.24	1	2	(23, 25)
26334.03	26336.59	-2.55	7	1	(41)
26359.84	26358.52	1.32	6	4	(20, 23, 25, 26)
26590.24	26586.87	3.37	10	1	direct submission
26708.58	26709.86	-1.28	8	0	(25)
26752.24*	26750.98	1.26	10	6	(23, 25, 36)
26752.24*	26752.89	-0.65	10	6	(37)
26761.12	26760.01	1.11	10	6	(19, 20, 36)
26779.45	26779.04	0.42	2	5	(26, 38)
26820.73	26819.12	1.61	10	6	(20, 26, 32, 36)
26837.16	26838.17	-1.01	10	6	(24, 27)
26859.75	26860.00	-0.25	4	0	(34, 39)
26891.66	26891.06	0.60	6	2	(36)
26906.45	26905.08	1.37	0	2	(36, 38)
26924.46	26923.17	1.30	10	5	(19, 20, 25)
27129.02	27127.53	1.49	9	5	(19, 20, 40)

2403 *Observed protein can be classified to two GenBank accessions

2404 *Italicized proteins are reported for the first time in this study by mass spectrometry*

2405

Table 3-2

A Comparison of Molecular Weights of α -Zein Proteins Measured via High-Resolution Mass Spectrometry to Database Proteins Previously Identified via Mass Spectrometry

Molecular weight (obs., HRMS)	Molecular weight (GenBank)	Molecular weight (reported)	Analysis type	CGM samples	DDGS samples	Literature
23231.84	23230.87	23232	CE-MS	8/10	6/6	(20)
23358.33	23358.96	23318/23358.5	MALDI-MS/CE-MS	9	6	(20, 23)
23361.24	23360.04	23362/23361	MALDI-MS/ CE-MS	9	6	(20, 24)
23366.54	23367.03	23365.3	CE-MS	3	2	(20)
24087.90	24086.86	24069/24085.7	MALDI-MS/CE-MS	10	6	(20, 23)
24137.61	24135.91	24137.3	CE-MS	10	6	(20)
24424.43	24423.12	24425/24426 (± 4)	CE-MS/ CE-MS	10	6	(19, 20)
24706.84	24705.60	24515	MALDI-MS	1	2	(23)
26359.84	26358.52	26308	MALDI-MS	6	4	(23)
26752.24	26750.98	26741	MALDI-MS	10	6	(23)
26761.12	26760.01	26758.8	CE-MS	10	6	(20)
26820.73	26819.12	26817	CE-MS	10	6	(20)
26837.16	26838.17	26838	MALDI-MS	10	6	(24)
26924.46	26923.17	26922.8/26925 (± 1)	CE-MS/CE-MS	10	5	(19, 20)
27129.02	27127.53	27128.6	CE-MS	9	5	(19, 20)
2406						
2407						
2408						
2409						
2410						
2411						
2412						
2413						
2414						
2415						
2416						
2417						
2418						
2419						
2420						

Table 3-3

A Comparison of Molecular Weights of α -Zein Proteins Measure via High-Resolution Mass Spectrometry to Non-Database Proteins Previously Identified via Mass Spectrometry

Molecular weight (obs., HRMS)	Molecular weight (reported)	Analysis type	CGM samples	DDGS samples	Literature
23217.76	23216.3	CE-MS	10/10	0/6	(20)
23141.98	23140.2	CE-MS	10	6	(20)
23379.00	23377	MALDI-MS	10	6	(24)
23404.27	23401 (± 1)	CE-MS	2	5	(19)
23437.09	23436.4	CE-MS	9	6	(20)
23995.94	23993.6	CE-MS	10	6	(20)
24071.90	24069	MALDI-MS	10	6	(23)
24096.55	24097	MALDI-MS	1	4	(24)
24559.48	24558.8	CE-MS	9	6	(20)
24694.62	24695 (± 1)	CE-MS	0	4	(19)
26386.02	26383.2	CE-MS	0	2	(20)
26632.19	26630.6	CE-MS	9	4	(20)
26811.46	26813 (± 4)	CE-MS	9	5	(19)
26828.15	26831.1	CE-MS	9	3	(20)
27186.14	27185.5	CE-MS	1	0	(20)

2421

2422

2423

2424

2425

2426

2427

2428

2429

2430

2431

2432

2433

2434

2435

2436 **Table 3-4**

2437

2438 Molecular Weights of α -Zein Proteins Which Met Deconvolution Criteria, Not Previously
2439 Reported Via Mass Spectrometry Analysis and No Database Entry

Molecular weight (obs., HRMS)	CGM samples	DDGS samples	Molecular weight (obs., HRMS)	CGM samples	DDGS samples
23241.83	1/10	0/6	24447.34	10/10	6/6
23308.89	9	4	24455.85	10	2
23331.97	0	2	24500.48	8	2
23394.45	0	2	24523.26	0	2
23407.36	0	5	24531.5	7	0
23442.62	6	6	24635.5	1	0
23455.25	2	6	26257.69	8	5
23458.20	10	6	26375.94	1	1
23470.26	1	0	26419.76	1	1
23476.11	0	6	26435.98	7	2
23510.95	0	6	26514.26	10	3
23519.50	10	0	26529.8	3	0
23523.17	0	6	26655.09	4	4
23554.11	0	3	26734.28	0	3
23599.38	2	4	26776.27	2	4
24010.05	10	4	26796.51	0	1
24108.57	8	6	26855.12	0	1
24148.26	2	0	26878.48	0	1
24155.42	5	6	26915.7	3	0
24164.22	10	6	26942.24	1	2
24195.96	0	2	26973.8	1	0
24213.00	10	6	27016.8	1	0
24240.38	1	0	27205.19	8	1
24441.77	0	1			

2440

2441

2442

2443

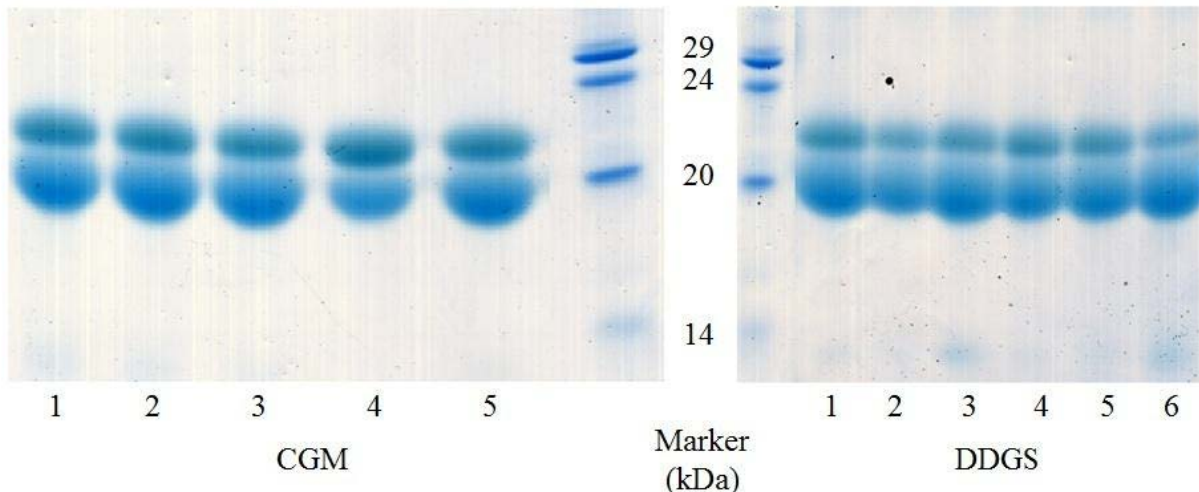
2444

2445

2446

2447

2448



2449

2450 **Figure 3-1.** SDS-PAGE of α -zein protein extracts from CGM and DDGS. For the five CGM
 2451 samples, all were extracted without sodium hydroxide and sodium bisulfite. A similar gel was
 2452 observed for the five identical extractions which used sodium hydroxide and sodium bisulfite.
 2453 CGM lane 1 was extracted with 88% aqueous 2-propanol, lane 2 with 70% aqueous 2-propanol,
 2454 lane 3 with 55% aqueous 2-propanol, lane 4 with 70% 2-propanol, 22.5% glycerol, and 7.5%
 2455 water, and lane 5 with 70% aqueous ethanol. For the six DDGS samples, lanes 1-3 were not
 2456 pretreated with enzyme while lanes 4-6 were pretreated. Lanes 1 and 4 were extracted with 88%
 2457 aqueous 2-propanol, lanes 2 and 5 were extracted with 70% aqueous 2-propanol, and lanes 3 and
 2458 6 were extracted with 70% aqueous ethanol. CGM gel adapted from Anderson and Lamsal (21)
 2459 and DDGS gel adapted from Anderson et al. (22)

2460

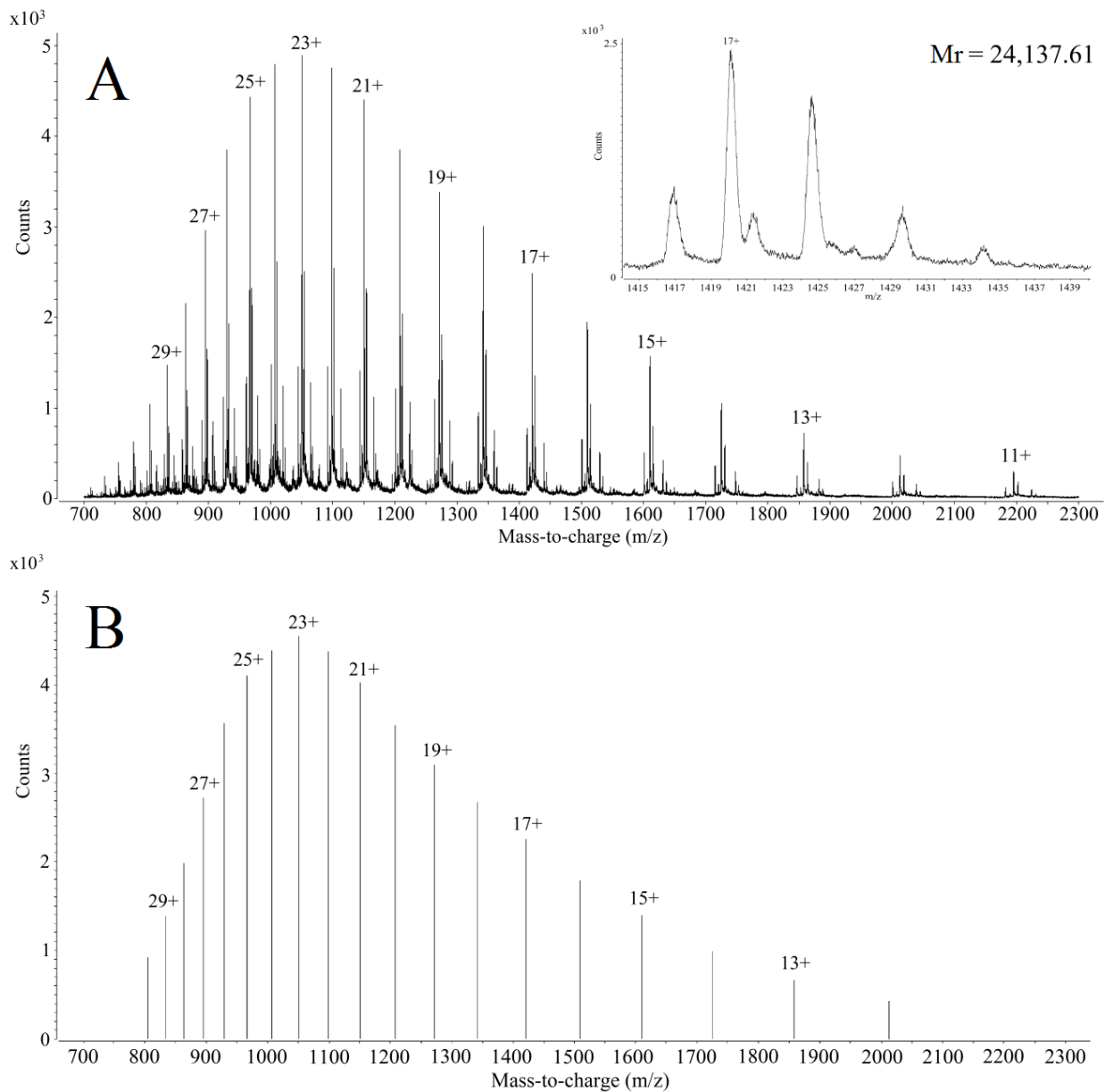
2461

2462

2463

2464

2465



2466

2467 **Figure 3-2.** Mass spectrum of a mixture of α -zein proteins. Peaks for the protein with Mr =
 2468 24,137.61 Da are labeled. Spectrum A is raw data integration of total ion chromatograph from
 2469 41.6 to 42.7 minutes. A zoomed in view of the 17+ peak is displayed in the inset. The peak
 2470 labeled 17+ belongs to the charge state progression for the protein shown in the deconvoluted
 2471 spectrum B. The other peaks in the inset belong to charge state progressions from other proteins.

2472

2473 **CHAPTER 4**
2474
2475
2476
2477 **ANALYSIS OF RESISTANT STARCHES IN RAT CECAL CONTENTS USING**
2478 **FOURIER TRANSFORM INFRARED PHOTOACOUSTIC SPECTROSCOPY**
2479
2480 Modified from a paper published in *Journal of Agricultural and Food Chemistry*¹
2481
2482 By
2483 Timothy J. Anderson,^{2,3} Yongfeng Ai,⁴ Roger W. Jones,² Robert S. Houk,^{2,3} Jay-lin Jane,⁴
2484 Yinsheng Zhao,⁴ Diane F. Birt,⁴ and John F. McClelland^{2,5*}
2485
2486 ¹Reprinted with permission of *Journal of Agricultural and Food Chemistry* 61(8):1818–1822
2487 ²Ames Laboratory-USDOE, Iowa State University, Ames, Iowa 50011
2488 ³Department of Chemistry, Iowa State University, Ames, Iowa 50011
2489 ⁴Department of Food Science and Human Nutrition, Iowa State University, Ames, Iowa 50011
2490 ⁵Department of Mechanical Engineering, Iowa State University, Ames, Iowa 50011
2491
2492
2493
2494
2495
2496
2497
2498
2499
2500 *Corresponding Author, Email johnfm@iastate.edu, Phone 515-294-7948, Fax 515-294-4748

2501 **Abstract**

2502 Fourier transform infrared photoacoustic spectroscopy (FTIR-PAS) qualitatively and
2503 quantitatively measured resistant starch (RS) in rat cecal contents. Fisher 344 rats were fed diets
2504 of 55 % (w/w, dry basis) starch for eight weeks. Cecal contents were collected from sacrificed
2505 rats. A corn starch control was compared against three RS diets. The RS diets were high-
2506 amylose corn starch (HA7), HA7 chemically modified with octenyl succinic anhydride, and
2507 stearic-acid-complexed HA7 starch. To calibrate the FTIR-PAS analysis, samples from each diet
2508 were analyzed using an enzymatic assay. A partial least squares cross-validation plot generated
2509 from the enzymatic assay and FTIR-PAS spectral results for starch fit the ideal curve with an R^2
2510 of 0.997. A principal component analysis plot of components 1 and 2 showed that spectra from
2511 diets clustered significantly from each other. This study clearly showed that FTIR-PAS can
2512 accurately quantify starch content and identify the form of starch in complex matrices.

2513

2514

2515

2516

2517

2518

2519

2520

2521 **Keywords** Resistant starch, fecal analysis, Fourier transform infrared photoacoustic
2522 spectroscopy, partial least squares, principal component analysis

2523

2524 **Introduction**

2525

2526 Foodstuffs contain a varied mixture of complex compounds and materials. One of these

2527 compounds, starch, has been characterized and studied for decades. Starch is commonly found

2528 in many foods as starch granules, which are a combination of amylose and amylopectin. The

2529 ratio of these two compounds varies with source material, but the amount of amylose in the

2530 normal starch granule is typically 15-30%, while amylopectin can reach 70% or 100% for waxy

2531 starch (1-3). Amylose can form single helical complexes with many chemicals, such as free fatty

2532 acids and iodine, and it can also form double helices (3). Recently, resistant starches containing

2533 high concentrations of amylose (up to 85%, high-amylose corn starch) and those with chemical

2534 modifications have increasingly been investigated (3). These starches have been dubbed

2535 resistant starch (RS), due to the fact that they resist degradation and absorption in the small

2536 intestine (4).

2537 The decreased digestibility of RS has garnered attention from researchers who study

2538 diabetes (5). With easily digestible starch, diabetics have difficulty controlling their blood

2539 glucose levels, but RS may impart many beneficial effects for diabetics through reduction in

2540 blood-glucose spikes (5-8). Another benefit of RS is the potential to control energy intake.

2541 Many researchers are attempting to find foods that digest slowly and decrease energy intake,

2542 which could help with weight maintenance (9). RS can also play a role as a prebiotic. Prebiotics

2543 encompass many of the dietary fibers, including RS, which are not readily digestible by humans.

2544 The undigested RS can be utilized by microbes within the gut and may release beneficial

2545 compounds for the host organism (10-13).

2546 There are five varieties of RS. Type 1 RS can be found in coarsely ground legumes or

2547 whole grain. The cell wall surrounding the Type 1 RS makes the starch physically inaccessible

2548 to digestion. Type 2 RS is individual C-type or B-type crystalline starch granules. Type 2 RS
2549 typically is raw banana and potato starch, and high amylose corn starch that retains the
2550 crystalline structure. Type 3 RS refers to retrograded amylose (14). Type 4 RS is chemically
2551 modified starch (10, 15). The latest RS is Type 5 RS, which is an amylose-lipid complex (16).

2552 Animal studies are often performed to evaluate RS digestibility from analysis of fecal
2553 samples, which are complex materials containing protein, carbohydrate, and lipid. Common
2554 quantitative methods for analyzing starch content are starch-hydrolysis enzyme assays. The
2555 enzyme assays are useful for starch quantification, but have many negative aspects for fecal
2556 studies. The enzyme assays cost approximately \$3 per sample, take about 20 minutes per
2557 sample, and consume at least 0.2 g dry sample for analyses in duplicate. Studies with mice or
2558 rats tend to produce large numbers of small samples, which may become time consuming and
2559 costly when hundreds of samples need to be analyzed.

2560 Our alternative proposed method of analysis is Fourier transform infrared photoacoustic
2561 spectroscopy (FTIR-PAS). Conventional FTIR relies on transmission of IR light through the
2562 sample to measure the absorption bands of the compounds of interest. Conventional FTIR does
2563 not work well with many food products due to their opaque nature, light scattering properties,
2564 and difficulties with sample preparation (17-19). Alternatively, FTIR-PAS directly measures the
2565 IR absorbance spectrum of opaque samples, needs minimal sample preparation, and is fast and
2566 nondestructive (20). FTIR-PAS uses a PAS accessory, which has a sample cell with a window to
2567 allow a modulated IR beam from the spectrometer to enter and illuminate the sample (21). The
2568 IR light absorbed by the sample heats it. The heat migrates to the gas/sample interface and
2569 produces a pressure wave in proportion to the absorbance by the sample. The resultant pressure
2570 signal is then picked up by a sensitive microphone, and the signal is converted into a

2571 wavenumber versus absorbance intensity spectrum (21). For further information pertaining to
2572 FTIR-PAS theory or explanation of various experimental methods, please see References 22 and
2573 23.

2574 A handful of studies have successfully analyzed starch and other food-based components
2575 using FTIR-PAS. One of the first food analyses utilized IR-PAS with a near infrared
2576 monochromator to determine the moisture content of protein powders (24). Later researchers
2577 applied FTIR-PAS to analyze protein and carbohydrate, but lacked statistical power to quantify
2578 the data (25). It was not until the mid-1990's that FTIR techniques with food materials began to
2579 couple spectral results with statistical techniques such as partial least squares (PLS) (26). PLS
2580 uses a small training set of samples analyzed via a non-FTIR standard method to calibrate the
2581 FTIR analysis. A multivariate model of the spectral data with the quantitative values can be
2582 produced to create a calibration to predict the composition of unknown samples from their
2583 spectra. This approach has been confirmed for determining lipid, protein, and carbohydrate
2584 concentrations in pea seeds (27).

2585 The present study went beyond food and single identity starch analysis by quantifying
2586 modified starch in rat cecal contents. Three types of RS were studied along with a control corn
2587 starch. The first RS studied was high amylose corn starch (HA7), a Type 2 RS. The second RS
2588 was octenyl succinic high-amylose corn starch (OS-HA7) which is a Type 4 RS. OS-HA7 is
2589 obtained from modifying starch with octenyl succinic anhydride, which forms ester bonds with
2590 hydroxyl groups of starch molecules. The third RS was high amylose corn starch complexed
2591 with stearic acid (RS5-HA7), a Type 5 RS. RS5-HA7 is based on a physical complex between
2592 amylose and stearic acid rather than chemical bonds.

2593 The main goal of this study was to determine if FTIR-PAS and PLS was a practical
2594 alternative to the enzymatic assay for starch content. To achieve this, we needed to determine
2595 whether FTIR-PAS analysis could produce a linear correlation while accounting for potential
2596 interferences from the complex sample matrix and RS modification. Beyond a quantitative fit of
2597 the starch, principal component analysis (PCA) was tested to determine if the different diets
2598 could be differentiated qualitatively.

2599

2600 **Materials and Methods**

2601 *Rat Animal Study*

2602 Fischer 344 rats were housed following the procedure of Zhao et al (28). The animals
2603 were on the feeding regimen for eight weeks before the animals were sacrificed. The trial
2604 contained 90 rats total (2 rats died before sacrifice), which were randomly assigned to four diet
2605 groups. The four diets consisted of the control (corn starch), HA7, OS-HA7, and RS5-HA7 diets
2606 described below. For purposes important to other companion studies based on this same diet
2607 trial, the control and RS5-HA7 diet groups each contained 29 rats and were broken down further
2608 into four subgroups per diet. The rats were given two injections of either saline or the
2609 carcinogen azoxymethane (AOM, Midwest Research Institute, Kansas City, MO) administered
2610 following the method of Zhao et al (28)., and some were fed an antibiotic treatment mixture of
2611 vancomycin and imipenem. The treatments resulted in the four subgroups within the control and
2612 RS5-HA7 diets that consisted of rats given both AOM and antibiotic, AOM and no antibiotic,
2613 saline and antibiotic, and only saline. Both HA7 and OS-HA7 diets contained 15 rats per diet
2614 group and were divided into only two subgroups. They were given either AOM and no antibiotic
2615 or neither. For purposes of the tests reported here, we have grouped samples only according to

2616 diet and not according to AOM or antibiotic treatment. The animal studies were performed in
2617 compliance with the guidelines of The Institutional Animal Care and Use Committee of Iowa
2618 State University.

2619

2620 *Starch Diets Fed to Rats*

2621 Four starch varieties were utilized for the feeding study: Control (corn starch, Cargill Gel
2622 03420; Cargill Inc., Minneapolis, MN), HA7 (AmyloGel 03003; Cargill Inc.), OS-HA7
2623 (processed HA7 bound to octenyl succinate in the Department of Food Science and Human
2624 Nutrition, Iowa State University), and RS5-HA7 (processed using HA7 and stearic acid in the
2625 Department of Food Science and Human Nutrition, Iowa State University) (16, 29). The
2626 starches were cooked before being added to the diets following the procedure of Zhao et al (28).
2627 The cooked starch was then added to a diet formulated on the basis of the standard diet
2628 recommended by the American Society for Nutritional Sciences for mature rats (AIN-93M) (30).
2629 Starch diets were prepared every other day and served fresh to the rats.

2630

2631 *Rat Cecal Samples*

2632 This study collected only the rat ceca and placed the contents into Corning 15-mL
2633 centrifuge tubes (Tewksbury, Massachusetts) on dry ice before storage at -80 °C. Due to two
2634 other companion studies obtaining samples prior to this experiment, much of the cecal contents
2635 from the samples was exhausted. Adequate material from only twenty-eight samples, seven
2636 from each of the four feeding groups, could be randomly obtained. The wet cecal samples were
2637 placed in aluminum weighing pans and dried in an oven at 105 °C for three hours. After drying,
2638 the cecal material formed dry wafers, which were ground using mortar and pestle. The ground

2639 cecal material was then placed in 1.7-mL microcentrifuge tubes purchased from Marsh Bio
2640 Products (Rochester, New York) and stored sealed at room temperature prior to analysis.

2641

2642 *Enzymatic Assay for Starch Content*

2643 The starch content of the cecal materials was measured using Total Starch Assay Kit
2644 (Megazyme International Ireland Ltd., Co.,Wicklow, Ireland) following AACC Method 76-13
2645 (31).

2646

2647 *FTIR-PAS*

2648 The FTIR-PAS analysis was performed using an MTEC Photoacoustics PAC300 detector
2649 mounted in a Digilab FTS 7000 FTIR spectrometer. The sample detector has a 1-cm interior
2650 diameter and a window at the top for the infrared beam to enter the chamber and illuminate the
2651 sample. The dried and ground cecal material was placed in a disposable aluminum cup, which
2652 was fully illuminated by the infrared beam. Immediately before analysis the detector was purged
2653 with helium gas to remove atmospheric water vapor and carbon dioxide, which have strong mid-
2654 infrared absorptions. Also, a desiccant, magnesium perchlorate, was added beneath the sample
2655 to remove any moisture that might evolve from the sample during analysis. Spectra were taken
2656 at 8 cm^{-1} resolution and a 2.5 kHz scan speed, with the co-addition of 256 scans.

2657

2658 *PLS and PCA*

2659 The spectra were correlated with starch levels determined by the enzymatic assay via PLS
2660 using commercial software (Thermo Galactic GRAMS/AI PLSplus IQ, Version 5.1) (32-34).
2661 PLS utilizes a training set of spectra from samples whose relevant properties are known and span

2662 the range of interest. In the present case, the enzymatic assay provided the known property
2663 values. PLS modeling determines a small set of basis-vector spectra, called factors, by which it
2664 can describe all of the training set spectra. Each training set spectrum is then just a weighted
2665 sum of the factors. The factors with the smallest weightings consist mostly of noise and are
2666 dropped from the model. PLS then performs a multiple linear regression correlating the factor
2667 weightings with the known values of the property being predicted. Once the PLS model is built,
2668 the correlated property can be determined for unknown samples directly from the model, as long
2669 as the properties of the unknowns fall within the range of those covered by the original training
2670 set.

2671 Because the starch level was determined for only 28 samples (seven per diet), the sample
2672 set was not split into separate training and validation sets. Instead, all of the samples were used
2673 in creating the PLS model, and a single-elimination cross validation was used to measure model
2674 quality. In such a cross validation, one member of the training set is removed, and a model is
2675 built from the remaining members. The removed spectrum is then analyzed as an unknown. The
2676 removed spectrum is returned to the training set, and then a different one is removed and the
2677 process is repeated. This is done until all training set members have been removed and analyzed
2678 as unknowns. Plots comparing the known values and the predicted values from the cross
2679 validations are included in Results and Discussion. The standard error of cross-validation
2680 (SECV) is a measure of model quality. It is the root-mean-square difference between the values
2681 of the predicted property determined during the cross-validation and their known values.

2682 The model with the lowest prediction residual error sum of squares (PRESS) value was
2683 selected as the most accurate model. PRESS is given by

$$PRESS = \sum_{i=1}^N (k_i - p_i)^2$$

2684 where k_i and p_i are the known and predicted values for the i^{th} sample, and there are N samples in
2685 the training set. In that most-accurate model, the $4000\text{-}397\text{ cm}^{-1}$ range of the spectra was used,
2686 the spectra were preprocessed using multiplicative scatter correction (MSC) (35) and by
2687 conversion to first derivatives (19-point Savitsky-Golay). The resulting model had ten factors.

2688 Classification of the spectra according to diet was done using PCA (36-37). The same
2689 $4000\text{-}397\text{ cm}^{-1}$ range and the same first derivative and MSC preprocessing were applied to the
2690 data as in the PLS modeling. This was sufficient to cleanly separate the samples into clusters
2691 according to diet.

2692

2693 **Results and Discussion**

2694 *Enzymatic Assay for Starch Content*

2695 Starch contents of the cecal material from the rats fed different diets are shown in Table
2696 5-1. The cecal content from the rats fed the OS-HA7 diet had the highest starch content, ranging
2697 from 47% to 50.1%, whereas that from the rats fed the control diet with normal corn starch had
2698 the lowest starch content, ranging from 0.3% to 1.1%. There was no significant difference among
2699 the food disappearance (used to estimate intake but includes losses) of the rats fed the different
2700 diets (data not shown). These results suggest that the OS-HA7 has the highest resistance to *in*
2701 *vivo* digestion, followed by RS5-HA7, HA7 and normal corn starch.

2702

2703

2704

2705 *FTIR-PAS*

2706 The FTIR-PAS data were measured from 4000 to 397 cm^{-1} . Spectra from all four diets
2707 are shown in Figure 4-1. All samples show many bands in common, but in the fingerprint region
2708 (1800 to 397 cm^{-1}), there are visible differences among the cecal samples from different diets. A
2709 study by Irudayaraj and Yang using FTIR-PAS identified bands in pure starch and protein
2710 spectra (38). However, due to the complexity of the cecal samples, the present spectra have
2711 substantial peak overlap, so manual interpretation is not sufficient. The use of chemometric
2712 software can analyze the data and draw out the quantitative and qualitative data needed.

2713 PLS was successfully used for starch to model the relation between the enzymatic assay
2714 results and the FTIR-PAS spectra of the rat cecal contents. Figure 4-2 shows the cross validation
2715 for the best fitting model. The plot correlates the known starch content (dry basis) with the
2716 starch content predicted by the PLS model. The diagonal line is the ideal (i.e., predicted =
2717 known). The SECV is 1.055 wt. % and R^2 is 0.997. The SECV is only 2% of the starch-content
2718 range in the sample set (0.3 to 50.1 wt. %), so the predictions are of good quality. The high
2719 quality of the predictions from the training set would allow unknown samples to be
2720 quantitatively analyzed for starch content using the chemometric model developed. Also since
2721 the model was able to accurately fit every modified starch, the model should be useful for any of
2722 the four starch diets utilized.

2723 Besides the quantitative starch information, qualitative information to identify which
2724 starch was measured is very useful. The spectral data was analyzed by PCA to aid in sample
2725 identification. The first two principal components from the PCA of the spectra cleanly separated
2726 the samples according to diet, as shown in Figure 4-3. These two components account for 83.5%

2727 of the variance in the data. The PCA analysis gives a simple and clearly visible means to match
2728 the cecal samples to the corresponding starch diets.

2729 Despite the similarity of the measured spectra for the different cecal materials,
2730 chemometric analysis produced a successful model of the data. The FTIR-PAS data coupled
2731 with the enzyme starch assay results clearly were able to produce a cross-validation plot that
2732 gave high-quality quantitative results. The first two principal component scores also were able
2733 to show clustering that would allow qualitative identification of starch in future unknown cecal
2734 samples. No clustering among the antibiotic or AOM subgroup treatments was observed using
2735 the PCA components. This finding should give credence to the robustness of FTIR-PAS to see
2736 through minor effects even within complex matrix materials.

2737 This study was proof of concept for FTIR-PAS analysis of starch to replace future high
2738 volume enzymatic assay analysis. Future work will incorporate timed fecal collections and
2739 FTIR-PAS starch analysis and metabolic analysis. This analysis would be used to track how the
2740 chemistry of the gut microbiome changes as the animal adapts over time to an RS diet.

2741

2742 **Abbreviations**

2743 Resistant starch (RS), Fourier transform infrared photoacoustic spectroscopy (FTIR-PAS),
2744 partial least squares (PLS), high-amylose corn starch (HA7), octenyl succinic high-amylose corn
2745 starch (OS-HA7), high amylose corn starch complexed with stearic acid (RS5-HA7), principal
2746 component analysis (PCA), prediction residual error sum of squares (PRESS), multiplicative
2747 scatter correction (MSC), standard error of cross validation (SECV).

2748

2749

2750 **Funding Sources**

2751 This project was supported by the Iowa State University (ISU) Plant Sciences Institute and was
2752 supported in part by the Department of Agriculture, CSREES award number 2009-65503-05798.

2753

2754 **Conflict of Interest Statement**

2755 John McClelland has a financial interest in MTEC Photoacoustics, Inc., the manufacturer of the
2756 photoacoustic detector used in this study.

2757

2758 **Acknowledgement**

2759 This research was performed at the Ames Laboratory. Ames Laboratory is operated for the U.S.
2760 Department of Energy by Iowa State University under contract no. DE-AC02-07CH11358.

2761

2762 **References**

1. Sajilata, M. G.; Singhal, R. S.; Kulkarni, P. R. Resistant starch-A review. *Compr. Rev. Food Sci. Food Saf.* **2006**, *5*, 1-17.
2. Atkin, N. J.; Cheng, S. L.; Abeysekera, R. M.; Robards, A. W. Localisation of amylose and amylopectin in starch granules using enzyme-gold labelling. *Starch-Stärke* **1999**, *51*, 163-172.
3. Jane, J. Structural Features of Starch Granules II. In *Starch: Chemistry and Technology*; 3rd ed.; BeMiller, J. N.; Whistler, R. L., Eds.; Academic Press Inc.: Orlando, FL, **2009**; pp. 193-236.
4. Champ, M.; Langkilde, A.-M.; Brouns, F.; Kettlitz, B.; Le Bail-Collet, Y. Advances in dietary fibre characterisation. 2. Consumption, chemistry, physiology and measurement of resistant starch; implications for health and food labeling. *Nutr. Res. Rev.* **2003**, *16*, 143-161.
5. Robertson, M. D. Dietary-resistant starch and glucose metabolism. *Curr. Opin. Clin. Nutr. Metab. Care* **2012**, *15*, 362-367.
6. Saltiel, A. R.; Kahn, C. R. Insulin signalling and the regulation of glucose and lipid metabolism. *Nature* **2001**, *414*, 799-806.
7. Ranganathan, S.; Champ, M.; Pechard, C.; Blanchard, P.; Nguyen, M.; Colonna, P.; Krempf, M. Comparative study of the acute effects of resistant starch and dietary fibers on metabolic indexes in men. *Am. J. Clin. Nutr.* **1994**, *59*, 879-883.
8. Eckel, R. H.; Grundy, S. M.; Zimmet, P. Z. The metabolic syndrome. *Lancet* **2005**, *365*, 1415-1428.
9. Bodinham, C. L.; Frost, G. S.; Robertson, M. D. Acute ingestion of resistant starch reduces food intake in healthy adults. *Brit. J. Nutr.* **2010**, *103*, 917-922.
10. Brown, I. L.; Wang, X.; Topping, D. L.; Playne, M. J.; Conway, P. L. High amylose maize starch as a versatile prebiotic for use with probiotic bacteria. *Food Aust.* **1998**, *50*, 603-610.
11. Marotti, I.; Bregola, V.; Aloisio, I.; Di Gioia, D.; Bosi, S.; Di Silvestro, R.; Quinn, R.; Dinelli, G. Prebiotic effect of soluble fibres from modern and old durum-type wheat varieties on *Lactobacillus* and *Bifidobacterium* strains. *J. Sci. Food Agric.* **2012**, *92*, 2133-2140.
12. Kritchevsky, D. Epidemiology of fibre, resistant starch and colorectal cancer. *Eur. J. Cancer Prev.* **1995**, *4*, 345-352.
13. van Munster, I. P.; Tangeman, A.; Nagengast, F. M. Effect of resistant starch on colonic fermentation, bile acid metabolism, and mucosal proliferation. *Digest. Dis. Sci.* **1994**, *39*, 834-842.
14. Englyst, H. N.; Kingman, S. M.; Cummings, J. H. Classification and measurement of nutritionally important starch fractions. *Eur. J. Clin. Nutr.* **1992**, *46* (Suppl. 2), S33-S50.
15. Baghurst, P. A.; Baghurst, K. I.; Record, S. J. Dietary fibre, non-starch polysaccharides and resistant starch-a review. *Food Aust.* **1996**, *48* (Suppl.), S3-S35.
16. Hasjim, J.; Lee, S.-O.; Hendrich, S.; Setiawan, S.; Ai, Y.; Jane, J. Characterization of novel resistant-starch and its effects on postprandial plasma-glucose and insulin responses. *Cereal Chem.* **2010**, *87*, 257-262.
17. Colthup, N. B.; Daly, L. H.; Wiberley, S. E. *Introduction to Infrared and Raman Spectroscopy*, 3rd ed.; Academic Press: New York, US, **1990**.

2807 18. *Laboratory Methods in Infrared Spectroscopy*, 2nd ed.; Miller, R. G. J., Stace, B. C., Eds.;
2808 Heyden and Sons: London, UK, **1979**.

2809 19. *Practical FT-IR Spectroscopy: Industrial and Laboratory Chemical Analysis*, Ferraro, J.
2810 R.; Krishnan, K., Eds.; Academic Press: New York, US, **1990**.

2811 20. Graham, J. A.; Grim, W. M., III; Fateley, W. G. Fourier transform infrared photoacoustic
2812 spectroscopy of condensed-phase samples. In *Fourier Transform Infrared Spectroscopy*,
2813 Ferraro, J. R., Basile, L. J., Eds.; Academic Press: Orlando, US, **1985**; Vol. 4; pp. 345-
2814 392.

2815 21. McClelland, J. F.; Jones, R. W.; Seaverson, L. M. A practical guide to FT-IR
2816 photoacoustic spectroscopy. In *Practical Sampling Techniques for Infrared Analysis*,
2817 Coleman, P. B., Ed.; CRC Press: Boca Raton, FL, **1993**; pp. 107-144.

2818 22. McClelland, J. F.; Bajic, S. J.; Jones, R. W.; Seaverson, L. M. Photoacoustic
2819 spectroscopy. In *Modern Techniques in Applied Molecular Spectroscopy*, Mirabella, F.
2820 M., Ed.; John Wiley & Sons, Inc.: New York, US, **1998**; pp. 221-265.

2821 23. McClelland, J. F.; Jones, R. W.; Bajic, S. J. Photoacoustic spectroscopy. In *Handbook of
2822 Vibrational Spectroscopy*, Chalmers, J. M.; Griffiths, P. R., Eds.; John Wiley & Sons
2823 Ltd.: Chichester, UK, **2002**; Vol. 2, pp. 1231-1251.

2824 24. Castleden, S. L.; Kirkbright, G. F.; Menon, K. R. Determination of moisture in single-cell
2825 protein utilising photoacoustic spectroscopy in the near-infrared region. *Analyst* **1980**,
2826 105, 1076-1081.

2827 25. Belton, P. S.; Saffa, A. M.; Wilson, R. H. Use of Fourier transform infrared spectroscopy
2828 for quantitative analysis: A comparative study of different detection methods. *Analyst*
2829 **1987**, 112, 1117-1120.

2830 26. McQueen, D. H.; Wilson, R.; Kinnunen, A. Near and mid-infrared photoacoustic analysis
2831 of principal components of foodstuffs. *TrAC-Trends Anal. Chem.* **1995**, 14, 482-492.

2832 27. Letzelter, N. S.; Wilson, R. H.; Jones, A. D.; Sinnaeve, G. Quantitative determination of
2833 the composition of individual pea seeds by Fourier transform infrared photoacoustic
2834 spectroscopy. *J. Sci. Food Agric.* **1995**, 67, 239-245.

2835 28. Zhao, Y.; Hasjim, J.; Li, L.; Jane, J.; Hendrich, S.; Birt, D. F. Inhibition of
2836 azoxymethane-induced preneoplastic lesions in the rat colon by a cooked stearic acid
2837 complexed high-amylose cornstarch. *J. Agric. Food Chem.* **2011**, 59, 9700-9708.

2838 29. Zhang, B.; Huang, Q.; Luo, F.; Fu, X.; Jiang, H.; Jane, J. Effects of octenylsuccinylation
2839 on the structure and properties of high-amylose maize starch. *Carbohydr. Polym.* **2011**,
2840 84, 1276-1281.

2841 30. Reeves, P. G. Components of the AIN-93 diets as improvements in the AIN-76A diet. *J.
2842 Nutr.* **1997**, 127 (Suppl. 5), 838S-841S.

2843 31. AACC International. *Approved Methods of the American Association of Cereal Chemists*,
2844 10th Ed., Method 76-13. The Association: St. Paul, US, **2000**.

2845 32. Haaland, D. M.; Thomas, E. V. Partial least-squares methods for spectral analyses. 1.
2846 Relation to other quantitative calibration methods and the extraction of qualitative
2847 information. *Anal. Chem.* **1988**, 60, 1193-1202.

2848 33. Fredstrom, S. B.; Jung, H.-J. G.; Halgerson, J. L.; Eyden, C. A.; Slavin, J. L. Trial of near-
2849 infrared reflectance spectroscopy in a human fiber digestibility study. *J. Agric. Food
2850 Chem.* **1994**, 42, 735-738.

2852 34. Franck, P. F.; Sallerin, J.-L.; Schroeder, H.; Gelot, M.-A.; Nabet, P. Rapid determination
2853 of fecal fat by Fourier transform infrared analysis (FTIR) with partial least-squares
2854 regression and an attenuated total reflectance accessory. *Clinical Chem.* **1996**, *42*, 2015-
2855 2020.

2856 35. Geladi, P.; MacDougall, D.; Martens, H. Linearization and scatter-correction for near-
2857 infrared reflectance spectra of meat. *Appl. Spectrosc.* **1985**, *39*, 491-500.

2858 36. Leardi, R. Chemometrics in data analysis. In *Food Authenticity and Traceability*, Lees,
2859 M., Ed.; Woodhead Publishing: Cambridge, UK, **2003**; pp. 299-320.

2860 37. Roldán-Marín, E.; Jensen, R. I.; Krath, B. N.; Kristensen, M.; Poulsen, M.; Cano, M. P.;
2861 Sánchez-Moreno, C.; Dragsted, L. O. An onion byproduct affects plasma lipids in healthy
2862 rats. *J. Agric. Food Chem.* **2010**, *58*, 5308-5314.

2863 38. Irudayaraj, J.; Yang, H. Depth profiling of a heterogeneous food-packaging model using
2864 step-scan Fourier transform infrared photoacoustic spectroscopy. *J. Food Eng.* **2002**, *55*,
2865 25-33.

2866
2867
2868
2869
2870
2871
2872
2873
2874
2875
2876
2877
2878
2879
2880
2881
2882
2883
2884
2885
2886
2887
2888
2889
2890
2891
2892
2893
2894
2895
2896
2897

2898 **Table 4-1**2899 Summary of enzymatic assay analysis of *in vivo* starch (dry basis) in cecal contents by rat

Diet	Rat#	Average Starch % (wt)	Standard Deviation
Control	87	0.3	0.2
	23	0.6	0.1
	27	0.8	0.0
	49	0.7	0.0
	84	0.8	0.0
	81	1.1	0.3
	70	1.0	0.1
	Average	0.7	
HA7	33	12.7	0.4
	40	19.4	0.5
	15	21.2	0.5
	9	21.3	0.5
	18	18.1	0.1
	22	20.5	0.1
	28	14.8	0.6
	Average	18.3	
OS-HA7	14	47.9	0.1
	16	47.9	0.1
	10	49.8	0.3
	44	47.1	0.4
	6	50.1	0.4
	50	50.0	0.1
	52	49.1	0.7
	Average	48.8	
RS5-HA7	12	24.0	0.1
	1	19.2	0.3
	20	17.1	0.6
	29	13.3	0.5
	43	28.1	0.2
	57	30.5	0.7
	64	21.5	0.4
	Average	21.9	

2900

2901

2902

2903

2904
2905
2906
2907
2908
2909
2910
2911
2912
2913
2914
2915
2916
2917
2918
2919
2920
2921
2922
2923
2924
2925
2926

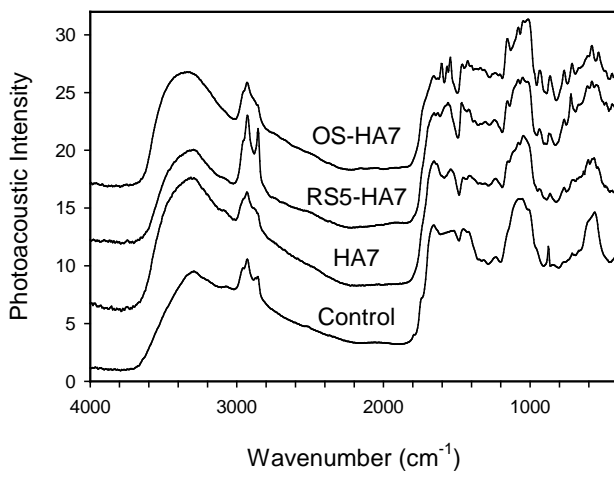


Figure 4-1. FTIR-PAS spectra

collected from rat cecal contents. The spectra are from single representative rats from each of the diet groups. Spectra scaled and displaced vertically.

2927

2928

2929

2930

2931

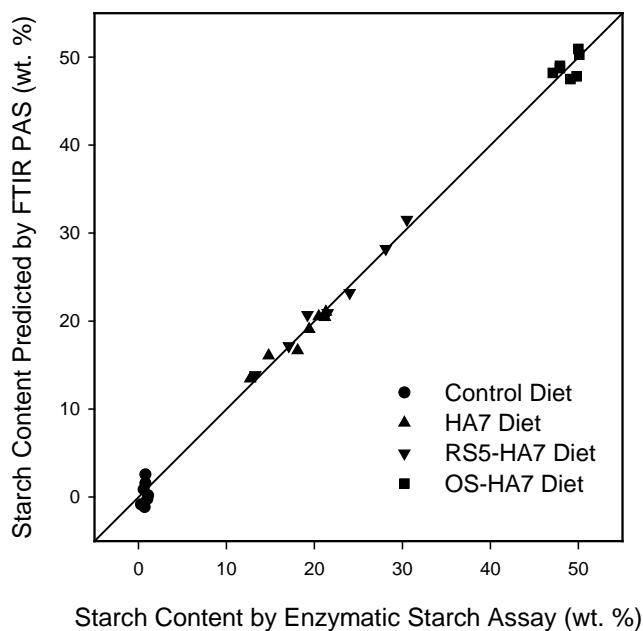
2932

2933

2934

2935

2936



2937 **Figure 4-2.** Plot of cross validation for starch content measured by enzymatic starch assay from
2938 each cecal sample (dry basis) from all four diets versus the predicted values by FTIR-PAS. The
2939 R^2 of the data to the ideal best fit line was 0.997.

2940

2941

2942

2943

2944

2945

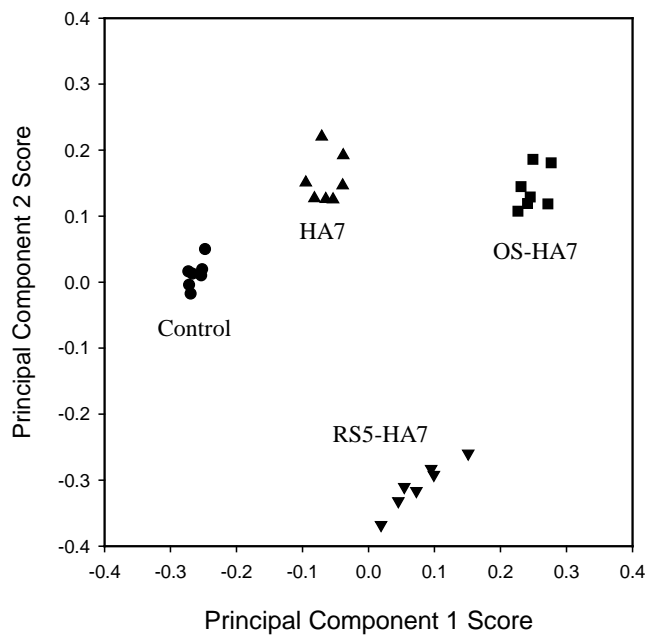
2946

2947

2948

2949

2950
2951
2952
2953
2954
2955
2956
2957
2958
2959



2960 **Figure 4-3.** Scores for the first two principal components in the PCA modeling of the spectra of
2961 28 dried cecal samples separate the samples according to the resistant-starch diets of the rats.

2962
2963
2964
2965
2966
2967
2968
2969
2970
2971
2972
2973
2974
2975
2976
2977
2978
2979
2980
2981
2982
2983

CHAPTER 5**General Conclusions**

2984 This dissertation concentrated on the use of mass spectrometry and FTIR-PAS for the
2985 analysis of metabolites, proteins, and starch from biological sources. Chapter 2 focused on the
2986 use of high resolution MS to determine if RS fed to rats had an effect on metabolites produced
2987 during digestion. It was startling to observe the sheer number of metabolites produced through
2988 direct infusion ESI MS. From the basic MS spectra that were obtained from the extracts from
2989 both cecal and distal colon contents, it was apparent the RS diets had an effect on the metabolites
2990 observed. The trend was that many of the low m/z ions for distal colon and cecal contents were
2991 similar despite diet, however many of the mid to high m/z ions were not shared. To determine if
2992 the apparent differences were statistically relevant PLS-DA was performed for cecal and distal
2993 colon content samples. The results showed that PLS-DA was able to accurately classify the
2994 cecal and distal colon content samples into distinct groups based upon the RS fed to the rats.
2995 The PLS-DA software was also able to determine biomarkers based upon accurate mass data.
2996 Future work would be to improve the fidelity of the study to include only RS parameters. The
2997 study included antibiotic and a carcinogen that potentially caused unnecessary metabolic
2998 variation among RS groups. Other interesting work would be to determine if metabolites shift
2999 over the time that an animal consumes the RS. By taking samples each week, rather than at the
3000 end of the study, these shifts would be apparent. Lastly, it would be paramount to attempt to
3001 accurately identify biomarker metabolites which consistently appear in multiple studies using
3002 LC-MS/MS in conjunction with standards.

3003 Chapter 3 centered on the identification of zein proteins from extracts procured from
3004 CGM and DDGS using a variety of solvent systems and with or without the use of a reducing

3009 agent. The zein extractions were tuned to extract primarily α -zein proteins. The use of high
3010 resolution MS was employed to find the accurate masses of the α -zein proteins in the extracts
3011 and to determine if the α -zein proteins varied based on extraction and source material. Previous
3012 MS studies had observed limited numbers of α -zein proteins, and generally had low resolution.
3013 The LC separation coupled to the high resolution MS discerned as many as 95 unique proteins,
3014 49 of the proteins had similar M_r values to previously reported proteins. It was unexpected that
3015 27 of the 49 proteins previously reported, were observed in both the CGM and DDGS extracts.
3016 The production of DDGS undergoes rigorous temperature and adulteration conditions, it was
3017 hypothesized that the zein extracted from DDGS many not contain fully intact zein proteins.
3018 Further work with α -zein extracts would include the full identification of the zein protein
3019 sequences using high resolution MS. The methods of choice would most likely include CID,
3020 ETD, or ECD. Such techniques would trap the charge state of choice for each zein protein of
3021 interest, fragment the protein, and then using software determine its protein sequence. These
3022 techniques would be amenable to protease digestion because most α -zein proteins would not be
3023 solubilized in aqueous solutions necessary for standard digestion conditions. Such digestions
3024 may be possible, but could be much more costly then seeking instrumental sequencing
3025 techniques.

3026 Chapter 4 applied FTIR-PAS to the same cecal samples used in Chapter 2. Rather than
3027 study the metabolites in the rat cecal contents, the main focus was the starch content. Very few
3028 techniques have the ability to determine how much starch is in a sample, and to determine the
3029 starch type. FTIR-PAS was utilized successfully for qualitatively and quantitatively determining
3030 the amount and type of RS remaining in the cecum of the rat. FTIR-PAS was able to analyze the
3031 bulk sample with minimal sample prep, which included grinding and oven drying. The main

3032 issue with FTIR-PAS was that it could not be utilized alone. A calibration had to be produced
3033 using approximately twenty cecal samples of known RS type, and measured for starch content
3034 using a bench-mark method. However, after calibrating for the twenty samples, it would be
3035 simple to measure the RS content and type for a near unlimited number of samples with minimal
3036 time and cost invested.

3037 Mass spectrometry is a method which is nearly indispensable to biological sample
3038 analysis. With future advances in ionization, chromatography, sensitivity, and resolution it may
3039 be relatively simple in the future to understand the near complete profile of compounds within a
3040 complex biological analyte. However, parallel techniques such as FTIR can interrogate the bulk
3041 properties of these same complex biological analytes with minimal sample preparation. If future
3042 improvements to FTIR techniques can decrease the number of techniques and apply it to most
3043 sample types, it would be vastly more accessible. One technique can provide valuable
3044 information, however the combination of two techniques used appropriately, such as MS and
3045 FTIR in tandem can provide a vast wealth of information from biological samples.

3046

3047

3048

3049

3050

3051

3052

3053

3054

3055 **ACKNOWLEDGEMENTS**

3056 A portion of this work was supported by the Iowa State University (ISU) Plant Sciences
3057 Institute and was supported in part by the Department of Agriculture, CSREES award number
3058 2009-65503-05798. This research was performed at the Ames Laboratory. Ames Laboratory is
3059 operated for the U.S. Department of Energy by Iowa State University under contract no. DE-
3060 AC02-07CH11358. Other funding was provided by the GAANN Fellowship.

3061 I would foremost like to thank Dr. Sam Houk for giving me the pleasure to join his lab
3062 while I overlapped the last year of my Masters in Food Science with my first year in the
3063 Chemistry PhD program. When things got rough during the time I had issues with my thesis he
3064 was always there with advice, assistance writing, and an untold number of Hershey chocolate
3065 kisses. During my PhD he allowed me a great deal of freedom to pursue my interests dealing
3066 with mass spectrometry and biological materials, while always being there with rock-solid
3067 advice. Second, I would like to thank Dr. John McClelland and Dr. Roger Jones for allowing me
3068 the ability to pursue and publish work within their lab. Dr. Jones' guidance and assistance
3069 writing two of my papers was exceptional. Third, I would like to thank Dr. Derrick Morast for
3070 teaching me everything he could about our instruments in Gilman and collaborating with me on
3071 our zein research paper. His mentoring and advice has been invaluable during my PhD.

3072 I would like to thank the Houk group members for their friendship, including Jeneé
3073 Jacobs, Jonna Berry, Katherine-Jo Galayda, Patrick McVey, Dr. Chris Ebert, Dr. Travis Witte,
3074 and Dr. Megan Mekoli. They were always of great help whether it be brainstorming, technical
3075 advice, or a productive group lunch on Friday. I would also like to thank my committee
3076 members for their assistance, Dr. Young-Jin Lee, Dr. Joseph Burnett, Dr. Jesudoss Kingston, and
3077 Dr. Emily Smith. I would like to further show my appreciation to Dr. Lee for meeting with me

3078 and discussing many ideas (some outlandish) pertaining to biological mass spectrometry and
3079 MALDI mass spectrometry. I would also like to thank Dr. Stan Bajic for his advice and
3080 assistance this year with our lab's ongoing the laser desorption project.

3081 I would like to thank the many friends I have in the department and I have made while
3082 my second stint in Ames. They made this time in Ames extremely enriching and enjoyable. I
3083 would like to thank my parents Karl Anderson and Katherine Anderson for their love and
3084 support in the past, and as I came back to graduate school. I would like to thank my brother John
3085 Anderson for his persistent, near daily calls and friendship. Last, I would like to thank my lovely
3086 wife Yeran, you were the one who convinced me to scale the cliff I considered a PhD. Your love
3087 and affection saw me through my toughest and best days during my Masters and PhD, thank you.

3088

3089